

Addis Ababa
University
(Since 1950)



ADDIS ABABA UNIVERISTY
COLLEGE OF NATURAL SCIENCES
SCHOOL OF EARTH SCIENCES

**PETROGRAPHY AND GEOCHEMISTRY OF BASEMENT ROCKS FROM
ABAY (BLUE NILE) RIVER GORGE, AROUND AGEMSA TOWN
WESTERN ETHIOPIA**

BY
SELAMAWIT ABDISSA MEKONNEN
ADVISOR: Prof. DEREJE AYALEW

**A Thesis Submitted to the School of Graduate Studies of Addis Ababa University, in
Partial Fulfillment of the Requirements for the Degree of Master of Science in
Geological Sciences (Petrology)**

JUNE,2018
ADDIS ABABA, ETHIOPIA

**ADDIS ABABA UNIVERSITY
COLLEGE OF NATURAL SCIENCES
SCHOOL OF EARTH SCIENCES**

**PETROGRAPHY AND GEOCHEMISTRY OF BASEMENT ROCKS FROM
ABAY (BLUE NILE) RIVER GORGE, AROUND AGEMSA TOWN
WESTERN ETHIOPIA**

**BY
SELAMAWIT ABDISSA MEKONNEN
ADVISOR: Prof. DEREJE AYALEW**

**A Thesis Submitted to the School of Graduate Studies of Addis Ababa University, in
Partial Fulfillment of the Requirements for the Degree of Master of Science in
Geological Sciences (Petrology)**

**JUNE, 2018
ADDIS ABABA, ETHIOPIA**

ADDIS ABABA UNIVERSITY
COLLEGE OF NATURAL SCIENCES
SCHOOL OF EARTH SCIENCES

**PETROGRAPHY AND GEOCHEMISTRY OF BASEMENT ROCKS FROM ABAY
(BLUE NILE) RIVER GORGE, AROUND AGEMSA TOWN WESTERN ETHIOPIA**

BY

SELAMAWIT ABDISSA MEKONNEN

Approved by the Examining Committee

Dr. Balemwal Atnafu

Head, School of Earth Sciences

Signature

Date

Prof. Dereje Ayalew

Advisor

Signature

Date

Dr. Mulugeta Alene

Examiner

Signature

Date

Dr. Tarekegn Tadesse

Examiner

Signature

Date

JUNE, 2018

ADDIS ABABA, ETHIOPIA

Declaration of originality

I hereby declare that this is my original work prepared under the supervision of Prof. Dereje Ayalew during the year 2018 for the partial fulfillment of the Degrees Masters of Sciences in Geological Sciences (Petrology). I further declare that this work is not presented or submitted to any other university or institution. All sources are well referenced and acknowledged.

Selamawit Abdissa Mekonnen

Signature

Date

I hereby declare this is her original work as part of her Master of Science in Geological Sciences (petrology).

Prof.Dereje Ayalew

Signature

Date

ACKNOWLEDGEMENT

I would like to thank very much to Dilla University for giving me an opportunity to start my master's degree in Addis Ababa University.

I would like also thank Addis Ababa University and School of Earth Sciences for providing me the opportunity and necessary support to pursue my master study.

My deepest gratitude goes to my Advisor Prof. Dereje Ayalew for his continuous and valuable comments, follow up and guidance from the pre-proposal formulation until the end of my thesis work.

I would like to thank the Deutscher Akademischer Austauschdienst (German Academic Exchange service) DAAD in region/in country scholarship for financial contribution. I wish to express my sincere appreciation to my friends Misgan Molla and Angesom Resom for their help starting from the proposal until the end of the work.

My greatest appreciation also goes to my dear parents for always supporting and encouragement during my study.

Last but not the least, the community of Agemsa town has a great place in my heart, I thank them all, for all support.

TABLE OF CONTENTS

CONTENTS	PAGES
ACKNOWLEDGEMENT	i
TABLE OF CONTENTS.....	ii
LIST OF FIGURES	vi
LIST OF TABLE	vii
ABSTRACT.....	x
CHAPTER ONE	1
1 INTRODUCTION	1
1.1 BACKGROUND OF THE STUDY	1
1.2 General description of the study area.....	2
1.2.1 Location	2
1.2.2 Accessibility.....	3
1.2.3 Topography and Drainage.....	3
1.2.4 Vegetation and Climate.....	4
1.2.5 Population and Land Use.....	5
1.3 Statement of the Problem	5
1.4 Objectives of the Study	6
1.4.1 General Objective	6
1.4.2 Specific Objectives	6
1.5 Materials and Methodology	7
1.5.1 Field Work	8
1.5.1.1 Laboratory and Data Analysis.....	8

1.5.1.1.1	Sample preparation and Geochemical analysis	8
1.5.1.1.2	Petrographic analysis	9
1.6	Expected Outcome and Significance of the Study	11
1.7	Previous Works	11
CHAPTER TWO		12
2	REGIONAL GEOLOGY	12
2.1	TECTONIC EVOLUTION OF THE EAST AFRICAN OROGEN (EAO)	12
2.1.1	Origin and Geology of the Arabian-Nubian Shield (ANS)	14
2.1.1.1	Origin of the ANS	14
2.1.1.2	Geology of the Arabian Nubian Shield (ANS)	15
2.1.2	The Mozambique Belt (MB)	15
2.2	Geology of the Ethiopian basement rocks.....	18
2.3	Geology and Geotectonic Evolution of Western Ethiopian Shield (WES).....	19
2.3.1	Litho-Stratigraphy.....	19
2.3.1.1	The Birbir Domain	21
2.3.1.2	The Baro and Geba Domain.....	21
2.3.1.3	The Didessa Domain	22
2.3.1.4	The Kemashi Domain.....	22
2.3.1.5	The Dengi Domain	23
2.3.1.6	The Sirkole Domain	23
2.3.1.7	The Daka Domain	23
2.4	Geotectonic Setting of the Western Ethiopian Shield (WES).....	24
CHAPTER THREE		26

3	GEOLOGY OF THE STUDY AREA	26
3.1	INTRODUCTION.....	26
3.2	Litho-Stratigraphy	28
3.2.1	The Orthogneiss Unit (Pmggn).....	28
3.2.1.1	Hornblende-Biotite Gneiss (ABS-7, ABS-16, ABS-17 Samples)	28
3.2.1.2	Granitic Gneiss (ABS-10, ABS-11 and ABS-12 Samples)	30
3.2.2	The Granite Unit	31
	CHAPTER FOUR.....	34
4	PETROGRAPHY AND METAMORPHISM	34
4.1	PETROGRAPHY	34
4.1.1	The Orthogneiss unit (Pmggn).....	34
4.1.1.1	Hornblende- Biotite Gneiss.....	34
4.1.2	Granitic Gneiss.....	35
4.1.3	The Granite Unit	37
4.2	Metamorphism	40
	CHAPTER FIVE.....	43
5	GEOCHEMISTRY	42
5.1	INTRODUCTION.....	42
5.2	Geochemistry of orthogneiss unit.....	46
5.2.1	Classification of orthogneiss.....	46
5.2.2	Trace Element Geochemistry of Orthogneiss	47
5.2.2.1	Zr variation diagrams for trace elements.....	47
5.2.2.2	Petrogenesis of Orthogneiss	50

5.2.2.3	Tectonic Setting of Orthogneiss.....	53
5.3	Geochemistry of Granite	54
5.3.1	Major Element Geochemistry of granite	54
5.3.1.1	Classification of Granite.....	57
5.3.2	Trace Element Geochemistry of Granite	59
5.3.2.1	Petrogenesis of Granite	59
5.3.2.2	Tectonic Setting of Granite	62
CHAPTER SIX.....		64
6	CONCLUSION AND RECOMMENDATION.....	64
6.1	CONCLUSION	64
6.2	RECOMMENDATION	66
REFERENCES		67
APPENDICES		76
Appendix I. Field data.....		76
Appendix II-Petrographic Data.....		78
Appendix III. Geochemical data		85

LIST OF FIGURES

Figure 1.1. Location map and digital elevation model (DEM) of the study area3

Figure 1.2. Physiographic map of the study area.....4

Figure 1.3. Schematic arrangement of Data used and methodology Adopted.....10

Figure 2.1. Tectonic evolution of the East African Orogen.....13

Figure 2.2. Sketch map of the East African Orogen.....17

Figure 2.3. Geographic distribution of Precambrian rocks in Eritrea and Ethiopia.....19

Figure 2.4. Generalized geology of the Tulu Dimtu Belt in western Ethiopia.....24

Figure 3.1. Geological map of study area27

Figure 3.2. Field Pictures of the Hornblende-Biotite Gneiss Unit.....29

Figure 3.3. Outcrop Pictures of the Granitic Gneiss Unit.....31

Figure 3.4. Field pictures of the Granite Unit.....33

Figure 4.1. A-D Microscopic Photo-pictures of Hornblende-Biotite Gneiss35

Figure 4.2. A-D Microscopic Photo-pictures of Granitic Gneiss36

Figure 4.3. Quartz-Alkali feldspar-Plagioclase classification Diagram.....38

Figure 4.4. A-H Microscopic Photo-pictures of Granite Unit.....38

Figure 5.1. The FAM triangular diagram for classification of orthogneiss46

Figure 5.2. Zr variation diagram for various trace elements (in ppm) of the orthogneiss48

Figure 5.3A. Chondorite normalized REE pattern for orthogneiss.....52

Figure 5.3B. Primitive mantle normalized mult-element variation diagram for orthogneiss.....52

Figure 5.4. Zr-Th-Nb tectonic discrimination plot for orthogneiss53

Figure 5.5. Harker Variation diagrams for granite55

Figure 5.6A. Chemical classification diagram for granite rock of the study area based on TAS..58

Figure 5.6B. Chemical classification diagram for granite rock of the study area based on Feldspar triangle58

Figure 5.6C. A/CNK ($Al_2O_3 / (CaO+Na_2O+K_2O)$) vs A/NK (Al_2O_3 / Na_2O+K_2O) plot granite rock.....58

Figure 5.6D. The K_2O vs. SiO_2 plot for classification of granite rock of the study area58

Figure 5.7A. Chondorite normalized rare earth element patterns for Granite.....61

Figure 5.7B. Primordial mantle normalized spider diagram for Granite61

Figure 5.8. Nb-Y, Ta- Yb, Rb- Yb+ Ta and Rb-Y+Nb tectonic discrimination diagrams for granite.....63

LIST OF TABLE

Table 5.1. Concentration of major and trace elements organized based on volatile free base recalculated values required for interpretation of the samples. Major oxides are in weight percent (wt %) and trace elements are in parts per million (ppm).....43

LIST OF ACRONYMS

- ALS	Australian Laboratory Science
- ASI	Alumina Saturation Index
- a.s.l	above sea level
- ANS	Arabian-Nubian Shield
- Bt	Biotite
- CAB	Calc- Alkali Basalt
- Chl	Chlorite
- Cpx	Clinopyroxine
- DEM	Digital Elevation model
- EAO	East African Orogen
- EMA	Ethiopian Mapping Agency
- GCD kit	Geochemical data kit tool
- GPS	Global Positioning System
- Hbl	Hornblende
- HFSEs	High Field Strength Elements
- HREEs	Heavy Rare Earth Elements
-IAT	Island Arc Tholeiitic
- ICP-AES	Inductively Coupled Plasma Atomic- Emission Spectrometry
- ICP-MS	Inductively Coupled Plasma Mass Spectrometry
- Kfs	K-feldspar
- LILEs	Large Ion Lithophile Elements
- LOI	Loss on Ignition
- LREEs	Light Rare Earth Elements
- MB	Mozambique Belt
- Mcr	Microcline
- ME-ICP06	Multi Element Inductively Coupled Plasma 06
- ME-MS81	Multi Element Mass Spectrometry 81

- mm	millimeter
- MORB	Mid-Ocean ridge basalt
- Msc	Muscovite
- My	Myremekite
- NMA	National Metrological Agency
- Plag	Plagioclase
- ppb	parts per billion
- PPL	Plane Polarized Light
- ppm	parts per million
- Pyr	Pyroxene
- OIB	Oceanic Island Basalt
- QAP	Quartz-Alkali feldspar-Plagioclase
- Qtz	Quartz
- REEs	Rare Earth Elements
- Syn-COLG	Syn-Collisional Granite
- Ser	Sericite
- VAG	Volcanic arc Granite
- WES	Western Ethiopian Shield
- WPG	With in Plate Granite
- wt. %	Weight percent
- XPL	Cross polarized Light

ABSTRACT

The geology Western Ethiopian Precambrian shield (WES) is known by low-medium grade metavolcano-sedimentary rocks, high grade gneiss and migmatites and ophiolite belts. The study area is a part of high grade metamorphic terrain of Western Ethiopian Precambrian shield that consists of both high grade Precambrian metamorphic and intrusive rocks. The high grade metamorphic rock is represented by orthogneiss, whereas the intrusive rock is represented by granite. The integration of field investigation, petrographic and whole rock geochemical analysis has been carried out to understand the petrogenic evolution and tectonic setting of the area. The presence of segregated mafic and felsic rich compositional bands both at the mesoscale and in the thin sections and the abundance of certain minerals such as hornblende and; plagioclase with lesser amount of clinopyroxine indicates that the orthogneiss of the study area has been subjected to high grade metamorphism that belong to upper amphibolite facies. Geochemically, the studied orthogneiss rock show calc-alkaline magma affinity. Except the granitic gneiss, all the remaining samples have relatively high concentrations of FeO, MgO and CaO and low concentration of SiO₂ content. Their REE abundance pattern shows nearly parallel trend in a negative general slope. The negative slope and calc-alkaline affinity combined with tectonic setting infer that the original rock of orthogneiss rock is originated from lower enriched mantle reservoir. The discrimination diagram Zr/117-Th-Nb/16 suggests that the original rock of orthogneiss of the study area were developed in the volcanic arc tectonic setting. The overall geochemical characteristic of granite shows high SiO₂ and Al₂O₃ contents 68.6-77.3 wt % ; 12.04-17.5 wt% and lower content of other major oxides. Such as, Fe₂O₃ 1.13-3.59 wt. %, MgO 0.02-0.62 wt % and CaO 0.83-1.69 wt.%. It display High K-calc-alkaline and peraluminous magma affinity. Their REE pattern shows only slight variation between the abundances of LREE and HREE elements which indicates moderate percentage melting. The discrimination diagrams Rb-(Y+Nb), Ta-Yb, Rb-(Y+Nb) and Nb-Y, suggested that the granite were developed in volcanic arc and syn-COLG environment.

Key words: Abay (Blue Nile) river Gorge, Palaeotectonic setting, Protolith, Metamorphism, Granite and orthogneiss.

CHAPTER ONE

1 INTRODUCTION

1.1 BACKGROUND OF THE STUDY

The geological formation of Ethiopia is classified into three major categories namely, the Precambrian basement, Late Paleozoic to Early Tertiary sediments; and the Cenozoic volcanic and associated sedimentary rocks (Mengesha Tefera et al., 1996). Among these, the basement rocks are the oldest rocks in the country which are formed during the Precambrian era and they range in age from 600–3000 million years. It includes different lithological types more or less intensively affected by metamorphism like gneisses, phyllite, quartzite, schists, and granitoids, mafites and ultramafites in dikes, bodies or complexes of variable sizes and importance (Getaneh Assefa et al., 1981). These Precambrian rocks are originally related to the pan African orogenic event particularly part of the so called Mozambique belt which has experienced during Paleozoic (Kazmin, 1971). The Precambrian rocks of Ethiopia are exposed in the peripheral parts of the country; in the north, west, southwest, and south and in the east (Asfawossen Asrat et al., 2001). Normally the Precambrian basement exposures are found in areas not intensively affected by Cenozoic volcanism and rifting and where the phanerozoic cover rocks have been eroded away (Mengesha Tefera et al., 1996).

In Ethiopia, the Precambrian rocks comprise both the Arabian Nubian Shield (ANS) in the north and the gneissic rocks of Mozambique belt (MB) in the south (Teklewold Ayalew, 1997). The two terrains hold distinctive lithotectonics which shows different lithological association, internal structure and grade of metamorphism. These are (1) granite-gneiss terrain, which contains both the high grade para and orthogneisses and deformed and metamorphosed granitoid; and (2) the ophiolitic fold and thrust belt which comprise on the other hand low-grade, mafic-ultramafic; and volcano-sedimentary assemblages. The terrains are bounded by, major faults and/or shear zone put on several deformation phases (B. Yibas, 2000 as cited in B. Yibas, 2002).

Based on lithological and structural mapping these rocks are classified in to three complexes; the Lower complex, composed of high-grade gneisses and represents the older (older than 2500M.y) cratonic basement, the Middle complex (clastic metasediments), is represented by the lower to middle Proterozoic platform cover and the Upper complex, consists of lower-grade metamorphic rocks in the sequence: ophiolitic rocks, andesitic metavolcanics and associated metasediments, clastic and to the lesser extent carbonate sediments (Kazmin et al.,1978).

According to Kazmin et al. (1978) the Western Ethiopian Precambrian shield comprises both the low-medium grade metamorphic rocks of Arabian-Nubian Shield (ANS) and high-grade reworked rock the of Mozambique belt (MB). In addition to this, the crystalline basement in the western Ethiopia consists of two major rock groups: namely high grade gneisses, which are often intensely migmatized, and volcano-sedimentary greenschist assemblages with associated linear belts of ultramafic rocks at Yubdo Daltti-Tullu Dimtu (from south to north). Plutonic rocks of variable composition and age intrude the basement rocks (Tesfaye Kebede et al., 1999). Abay (Blue Nile) River gorge has exposed part of western Ethiopian Precambrian shield. Exposures in this gorge start with Neoproterozoic rocks age in ~750Ma. Mesozoic sedimentary rocks are sandwiched unconformably between the Neoproterozoic basement rocks and Early–Late Oligocene volcanic rocks. No Paleozoic sedimentary rocks are exposed within the Gorge of the Nile (Gani and Abdelsalam, 2006).

1.2 General description of the study area

1.2.1 Location

The present research work is conducted in western Ethiopian Precambrian shield; specifically in the Abay (Blue Nile) River gorge located in the boarder of Oromia and Amahara national regional state. The area lies on Bure map sheet (NC-37/5) at 1:250,000 scale according to Ethiopian map Agency (EMA) and it is bounded by 10°00'-11°00'N latitudes and 36°00'-37°00'E longitudes The area is about 450 km from Addis Ababa, 130 km NE of Nekemte town (Figure 1.1).

1.2.2 Accessibility

The study area is accessed by the main road that joins Addis Ababa through Nekemte-Guttin-Gida Kiremu-Agamsa-Bure road. The road from Addis Ababa to Nekemte is asphalt and the remaining route from Nekemte to Bure is an all weathered gravel road. The study area is only accessible by field car.

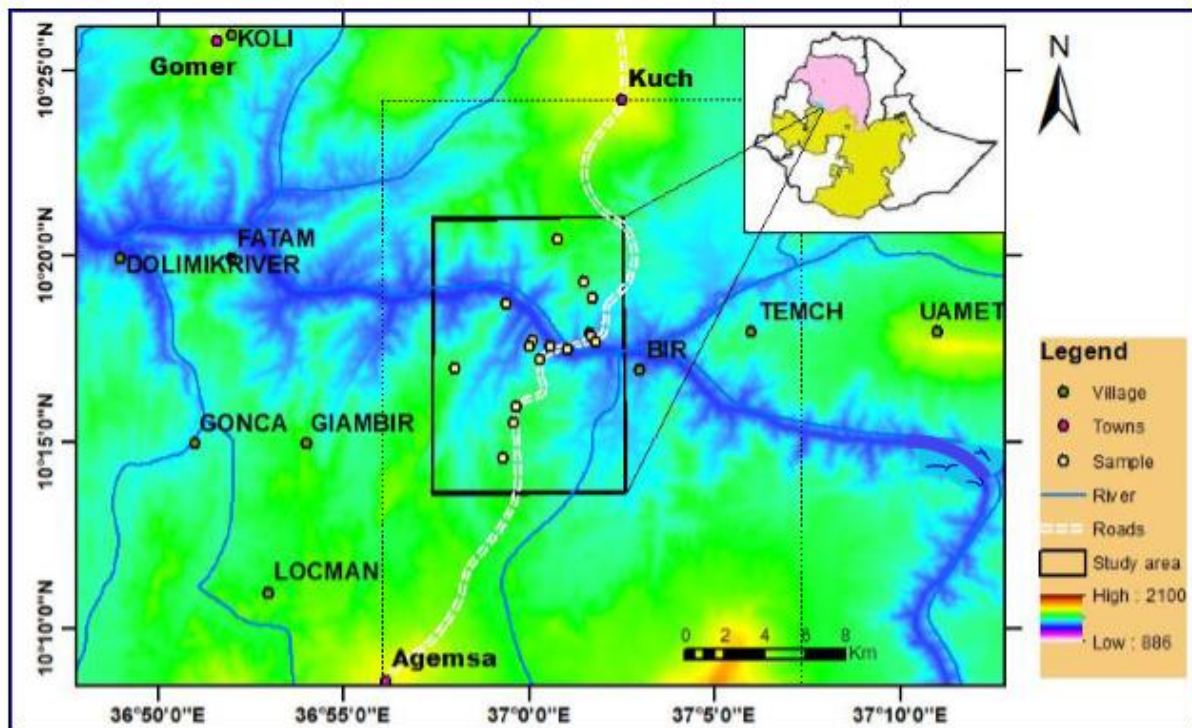


Figure 1.1. Location map and digital elevation model (DEM) of the study area.

1.2.3 Topography and Drainage

The study area is a part of Western Ethiopian shield which encompasses varied topography ranging from the deeply dissected wide canyon or gorge along the Abay (Blue Nile) River course to very rugged rocky mountainous terrains which surrounds the gorge. The elevation of the area is ranges from ~800 m (Near to the Abay gorge) and ~1600 m a.s.l (Around Agamsa town).The

drainage patterns of the study area is mainly controlled catchment of the Abay River. Most of the streams flow seasonally and joining with the main Abay River. The drainage pattern in the area is basically dendritic to angular in which Dura, Fetam, Bir, Temch, Gonka /Dubak and Aleltu are among the tributaries to the major Abay River.

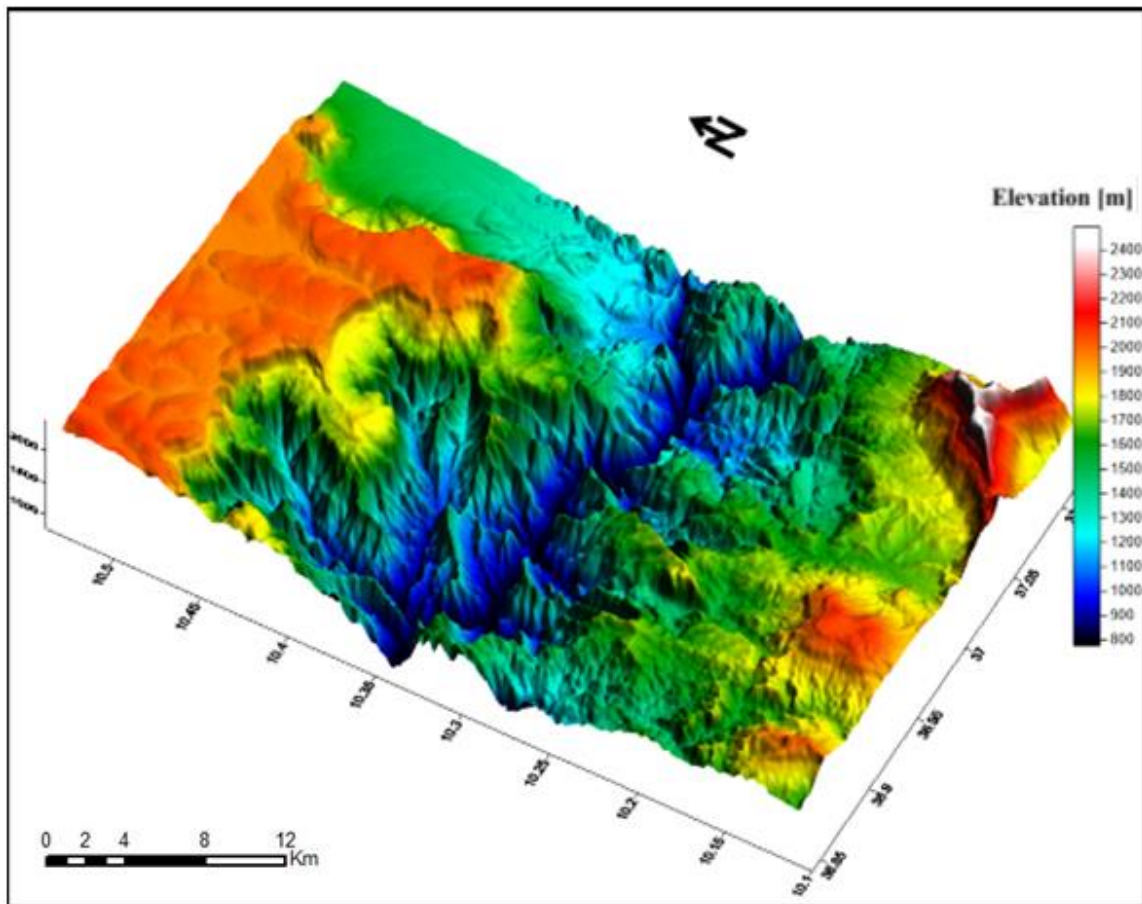


Figure 1.2. Physiographic map of the study area.

1.2.4 Vegetation and Climate

The climatic condition of the study area is represented by semi-arid climate or “Kola with a mean annual temperature 25°C (NMA, 1981). The main rainy season in the area is between

June-September and the dry season is between October-January. Generally the Area is highly rugged, inaccessible with very hot weather condition and is covered by thorny bush vegetation.

1.2.5 Population and Land Use

With the exception of Nekemte town, which is small in size is sparsely populated. The inhabitants of the area are Amahara, Oromo and Gumuz whose native languages are Oromiffa, Amaharic and Gumuzigna. Most of the populations are Protestants; few are Muslims and orthodox Christianity followers and generally relay on agricultural activities except the semi nomadic tribes of the Gumuz people close to the Abay River practiced in none well developed agriculture.

1.3 Statement of the Problem

In general the Precambrian geology of Ethiopia is not well understood (Asfawossen Asrat et al., 2001). In contrary to this, the Precambrian rocks of western Ethiopia is extensively studied particularly in the central Wellega area (e.g. Kazmin, 1969; De wit and Aguma, 1977; De wit et al., 1977; Senbeto Chewaka, 1980 as cited in Tesfaye Kebede et al., 1999). Even though the focus area of the present study, Abay (Blue Nile) River Gorge is a part of western Ethiopian shield, when compared to the other part of Western Ethiopian Precambrian shield this area is the least studied one. Particularly, no work has been conducted so far on the geochemistry of basement rocks of this area. In order to reduce this gap, the present work has been designed to study the petrography and geochemistry of basement rocks from Abay (Blue Nile) River Gorge. The results of petrography and geochemical analysis along with field investigation will help other researchers for the broad discussion of the nature of the rocks.

1.4 Objectives of the Study

1.4.1 General Objective

The general objective of this study is investigating the petrographical and geochemical characteristics of basement rocks from Abay (Blue Nile) River gorge, around Agemsa town, Western Ethiopia, using field investigation, petrographic and geochemical results.

1.4.2 Specific Objectives

In order to investigate the petrography and geochemistry of rocks in the study area, the main specific tasks to be carried out:

- To conduct petrological as well as geochemical analysis (thin section, major and trace element geochemistry).
- To determine the nature of protolith (parent rock).
- To relate the different metamorphic mineral assemblages with degree of metamorphism.
- To understand the petrogenesis of the rocks using the data collected and generated.
- To understand palaeotectonic environment of the rocks.

1.5 Materials and Methodology

The present study followed three general methods and approaches to achieve the general and specific objectives of the proposed research. These are pre-field work, field work and post field work. In the pre-field work collecting the literatures, identifying the problem, deciding the objectives and collecting topographic maps of the study area has been done. During the field work collecting the representative fresh samples from the outcrops, lithological descriptions of samples in hand specimens and taking GPS locations of the outcrop are the main activities that were employed. Post field works included, analyzing, synthesizing, presenting and interpreting of data and writing of this thesis.

During the initial stage (pre field work); field planning, literature survey and organization, relevant software identification and training, topographic map collection and processing, understanding the methods, results and findings of the concerned previous researchers and finally understanding the theoretical frame work of previous researchers plus delineating the study area are conducted before the actual field work.

Following the initial stage; description, sampling, labeling and packing of the lithologic samples are done during the field work. In addition, sampling locations are recorded in the excel sheet for further feeding and processing using ARC GIS.

Once the samples are described, labeled and packed in the field, sample preparation is conducted during the post field work. The samples are prepared for petrography and geochemistry where the sample preparation involves removing of the weathered parts and cutting to the appropriate size. Fourteen (14) samples are sent to the Institute of Geological Survey of Ethiopia for thin section preparation. In addition, 10 powdered samples are again prepared at the Institute of Geological Survey of Ethiopia and sent to the Australian Laboratory Science (ALS) in Ireland for Geochemical Analysis.

Subsequently, the prepared thin sections are studied using standard petrographic microscope at the petrography lab of the School of Earth Sciences, Addis Ababa University and the modal percentage of the minerals are well analyzed. The analyzed data (petrographic and geochemical data) are collected, presented, synthesized and interpreted for further discussion together with the

field observation. Finally all the data (field investigation, petrographic and geochemical data) together with the ideas of previous researchers are systematized, integrated and discussed.

Data synthesis has been done by collecting and integrating a variety of information for the purposes of interpreting the results. The other techniques to synthesize the data are Microsoft Excel, Win rock, geochemical tool (GCD kit) for petrographic and geochemical analysis. All the data both collected in the laboratory and from the literature reviews were analyzed, interpreted and presented together. Presentation will be in the form of texts, tables and figures.

During the different phases, a variety of tools are used, including topographic and geological maps at a scale of 1:250,000, ArcGIS, Google earth, DEM, Global mapper, Win rock, GCD kit and Microsoft excel 2007. In the following sections the main methods that applied in the research work is discussed below. The details of the research methodologies in each stage of the study are discussed below.

1.5.1 Field Work

Field work has been carried out from February 10 to February 20, 2017. Of the ten days in the field two days were visited the area in order to know the exposure of the outcrop, while the rest eight days were spent on the area to collect the representative and fresh rock samples for petrographic and geochemical analysis. Geological and topographic map of Bure sheet at the scale of 1:250,000 are used during the field work.

1.5.1.1 Laboratory and Data Analysis

1.5.1.1.1 Sample preparation and Geochemical analysis

Ten representative rock samples were collected from the study area to determine the major and trace element concentration of the rocks. The samples were prepared in the powdered form after removing the weathered part from the surface of rock sample. Then, samples were crushed to 70% less than 2mm, riffled to split of 1kg and the splits were pulverized to 85% passing 75 microns. The sample preparation has been done at the Institute of Geological Survey of Ethiopia, Addis Ababa. Finally, the pulverized samples were shipped to Australian Laboratory Science (ALS), Ireland for whole rock analysis. Major elements are analyzed using Multi element

Inductively Coupled plasma 06 (ME-ICP06) whereas trace elements are analyzed using Multi element mass spectrometry 81 (ME-MS81).

1.5.1.1.2 Petrographic analysis

Fresh and representative samples were collected from the study area based on their mineralogical and textural variations. Fourteen thin sections are prepared at the Institute of Ethiopian Geological Survey, Addis Ababa. Thin sections have been examined under Petrographic microscope (Leica microscope) at laboratories of school of Earth Sciences, Addis Ababa University. Each rock sample is studied under petrographic observation in order to determining the mineralogy, texture, composition, grain size, grain shape, structure and modal percentage of minerals in the rock. Finally based on the volume percentage of the minerals the name of the rock is given.

Schematic arrangement of data

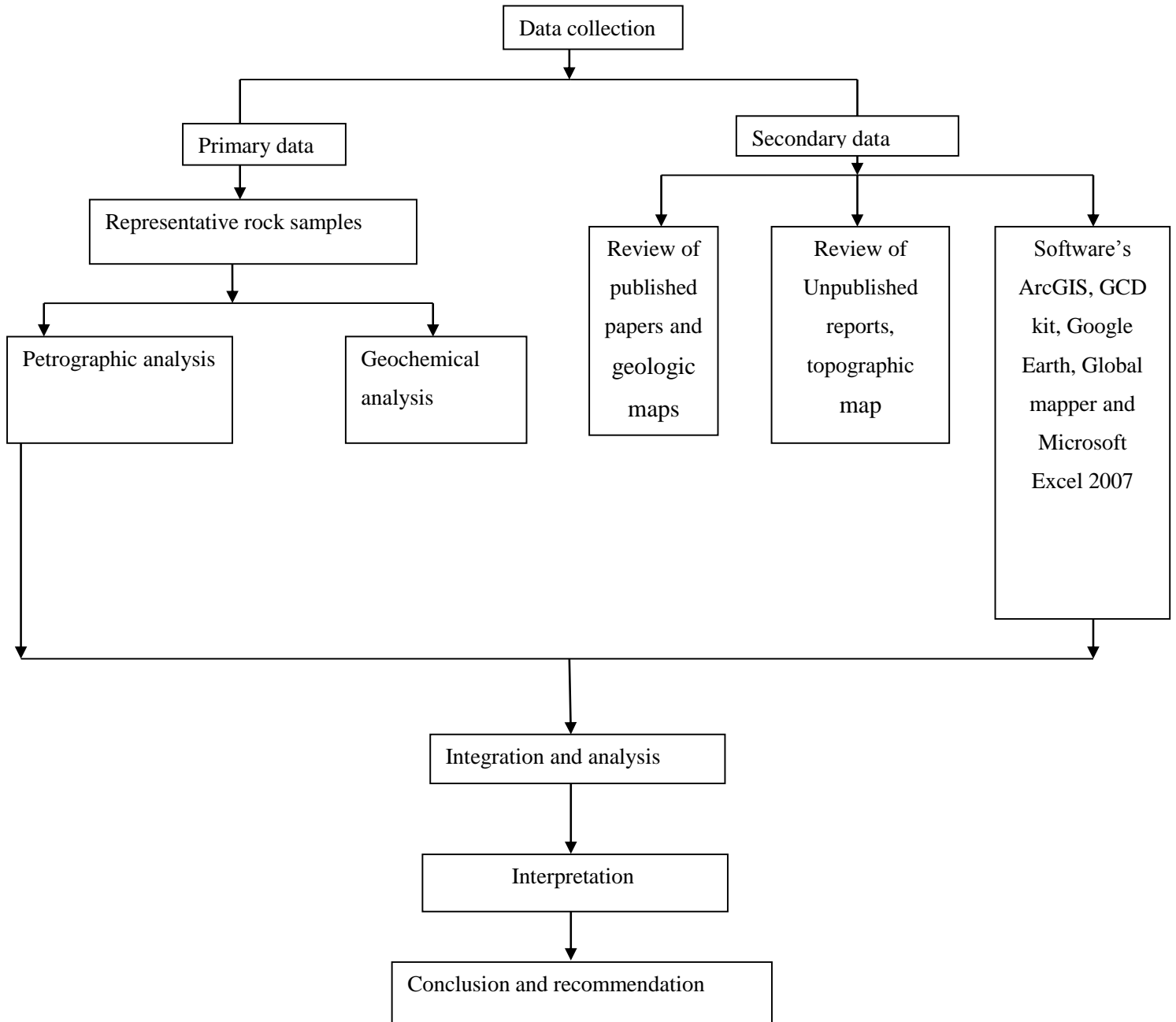


Figure 1.3. Schematic arrangement of Data used and methodology Adopted.

1.6 Expected Outcome and Significance of the Study

The geochemistry of the Abay (Blue Nile) river gorge area is not studied before. However the petrography characteristics of the rocks are only studied by Institute of Ethiopian geological survey at 1:250,000 scale. This new result of geochemical and additional information of petrological data will help others for further study of the petrogenesis of the rock, metamorphic and tectonic history of the area.

1.7 Previous Works

The Western Ethiopian Precambrian shield has been studied by different authors based on different perspectives. These include (Kazmin, 1969; De Wit and Aguma, 1977; De Wit et al, 1977; Senbeto Chewaka, 1980 as cited in Tesfaye Kebede et al, 1999). These studies were mainly targeted on the classification of the Precambrian geology of the area. They have identified the Pan-African low grade volcano-sedimentary rocks (ANS) and the high-grade gneissic rocks of (MB). Moreover, another study has been conducted by (Mengesha Tefera and Seife Michael Berhe, 1987; Moore et al., 1987 as cited in Teklewold Ayalew and Johnson, 2002). These studies also aim to the classified the rocks of the area into three lithotectonic domains were recognized. More specific works have been conducted in the area regarding geology, petrogenesis, geochemistry, tectonic setting, and evolution of the area; include study by Tesfaye Kebede et al. (1999); Tesfaye Kebede and Koebrel, C. (2001b, 2003); Grebonnikov, A.V (2014); Tadesse Alemu and Tsegaye Abebe (2007); Johnson et al.(2004); Allen and Gebremedhin Tadesse (2003, 2005); Teklewold Ayalew (1997); Teklewold Ayalew and Johnson (2002), Teklewold Ayalew and Peccerillo (1998); Braathen et al. (2001); Tadesse Yihunie and Fekadu Hailu (2007). The age of Precambrian rocks of western Ethiopia has been constrained by dating of granitoids conducted by Blades et al.(2015); Teklewold Ayalew et al. (1990); Tesfaye Kebede et al.(2001).The petrography of the Precambrian rocks of the Abay (Blue Nile) River gorge has studied by geological survey of Ethiopia compiled by Lulu Tsige (2008) as part of the Bure map sheet project work.

CHAPTER TWO

2 REGIONAL GEOLOGY

2.1 INTRODUCTION: TECTONIC EVOLUTION OF THE EAST AFRICAN OROGEN (EAO)

The East African orogeny (EAO) is one of the largest orogenic belts on earth, stretching ~6000 km N-S along the eastern flank of Africa (Stern et al, 2012). The EAO developed due to the collision of East and West Gondwana (Figure 2.1) during the late Proterozoic, which finally formed the greater Gondwana land (Stern, 1994). According to Stern (1994), the tectonic evolution of the east African orogen (EAO) comprises: (1) Rodinia rifting and break-up at ~900-850 Ma; (2) seafloor spreading, arc and back-arc basin formation, and terrane accretion from 870 to 690 Ma; (3) continent-continent collision from 630 to 600 Ma, and (4) further crustal shortening, lateral escape, orogenic collapse and extension leading to the formation of NW-SE faults during 600 to 540 Ma (Stern,1994). The Evolution of the EAO is a result of a Neoproterozoic-lower Paleozoic (Cambrian) Wilson Cycle that initiated with the breakup of Rodinia 870–800 Ma: and led to the final amalgamation of Gondwana in Cambrian time (Kusky et al., 2003; Li et al., 2008 as cited in Stern et al, 2012).

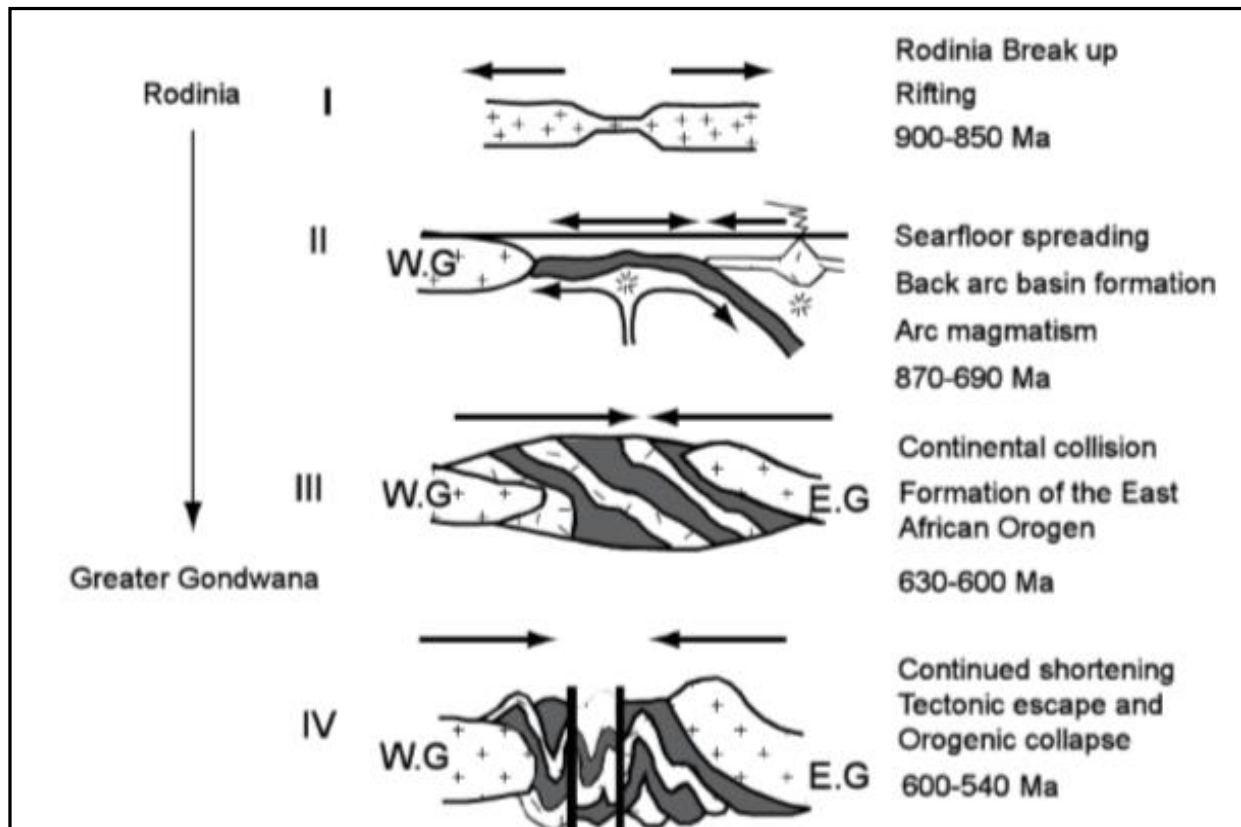


Figure 2.1. Tectonic evolution of the East African Orogen that resulted in the greater Gondwana Super continent (Stern et al., 2006). W.G=West Gondwana and E.G=East Gondwana.

During the Neoproterozoic the EAO comprises two major segments namely Arabian–Nubian Shield (ANS) in the north and Mozambique Belt in the south (Stern, 1994; Kröner and Stern, 2005; Lulu Tsige and Abdelsalam, 2005) (Figure 2.2).

2.1.1 Origin and Geology of the Arabian-Nubian Shield (ANS)

2.1.1.1 Origin of the ANS

The basement rocks exposed in the northeast Africa and western Arabia is known as ANS (Abdelsalam and Stern, 1996). Among the regions of Africa this belt is the largest tract of mostly juvenile Neoproterozoic crust and was affected by the pan-African orogenic cycle (Kroner and Stern, 2004). The ANS covers the northern half of the East African Orogen and stretches from southern Israel and Jordan as far as Ethiopia and Yemen, where it forms transition into the Mozambique Belt. ANS is distinguished from the Mozambique Belt by its dominantly juvenile nature, relatively low grade of metamorphism, and abundance of island-arc rocks and ophiolites (Kroner and Stern, 2004).

It was formed by as a result of a multistage process, whereby juvenile crust was produced above intra-oceanic convergent plate boundaries (juvenile arcs) and perhaps oceanic plateau (*Ca.* 870-630 Ma), and these juvenile terranes collided and coalesced to form larger composite terranes. In the course of its Neoproterozoic evolution, numbers of tectono-metamorphic and igneous cycles have processed the ANS; but two major tectono-metamorphic phases were the most prominent (Abdelsalam and Stern, 1996; Johnson and Woldehaimanot, 2003). The first phases, the older phase at around 750 Ma followed the termination of most island-arc igneous activity and probably concerns to the accretion and assembly of ANS island arcs (Abdelsalam and Stern, 1996; Johnson and Woldehaimanot, 2003). The second phase is subsequent tectono-metamorphic phase which followed a period of reduced igneous activity at around 700Ma causing thickening of the previously sutured island-arc complexes and formed tight, roughly N–S trending upright folds (Avigad et al., 2007 as cited in Avigad and Gvirtzman, 2009).

The Arabian Nubian shield was sandwiched between fragments of East and West Gondwana (Figure 2.2) and knowing the accurate timing of the collision is still being resolved. However, it appears to have occurred after ~630Ma when high-magnesium andesite 'schistose dykes' were emplaced in southern Israel but before the ~610Ma post-tectonic 'Mereb' granites were emplaced in northern Ethiopia (Kroner and Stern, 2004).

2.1.1.2 Geology of the Arabian Nubian Shield (ANS)

The ANS consists of extensive low-grade Neoproterozoic volcano sedimentary sequences with associated dismembered ophiolites aligned along suture zones (Vail, 1983, Seife Michael Berhe, 1990, Stern et al., 1990, Stern, 1994, Abdelsalam and Stern, 1996 as cited in Braathen et al., 2001). It also consisting of supracrustal metavolcanics including volcanoclastics and immature sediments mostly metamorphosed in the greenschist facies, variously deformed and intruded by granites, gabbros, and dikes (Avigad et al., 2007). In Ethiopia, the ANS is interleaved together with the Mozambique Belt which forms the southern half of the EAO and accommodated the most intense collision between East and West Gondwana fragments (Stern, 1994). The western margin of ANS is defined by juxtaposition of ophiolite-decorated volcano-sedimentary sequences and juvenile Neoproterozoic arc magmatic terranes. Highly deformed mafic-ultramafic bodies also found within low-grade (ANS) terrains making linear belts which are interpreted as dismembered ophiolitic rocks (Teklewold Ayalew et al., 1990; Abdelsalam and Stern, 1996). The ANS is exposed in the upper to middle crustal level, comprises relatively low grade metamorphic rocks and contains abundance of ophiolites, subduction- or collision-related granitoids, island-arc or passive continental margin assemblages makes the ANS distinct from MB (Kröner and Stern, 2004).

2.1.2 The Mozambique Belt (MB)

The MB is a broad belt which defines the southern Part of the East African Orogen and mainly consists of medium- to high-grade gneisses and voluminous granitoids. It extends south from the Arabian-Nubian Shield into southern Ethiopia, Kenya and Somalia via Tanzania to Malawi and Mozambique including Madagascar (Kroner and Stern, 2004). The Mozambique Belt, a part of the Pan African East African Orogen is a roughly N-S oriented mountain range formed by the collision of East and West Gondwana (Tenczer et al., 2005). The reasons of this collisional event are believed to be a long-lived subduction system along which island arcs were accreted between 750-500 Ma (Tenczer et al., 2005).

According to Kroner and Stern (2004) there is no overall model for the evolution of the MB, although most workers agreed that it was resulted from collision between East and West

Gondwana. In addition, the observable difference in rock types, structural style, age and metamorphic evolution suggests that the belt as a whole constitutes of a Pan-African Collage of terranes accreted to the eastern margin of the combined Congo and Tanzania cratons. Significant volume of older crust of the cratons were reconstituted during this event. This study also claims that the tectonics related to this event resulted in the formation of thrust propagating onto different cratons. The propagation of these thrusts formed the Pan-African metamorphic overprint with a gradient from greenschist facies to high pressure granulite facies in different Cratons of Africa (Tenczer et al., 2005). Closure of the oceanic basin occurred at ~760Ma and was followed by the formation of major north trending transcurrent faults at ~635Ma (Abdelsalam and Stern, 1996). In Ethiopia, the MB is exposed in the south and south-west and forms a front with the ANS, a lower grade (greenschist facies) calc-alkaline volcano-sedimentary terrain to the north (Asfawosson Asrat and Barbey.P, 2003). In general the Mozambique belt rocks are the well-exposed in Kenya, Southern, Eastern and Western Ethiopia, Northern Somalia and to lesser extent Northern Ethiopia (Kazmin et al., 1978; Taddesse Alemu and Tsegaye Abebe, 2007).

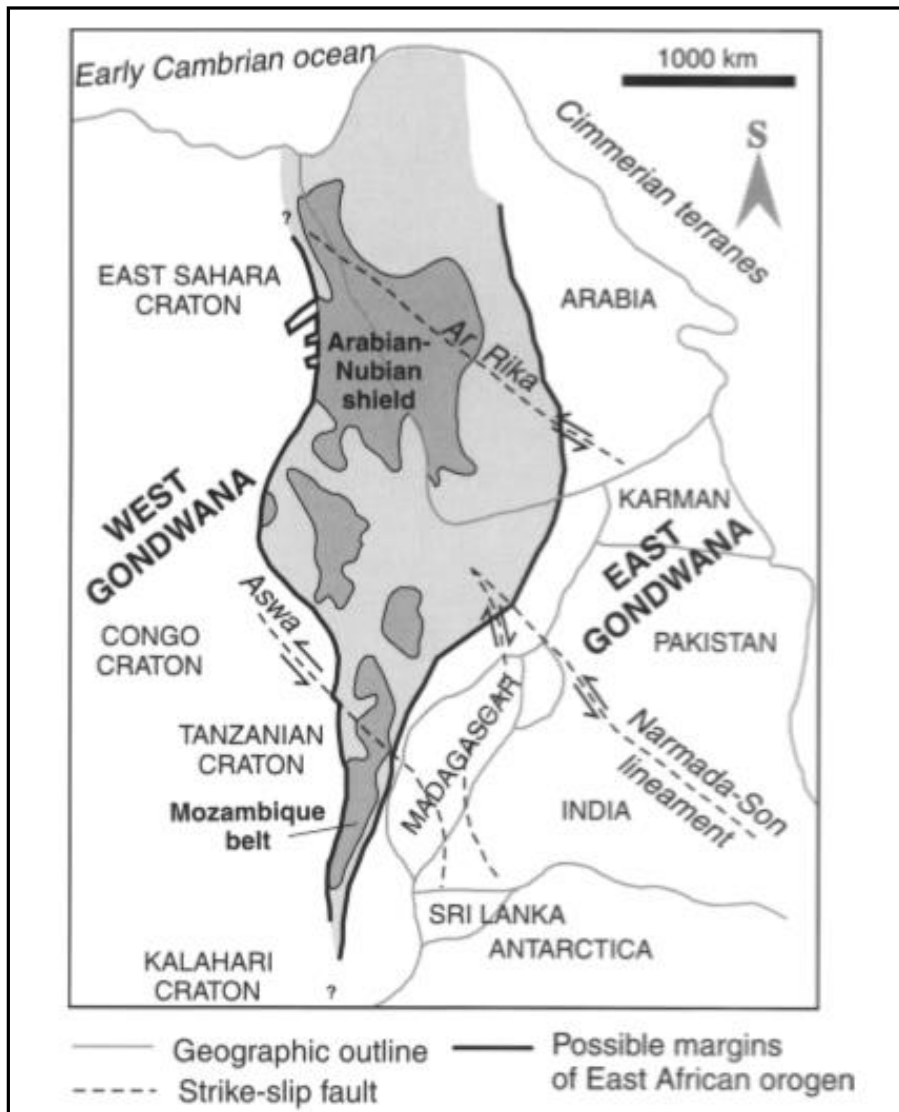


Figure 2.2. Sketch map of the East African orogen showing the location of the Arabian-Nubian shield relative to the Mozambique Belt and adjacent cratonic margins (after modified Stern, 1994 as cited in Johnson and Woldehaimanot, 2003).

2.2 Geology of the Ethiopian basement rocks

The Ethiopian basement rocks are exposed in the north, in the west, in the southwest, in the south and in the east parts of the country (Asfawosson Asrat et al., 2001) (Figure 2.3). It consists of a wide variety of volcano-sedimentary and plutonic rocks metamorphosed to varying degrees of metamorphism (greenschist to amphibolite facies), medium to high grade gneisses and schists, metamorphic rocks occur (Kazmin,1971 as cited in Asfawosson Asrat et al., 2001). According to Abbate et al. (2015) Neoproterozoic crystalline basement rocks range in age from 880 to 550 Ma and constitutes the crustal backbone of the Ethiopian region with wide coverage in the southern and western Ethiopia and, to a lesser extent, in the northern most Ethiopia. Likewise, these crystalline basement exposures of the EAO in Western Ethiopia occupy a particular interest, lying between the predominantly gneissic Mozambique belt (MB) in the south, and the greenschist-facies volcanic-arc complex of the Arabian Nubian shield (ANS) in the north (Braathen et al, 2001). The Proterozoic terrains in Ethiopia are related to the East African Orogen (Stern, 1994), N–S elongated mega collisional structure stretching from Israel to Madagascar and produced between West and East Gondwana by the closure of the Mozambique ocean (Abbate et al., 2015) .

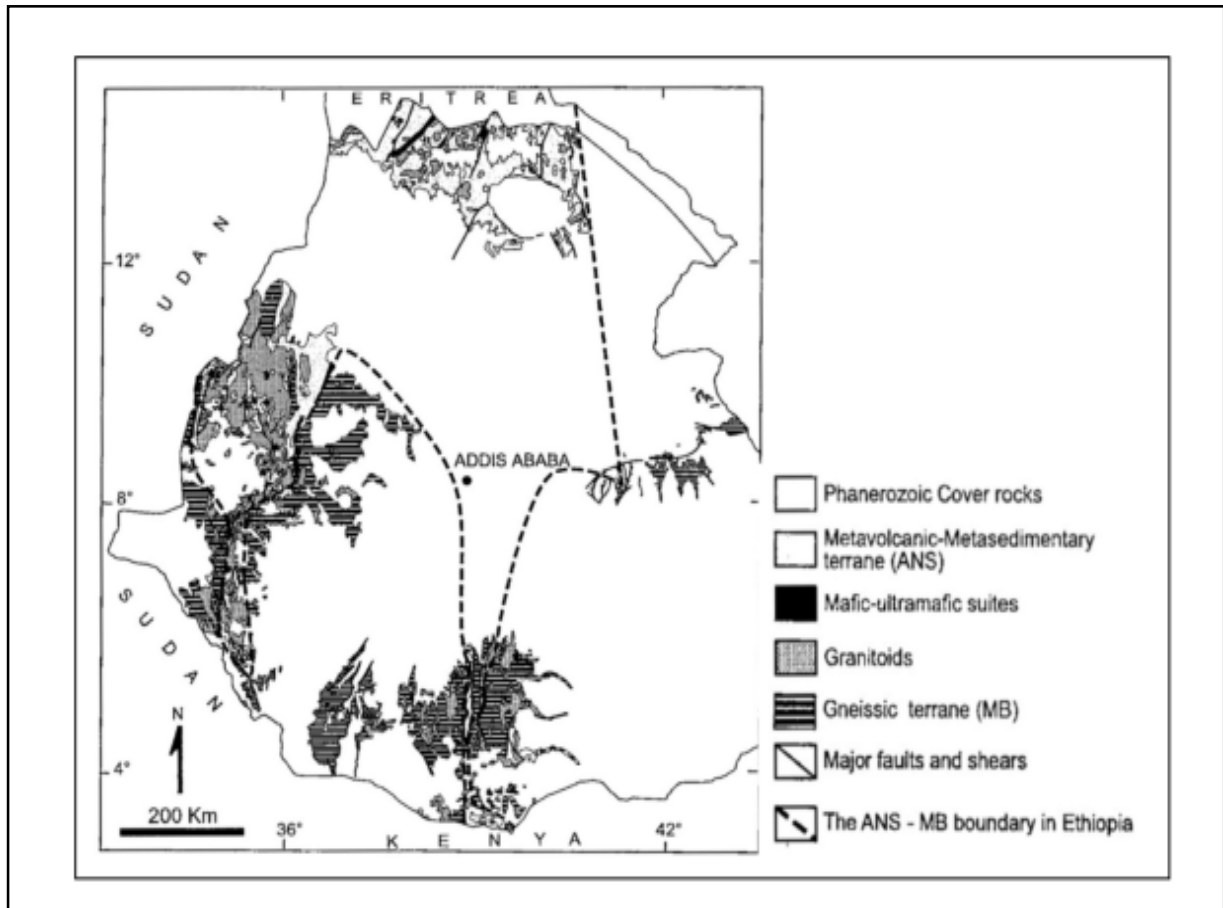


Figure 2.3. Precambrian rock exposures in Ethiopia with the proposed boundary between the ANS and the MB in Ethiopia (Asfawossen Asrat et al., 2001).

2.3 Geology and Geotectonic Evolution of Western Ethiopian Shield (WES)

2.3.1 Litho-Stratigraphy

The Western Ethiopian shield comprises both the low-medium grade metamorphic rocks of Arabian-Nubian Shield (ANS) and high-grade reworked rocks of Mozambique belt (MB) (Kazmin et al., 1978). Braathen et al. (2001) presented that the Precambrian rocks of Western Ethiopia shows a division of two provinces: Archaean to Palaeoproterozoic gneisses in the east,

Neoproterozoic and Palaeoproterozoic gneisses to the west. The Precambrian rocks of this region comprises of high-grade gneiss and migmatite in the east and west and low-grade metavolcano-sedimentary rocks at the middle and bounded in either side by two parallel NNE-SSW trending ophiolitic belts (Tulu Dimtu and Asosa-Kurmuk) (Tadesse Alemu and Tsegaye Abebe, 2007).

The lower complex (considered to be Archaean) containing various gneiss and migmatite, mainly granitic composition and supposed to represent the older cratonic basement in the country (Asfawossen Asrat et al., 2001). Eventually, these rocks are coarse grained, well foliated and banded, strongly deformed and metamorphosed to amphibolite facies and overlain by the Upper Complex which consists of metavolcanic and metasedimentary rocks of low grade greenschist to amphibolite facies (Benzu Gold Mining Ethiopia PLC, 2013). The low-grade metavolcano-sedimentary rocks referred to as upper complex have been considered as the southern continuation of the Pan-African Arabian-Nubian shield (Kazmin, 1972; UNDP, 1972 as cited in Tadesse Alemu and Tsegaye Abebe, 2007).

The metavolcano-sedimentary lithology includes graphitic phyllite, carbonate schists, marble and ultrabasic to acidic intrusive related to the Upper complex intruding the Lower Complex (Benzu Gold Mining Ethiopia PLC, 2013). Geochronological investigations from plutonic rocks suggest that the age of low-grade rocks range from ~830 to ~540 Ma (Teklewold Ayalew et al., 1990). Based on field, lithologic geochemical and geochronological evidence the low-grade rocks of western Ethiopia were correlated to the juvenile Pan-African assemblages of northern Ethiopia, Eritrea and southeastern Sudan (Tadesse Alemu and Tsegaye Abebe, 2007).

The western Ethiopian Precambrian shields (WES) has been sub-divided in to several domains using different classification schemes (Allen and Gebremedhin Tadesse, 2003). They can be group into three lithotectonic units; the Birbir Domain, Geba domain and Baro domain (Teklewold Ayalew and Peccerillo, 1998; Mengesha Tefera and Seife Michael Berhe, 1987 as cited in Teklewold Ayalew and Johnson, 2002). This classification was mainly based on grade of metamorphism and lithological similarities within the same domain (Teklewold Ayalew and Peccerillo, 1998).

2.3.1.1 The Birbir Domain

The main unit characterizing this domain includes an assemblage of deformed and metamorphosed volcano sedimentary rocks and associated ultramafic to felsic magmatic rocks bounded by dominantly orthogenetic Geba and Baro domain (Johnson et al., 2004). In addition to this, it comprises metasedimentary rocks, and metavolcanics altered sub-volcanic sills, dykes and mylonitic quartz diorite. The metasediments are weakly to strongly schistose metagreywacke and pelite, with subordinate coarse volcanoclastic and carbonate rocks (Teklewold Ayalew and Johnson, 2002).

2.3.1.2 The Baro and Geba Domain

The Baro and Geba domain is exposed in the eastern and western part of the western Ethiopian Precambrian shield. The easterly Geba domain is dominated by rather monotonous quartzofeldspathic gneisses. The predominant rock types are strongly foliated; medium- grained biotite and hornblende-biotite gneisses. Some of the gneisses are migmatitic and contains numerous sub-concordant lenses of granitic and pegmatitic material. A uniform granitoid composition and lenticular texture over hundreds of square meters of the outcrop suggests that the majority of biotite-gneiss and hornblende-biotite are tonalitic or granodioritic orthogneisses. Rare garnet-bearing and commonly epidotised rocks are more probably paragneisses. Although the westerly Baro domain is similarly dominated by orthogneissic biotite-gneiss and hornblende-gneiss, paragneisses characterize the eastern margin of the Baro close to the contact with the Birbir (Teklewold Ayalew and Johnson, 2002).

Another subdivision of the western Precambrian terrane was proposed by Allen and Gebremedhin Tadesse (2003). Accordingly, the major divisions are: from East to West (Figure 2.4): Didessa domain, Daka domain, Kemashi domain, Sirkole domain and Dengi domain.

2.3.1.3 The Didessa Domain

This domain displays distinct lithological and structural characteristics that differentiated it from the adjacent Kemashi domain to the west. This domain extends approximately 5Km east of Didessa River in Wollega area covering about 70Km up to about 25Km west of Gimbi town. It is differentiated from the adjacent Kemashi domain to the west by distinctive lithological and structural characteristics. The rocks within this domain are moderate grade para-gneisses which consist of interlayered biotite-amphibole gneiss, garnet-biotite gneiss and quartzofeldspathic gneiss and ortho-gneisses which consists banded mafic gneiss. Banded mafic gneisses in ortho-gneisses of Didessa domain contain ultramafic bands derived from a layered mafic intrusive body and very coarse granitoid gneiss and intruded by Neoproterozoic intrusive rocks. This domain makes a contact with the nearby Kemashi which is marked by the N-S trending Chugi Shear Zone, consisting of strongly N-S cleaved phyllonitic rocks derived from the Didessa Gneiss.

2.3.1.4 The Kemashi Domain

This is a narrow 10-15Km wide domain paralleling the trend of Tulu Dimtu belt. Sequences of metasedimentary rocks of marine origin, mafic to ultramafic metavolcanics and associated plutonic rocks wide variety make up the domain. The metasedimentary rock consists of dark, highly pyritised, pelitic to psammitic schists, intercalated with chert, graphitic phyllite and marble.

2.3.1.5 The Dengi Domain

The main units characterizing this domain include deformed and metamorphosed volcano-sedimentary sequence, a coarse grained para-and ortho gneissic unit and mafic to felsic intrusive bodies intruding to the later. It crops out to the west of Kemashi Domain and has 120 Km width and indicates two pulses of magmatism at 850-840 Ma and 780-760Ma in similar way to Didessa domain (Blades et al, 2015).

2.3.1.6 The Sirkole Domain

The Sirkole domain was to occupy west of Assosa town extending into Sudan, and therefore its western limits is unknown. It consists of different N-S elongated blocks of which have only a few Km widths. Alternating sequences of moderate grade polydeformed and metamorphosed gneisses and low- to moderate-grade metasedimentary rocks and mafic to felsic metavolcanic rocks intruded by deformed and undeformed granitoid plutons are the characteristics of this domain.

2.3.1.7 The Daka Domain

The predominant rocks in this domain are gneissic and they encompass three lithological units Daka Domain's another gneissic unit is a banded orthopyroxine-bearing granulite facies unit known as Daka gneiss. It crops out in south of the other two units and is in tectonic contact with the other two along the E-W trending Daka River Thrust. This occurrence is significant as granulite facies terranes are rare within the northern part of the EAO.

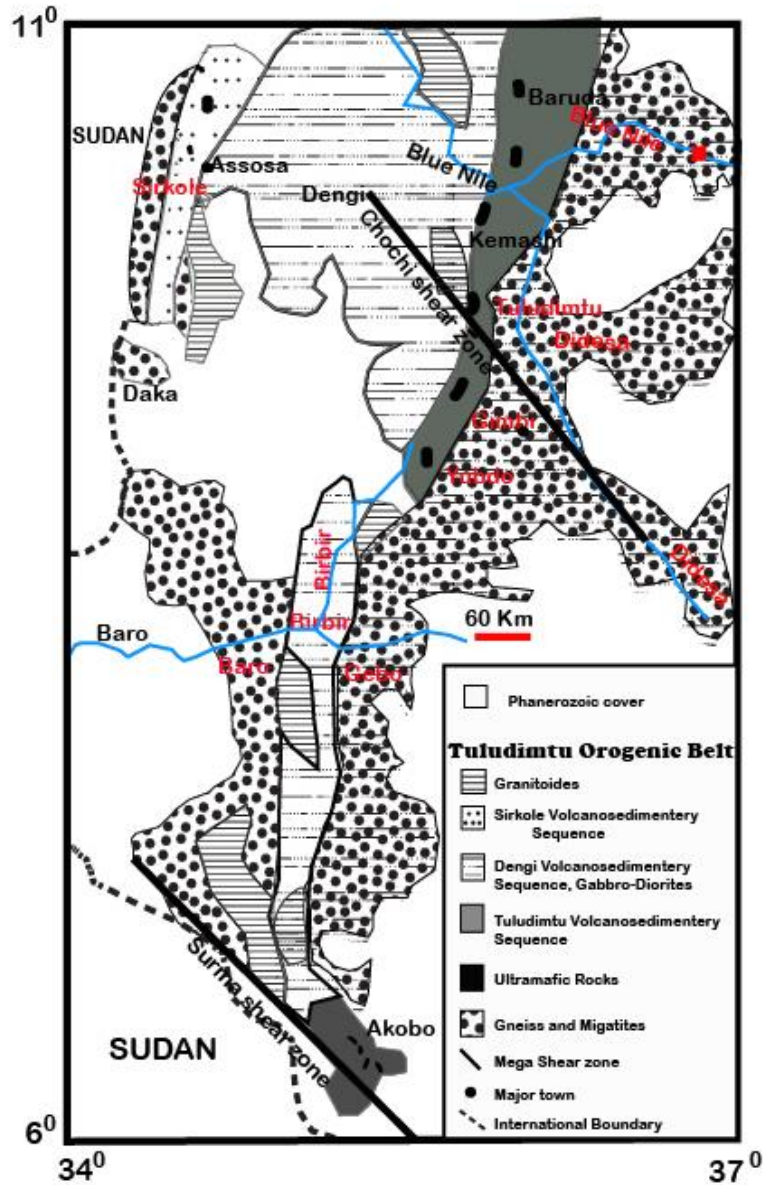


Figure 2.4. Generalized geology of the Tulu Dimtu Belt in western Ethiopia (Allen and Gebremedhin Tadesse, 2003).

2.4 Geotectonic Setting of the Western Ethiopian Shield (WES)

The WES is located close to the transition between the Arabian Nubian Shield and the Mozambique Belt adjacent and East of the 'Eastern Saharan Meta-craton (Abdelsalam and Stern, 1996). It extends northwards from 6°N and it covers about 650km², which is the largest

Precambrian block in Ethiopia (Tadesse Alemu and Tsegaye Abebe, 2007). Geotectonically it is evolved through different processes starting from early rifting and associated sedimentation, followed by subduction and island arc formation, arc-accretion and, finally, continent-continent collision (Kazmin et al., 1978). The reason of the latter stages was resulted from the collision of east and west Gondwana (Stern, 1994) caused severe E-W crustal shortening. Different evidences have shown concluded that bodies within the WES have an intrusive nature (Grenne et al., 1998; Aberra Mogessie et al., 1999 as cited in Teklewold Ayalew and Johnson, 2002). It was emplaced into an extensional back-arc-rift setting (Braathen et al., 2001).

According to Tesfaye Kebede et al. (1999) these intrusive bodies occur as a wide compositional spectrum from gabbro to granite characterizes the volcano-sedimentary assemblages. Granitoid intrusions into the high-grade terrane, however, are restricted both compositionally (diorite/granodiorite to granite) and geographically they occurred only in a few location. Among this, A-type granitoids are one of the intrusive bodies from western Ethiopia, Wellega area and contains three domains namely the Ganjii monzogranite, the Homa gneissic granite and Tuppi granite. These granitoid bodies are understood as they were either intruded into greenschist facies volcano-sedimentary sequence or emplaced at the contact between low- and high-grade terranes (Tesfaye Kebede and Koeberl, 2003). They are composed of Fe-rich biotite, Ferro-hornblende, alkali-amphiboles and alkali pyroxenes. High total alkalis, high FeO_T/MgO (particularly in the peralkaline varieties and syenite), enriched rare earth element (REE), Y, Nb, Ta and low CaO, MgO, and Sr abundance characterize these granitoids (Tesfaye Kebede and Koeberl, 2003). The granitoid rocks in the area are categorized as pre- to post-deformation granitoids of within plate and volcanic arc settings.

Teklewold Ayalew and Peccerillo (1998) concluded that pre- to syn-tectonic granitoids appear to be the product of magmatic arc activity (VAG), whereas the other granites fall in the field of within-plate granite (WPG). Generally, metamorphism in WES occurred in wide range of metamorphic grades beginning from low grades like greenschist facies and lower amphibolite as in Birbir domain to very high-grades like upper amphibolite and granulite facies as in Geba and Baro domains (Teklewold Ayalew and Peccerillo, 1998).

CHAPTER THREE

3 GEOLOGY OF THE STUDY AREA

3.1 INTRODUCTION

The study area is a part of high grade metamorphic terrain of Western Ethiopian Precambrian shield (WES) that is dominated by both Precambrian high grade metamorphic and intrusive rocks (Figure 3.1). The high grade metamorphic rock is represented by migmatitic gneiss (orthogneiss consists of hornblende-biotite gneiss and granitic gneiss) that are exposed in the east central, southeast and southwest part of the study area, whereas the Precambrian intrusive rock is represented by granite that is exposed in the western, northwest, and southwest part of the study area. Both rock units cover the largest portion of the study area. The orthogneiss rocks unit are relatively foliated and banded. Most of the rocks of the study area are affected by secondary structures, like joints, fractures, quartz veins and fault. They are generally exposed in a relatively low-lying and rugged topography. The following description gives an account on the geology (i.e. the rock type, description including the mineralogy and texture) of rock of the study area.

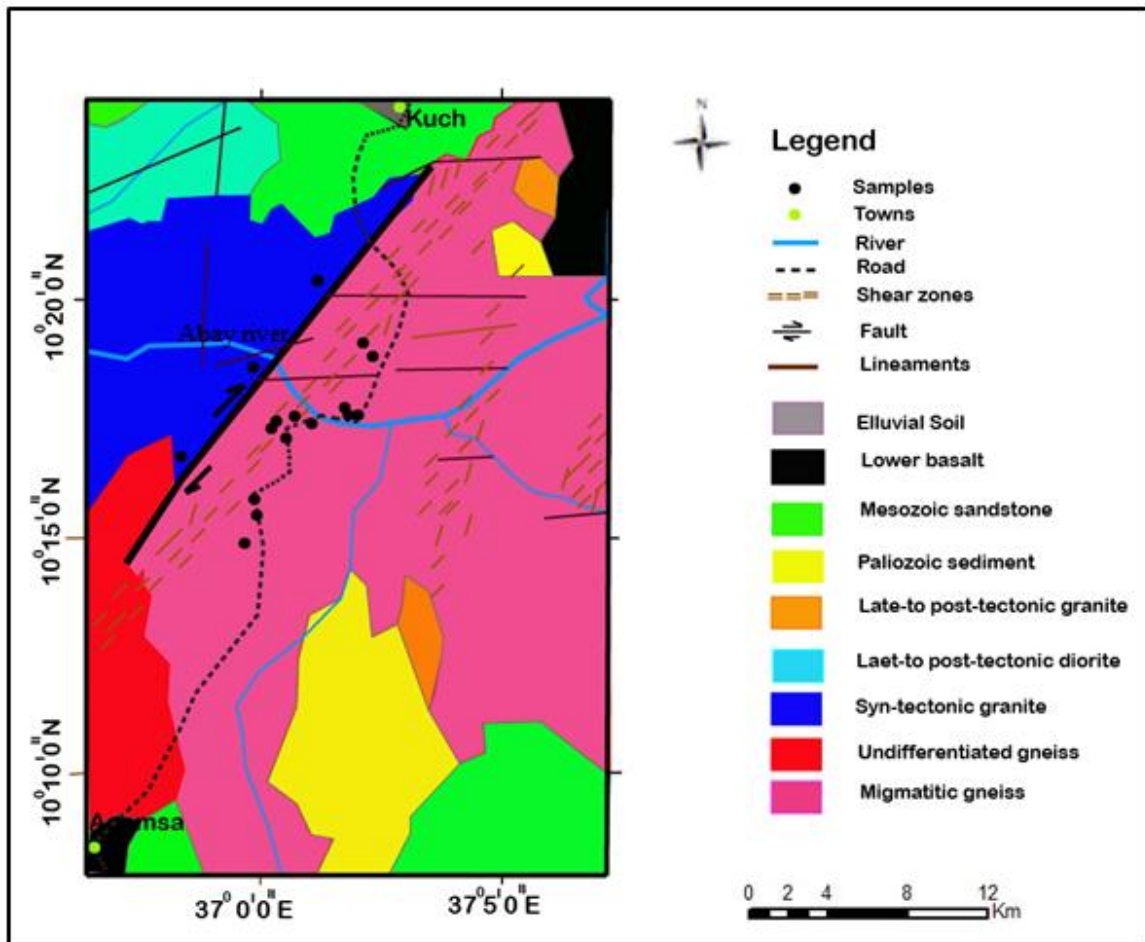


Figure 3.1. Geological map of study area (modified and adopted from geological map of bure sheet compiled by Lulu Tsige and Endashaw Hailu, 2007).

3.2 Litho-Stratigraphy

3.2.1 The Orthogneiss Unit (Pmgn)

This unit is the most dominant rock unit in the area. It covers the large part of the study area. Based on mineral content, the rock unit is divided into two namely, the Hornblende-Biotite Gneiss and Granitic gneiss. The contact of this unit with the adjacent rock is mostly gradational.

3.2.1.1 Hornblende-Biotite Gneiss (ABS-7, ABS-16, ABS-17 Samples)

This rock unit is mainly exposed in the southwest part of the study area (Fig.3.2). It is mostly characterized by compacted but at some place it is friable, medium to coarse grained and shows dark to dark gray color in fresh outcrop and light grey to greenish grey in weathered surface and; foliated fabric. It is mainly composed of medium to coarse grained minerals with commonly visible minerals like plagioclase, hornblende and biotite. Both the dark minerals and light colored minerals are strongly flaky and oriented in different fashion finally it gives the gneissosity structure. The gneissosity of the rock is greatly deviates from the generally N-S trending to W-E trending and defined by segregation of mafic (hornblende and biotite) and felsic (quartz and plagioclase) minerals. This compositional variation has been probably formed due to metamorphic differentiation which is formed in the progressive deformations of high grade metamorphism. Generally, this rock unit shows mesoscale fault with strike of $S60^{\circ}W$ and its dip $70^{\circ}NW$ (Figure 3.2 C) and foliations cross cut by quartz veins (Figure 3.2 A). It is highly fractured and in some part the rock is highly sheared. It is commonly exposed in relatively low-lying and rugged topography. It has an estimated thickness of ~150m. Petrographic examinations of ABS-7 is composed of 40% hornblende, 35% plagioclase, 10% quartz, 8% biotite, 3% chlorite and 3% pyroxene and 1% opaque, whereas ABS-16 contains 38% hornblende, 30% plagioclase, 15% quartz, 5% biotite, 5% pyroxene, 4% sphene, 2% opaque and 1% apatite and; ABS-17 consists of 48% hornblende, 25% plagioclase, 10% biotite, 5% quartz, 5% pyroxene, 4% sphene, 2% opaque and 1% apatite. Chlorites occur as alteration product of hornblende mineral.

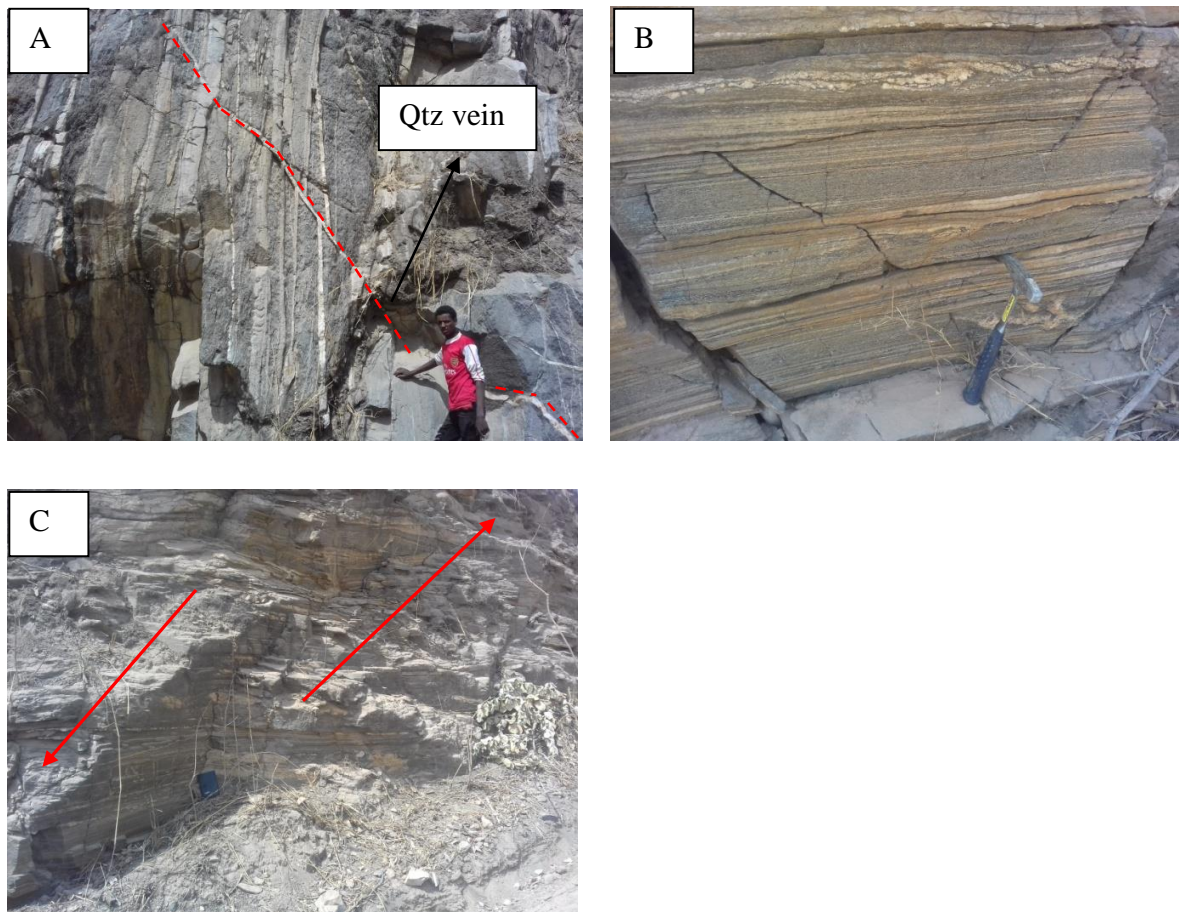


Figure 3.2. Field pictures of hornblende-biotite gneiss. (A) This rock unit is strongly foliated, shows vertical compositional banding cross cut by quartz vein ($037^{\circ}01'03.2''E$: $10^{\circ}17'28.6''N$). (B) This rock unit is also strongly foliated shows horizontal compositional banding ($037^{\circ}01'47''E$: $10^{\circ}17'39.8''E$). (C) Photograph shows a mesoscale (out crop level) fault and highly fractured unit at the same location with outcrop (B).

3.2.1.2 Granitic Gneiss (ABS-10, ABS-11 and ABS-12 Samples)

This rock unit is mainly exposed in the east central and southeast part of the study area (Figure 3.3); associated with granite and hornblende-biotite gneiss rock. It is characterized by light gray color in the weathered outcrop and whitish to light pink color in the fresh outcrop; it is medium to coarse grained with flaky mineral like biotite. From the representative samples of this unit, it is mainly composed of K-feldspar, quartz, plagioclase and biotite, muscovite/sericite, chlorite, apatite, zircon and opaque minerals. K-feldspar is a major constituent in the rock characterized by light pink color. At places (Figure 3.3 C) it shows clear segregation of mafic and felsic minerals. The strike orientation of the foliation is N35°E and its dips amount 65°NW. It has been cut by two perpendicular quartz veins and they have two general trends; nearly N-S and E-W. The rock also has been subjected to sericitization and chloritization alteration processes. Locally it has been fractured, weathered and altered. It is commonly exposed in a relatively low-lying and rugged topography. Generally, the rock shows gneiss texture and the outcrops possess different sets of joints. The petrographic study of ABS-10 sample indicates that this rock is composed of 40% K-feldspar (microcline), 30% quartz, 15% plagioclase, 10% biotite, 2% sphene and 2% opaque, whereas ABS-11 composed of 45% K-feldspar, 35% quartz, 10% plagioclase 5% biotite, 2% muscovite/sericite, 2% chlorite, 2% opaque, and 1% apatite. Similarly another thin section ABS-12 shows 45% K-feldspar, 30% quartz, 15% plagioclase, 5% biotite, 3% muscovite/sericite 1% opaque and 1% zircon.

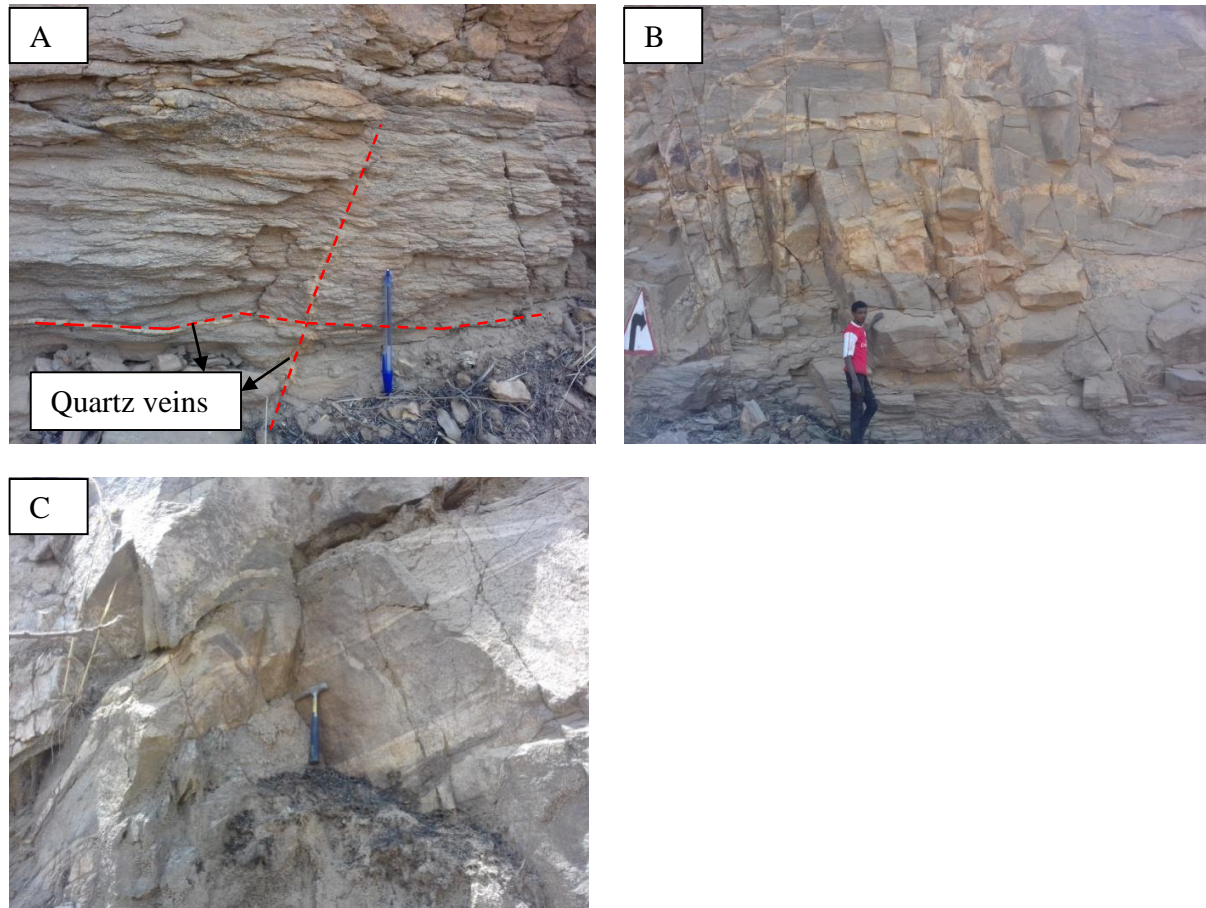


Figure 3.3. Outcrop photo pictures of granitic gneiss unit. (A) This rock unit is cut by two perpendicular quartz veins ($037^{\circ}00'06.7\text{E};10^{\circ}17'43.9\text{N}$); (B) fractured and altered granitic gneiss unit ($037^{\circ}00'37.6\text{E};10^{\circ}14'49.7\text{N}$). (C) this rock unit show weak foliation ($037^{\circ}00'16.8\text{E};10^{\circ}17'11.4\text{N}$).

3.2.2 The Granite Unit

This rock unit is the most dominant rock unit in the study area. It covers the larger part of the area and is found intruding the high grade domain of the gneiss rock. It occurs in various grain sizes, ranging from very coarse grained to medium grained with similar mineral assemblage. The constitute minerals are K-feldspar (microcline), quartz, plagioclase, biotite, muscovite/sericite, chlorite, zircon and opaque. It is generally exposed in a relatively low-lying and rugged topography along the Abay (Blue Nile) River Gorge. It has a gradational contact with orthogneiss rock unit. Samples coded by ABS-4 and ABS-8 are from a thin and small outcrop mainly exposed in the southwest part of the study area. It is mostly characterized by very coarse

grained texture ($\sim >10\text{mm}$) and it is compacted and show pinkish and whitish in the fresh surface, and light to dark grey in the weathered surface. It is dissected by one systematic joint and its strike $S30^\circ E$ and its dip $65^\circ NE$. It has an estimated thickness of $\sim 100\text{m}$. Petrographic examinations of ABS-4 indicates that this rock is composed of 55% K-feldspar (microcline), 25% quartz, 15% plagioclase, 2% biotite, 1% muscovite/sericite, 1% zircon and 1% opaque, whereas ABS-8 is composed of 35% plagioclase, 30% quartz, 25% K-feldspar(microcline), 3% muscovite/sericite, 3% biotite, 3% opaque and 1% zircon. Other sample coded by ABS-9 and ABS-13 cover relatively smaller part of the study area. It is mainly exposed in the northwest and southwest part of the study area (Figure 3.4). Mostly characterized by friable, coarse grained ($\sim 5\text{-}10\text{mm}$) and shows pinkish and whitish color in the fresh outcrop and light-gray to dark gray in the weathered surface. It shows a large phenocrysts grain of K-feldspar (microcline) embedded in relatively fined grained mass of plagioclase and quartz. The quartz veins featuring throughout the body of this unit and show the same orientations (parallel orientation). The alteration features is quite common and represented by sericitization of plagioclase and K-feldspar were apparent. It has an estimated thickness of $\sim 500\text{m}$. Locally it has been fractured, weathered and altered. Petrographic examination of this rock ABS-9 shows 45% K-feldspar (microcline), 30% quartz, 10% plagioclase, 8% biotite, 4% muscovite/sericite, 3% opaque, whereas ABS-13 is composed of 50% K-feldspar (microcline), 20% quartz, 15% plagioclase, 6% biotite, 5% muscovite/sericite and 4% opaque. Samples coded by ABS-1, ABS-2, ABS-6, and ABS-15 cover relatively large part of the study area. It exposed in the west, southwest and northwest part of the study area. It appears medium grained ($\sim 1\text{-}5\text{mm}$), light pink, light gray to whitish and pale pink in the fresh outcrop and light dark in the weathered surface. It is cut by one set of joints and its strike varies from $N70^\circ\text{-}85^\circ W$ and its dip amount varies from $70^\circ\text{-}80^\circ SW$. Locally it has been fractured and weathered. The petrographic study of ABS-1 shows 45% K-feldspar (microcline), 25% quartz, 20% plagioclase, 6% biotite, 2% opaque and 2% muscovite/sericite, whereas ABS-2 contains 50% K-feldspar (microcline), 20% quartz, 15% plagioclase, 10% biotite, 3% muscovite/sericite and 2% opaque. Similarly another thin section ABS-6 is composed of 45% K-feldspar (microcline), 25% quartz, 20% plagioclase, 5% biotite, 3% opaque and 2% muscovite/sericite and ABS-15 composed of 50% K-feldspar, 30% quartz, 10% plagioclase, 5% biotite, 3% muscovite/sericite and 2% opaque.

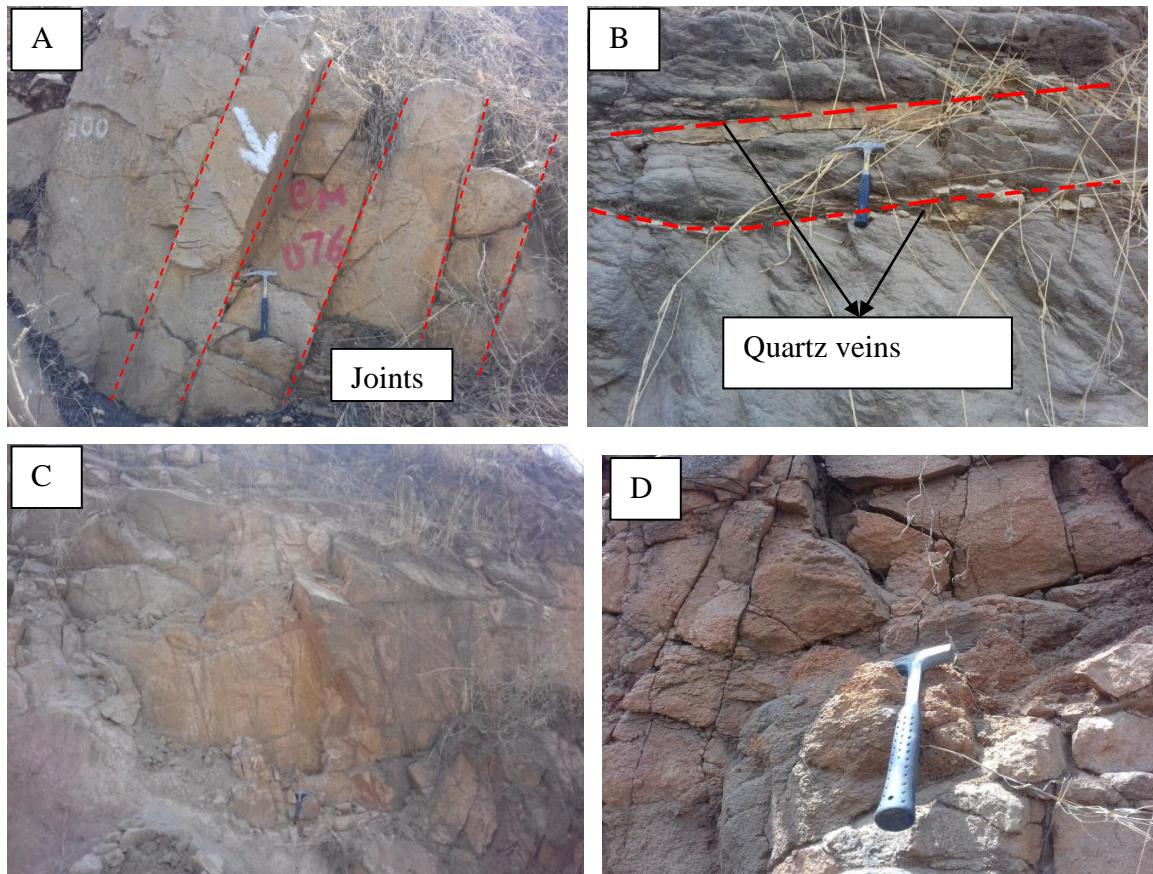


Figure 3.4. Field pictures of the granite unit. (A) This rock unit is dissected by one systematic joints, oriented $S110^{\circ}E/65^{\circ}NE$ and its joint spacing is approximately 1-2m ($036^{\circ}59'22.5''E:10^{\circ}14'39.3''N$), (B) The Granite unit cut by two parallel quartz veins ($036^{\circ}59'35.8''E:10^{\circ}15'30.8''N$), (C) highly altered, weathered and fractured granite unit ($037^{\circ}00'01.5''E:10^{\circ}17'34.8''N$), (D) fractured and pinkish granite unit ($037^{\circ}01'28.5''E:10^{\circ}19'17.9''N$).

CHAPTER FOUR

4 PETROGRAPHY AND METAMORPHISM

4.1 PETROGRAPHY

The aim of studying petrographic characteristics of the rocks is used to determine the nature of the rock, protolith and metamorphic history of the area. The petrographic analyses of the representative samples from the two units have been examined. The thin sections are analyzed by using both plane polarized light (PPL) and cross polarized light (XPL). The analyzed samples show both igneous and metamorphic textures. In gneiss rock the mafic minerals (hornblende and biotite) and felsic mineral (feldspar and quartz) show preferred orientation and define the gneissosity structure. The petrographic description and analysis of the rock units are described below.

4.1.1 The Orthogneiss unit (Pmggn)

4.1.1.1 Hornblende- Biotite Gneiss

Petrographic studies of the representative samples (Figure 4.1 A-D) from hornblende-biotite gneiss unit indicate that this unit is mainly composed of hornblende, plagioclase, biotite, pyroxene and quartz. Trace amount of chlorite, sphene and opaque minerals also constitute the rock unit. Among the feldspar minerals plagioclase dominates the rock unit characterized by anhedral to subhedral shape and clearly shows twinning (polysynthetic twinning). This rock unit exhibits granular and foliated texture. The abundance of certain minerals such as hornblende, plagioclase, biotite and small amount of clinopyroxine indicates that this rock is derived from mafic rock most probably basalt. Alteration of hornblende to chlorite is commonly developed. Most of minerals show preferred orientation and the foliations are defined by mafic (hornblend) and felsic (plagioclase and quartz) minerals (see appendix II D).

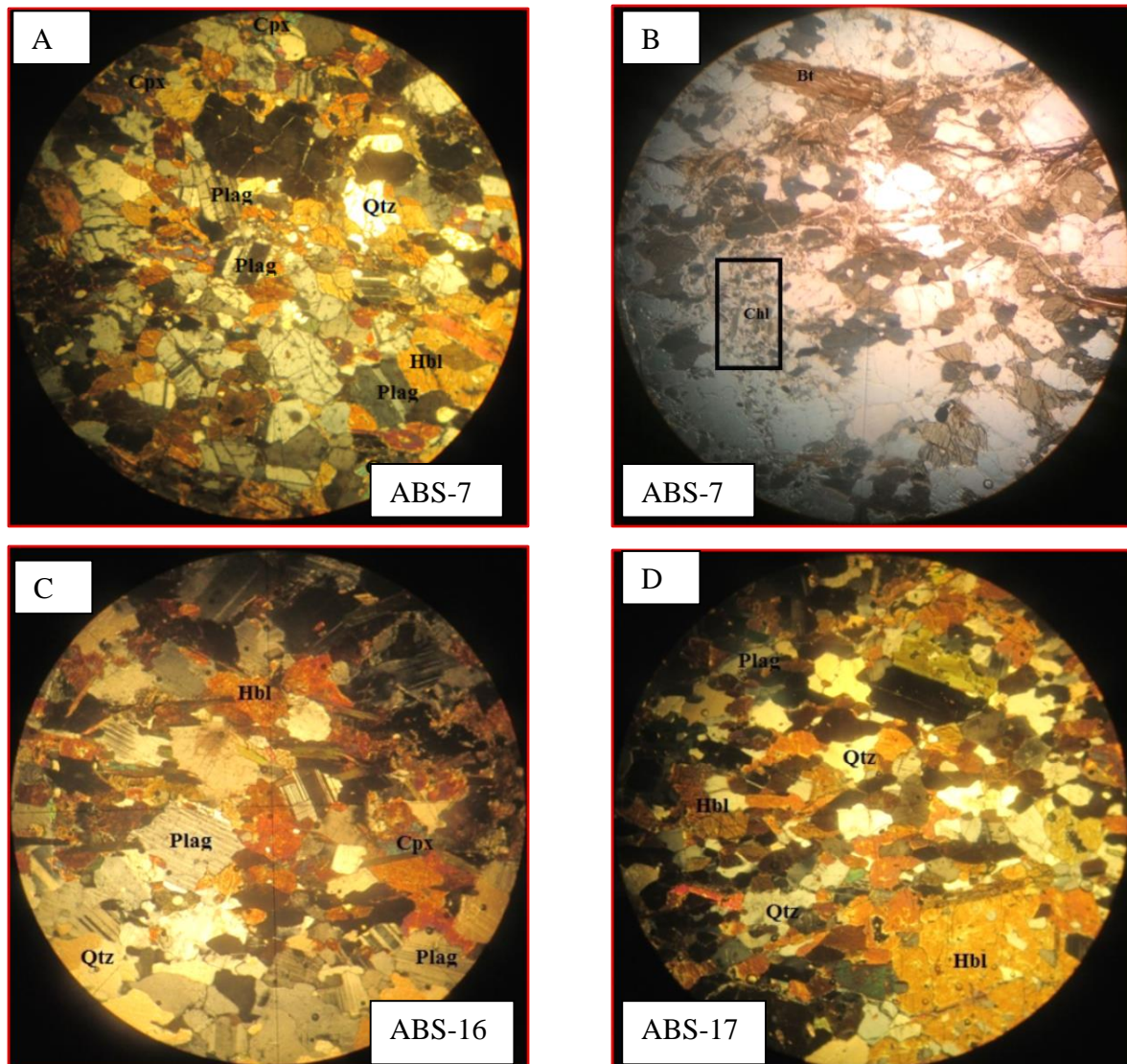


Figure 4.1. A-D: Microscopic photo pictures of the Hornblende-Biotite Gneiss unit. (A and D) this sample exhibits granular and foliated texture. (B) Shows alteration of hornblende to chlorite. (C) part of hornblende-biotite unit with visible Clinopyroxene surrounded by hornblende and plagioclase show clear polysynthetic twinning.

4.1.2 Granitic Gneiss

Petrographic study of the representative rock samples (Figure 4.2 A-D) from the granitic gneiss unit indicates that this rock is mainly composed of K-feldspar, quartz, plagioclase and biotite.

Trace amount of muscovite/sericite, opaque, chlorite, sphene and zircon also constitute the rock unit. Exhibiting granular and weak foliation defined by felsic (plagioclase, K-feldspar and quartz) and mafic (biotite) minerals. The abundance of certain mineral assemblage such as K-feldspar, quartz and plagioclase and granular texture indicates that the protolith of the rock is felsic igneous rock most probably granite (see appendix II D).

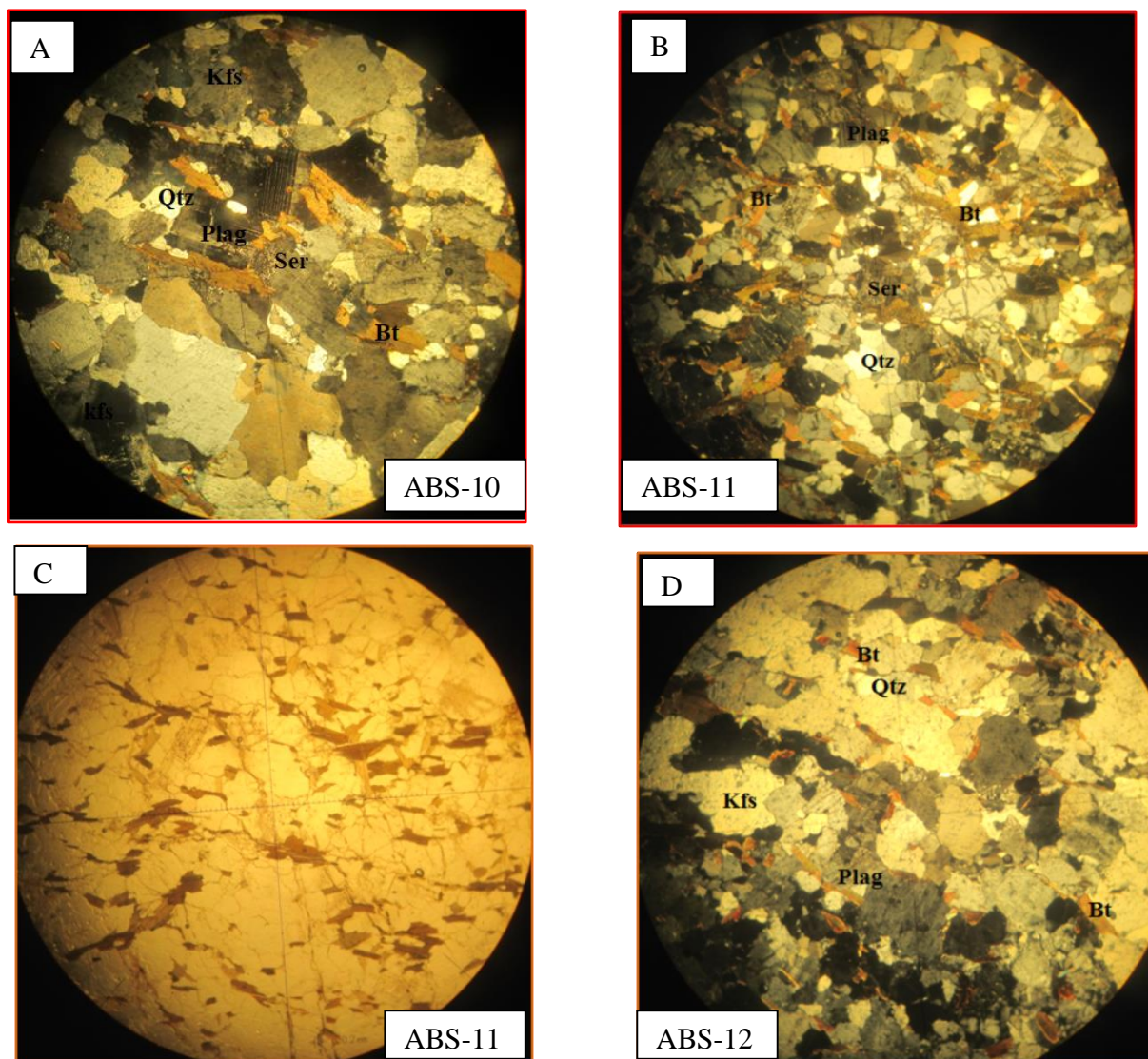


Figure 4.2. A-D: Microscopic photo-pictures of granitic gneiss unit. (A) part of granitic gneiss unit exhibit granular texture and clear alteration of plagioclase to sericite. (B and D) samples

show faint foliation. (C) the same view of picture B under PPL, the biotite grain shows brown color.

4.1.3 The Granite Unit

The granite of the study area is represented dominantly by grayish, whitish and pinkish color as discussed in chapter three. The petrographic classification of the granite ranges from syenogranite to monzogranite. This classification is based on petrographic name of the granite presented below and assigned based on modal mineral composition obtained by point counting, which were then plotted on QAP (Figure 4.3) (after Streckeisen 1976) for classification. The samples coded by ABS-1, ABS-2, ABS-3, ABS-4, ABS-6, ABS-13 and ABS-15 are syenogranite unit. The remaining one sample ABS-8 is the monzogranite unit. The most common mineral assemblages are K-feldspar (microcline), quartz, plagioclase, biotite and muscovite/sericite and; accessory minerals such as zircon, chlorite and opaque. Biotite is the only mafic mineral in this rock unit.

The alteration features are quite common represented by sericitization of K-feldspar (microcline) and plagioclase were apparent. Some of the quartz crystals show little undulose extinction and it occurs as anhedral to subhedral crystal habit. In some thin sections quartz grains occur as clusters between the feldspar and myremekite (intergrowth of quartz with feldspar) also common (Figure 4.4 C). The Plagioclase mostly occurs as anhedral to sub-hedral and twinning is a typical feature. Some of the plagioclase grains contain inclusions of opaque and biotite. K-feldspar is dominated by microcline and occurs as anhedral to subhedral crystal habit. In the perthite, the exsolved plagioclase component occurs within host microcline as microscopic lamellae. The presence of microcline and perthite indicate unmixing of sodium and potassium feldspars. Granular, intergranular, graphitic, perthite and myremekite textures are common as well. Biotite displays fine aggregate to flaky texture. Zircon has a typical idiomorphic shape and appears light gray color (in PPL). They have high relief than the other minerals which constitutes the granite unit. Sericite is fine grained occurs as the alteration result of feldspars and it has high interference color. The opaque minerals observed in the rock range between anhedral and subhedral crystal shape with some visible euhedral grain shape.

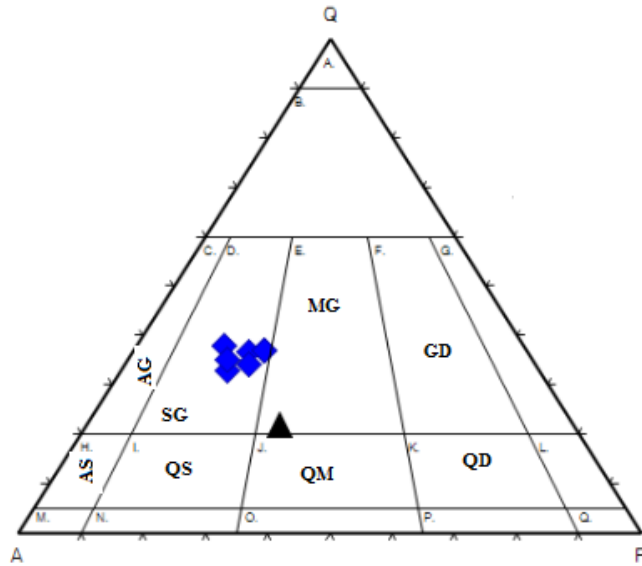
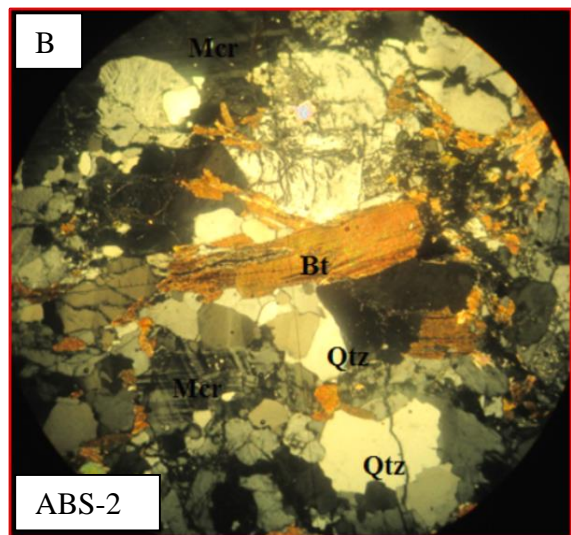
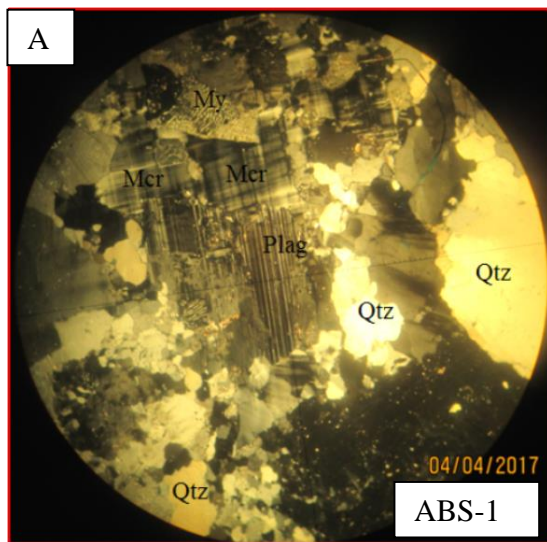
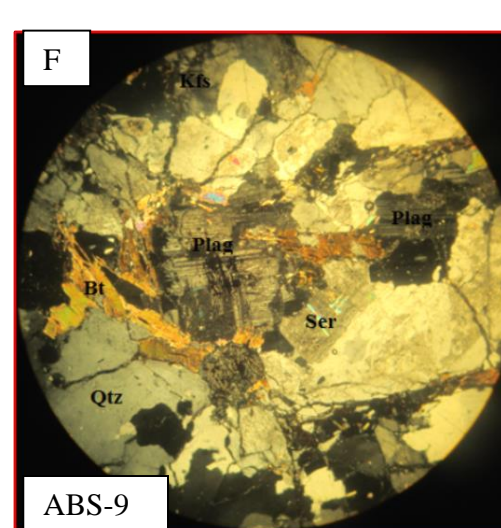
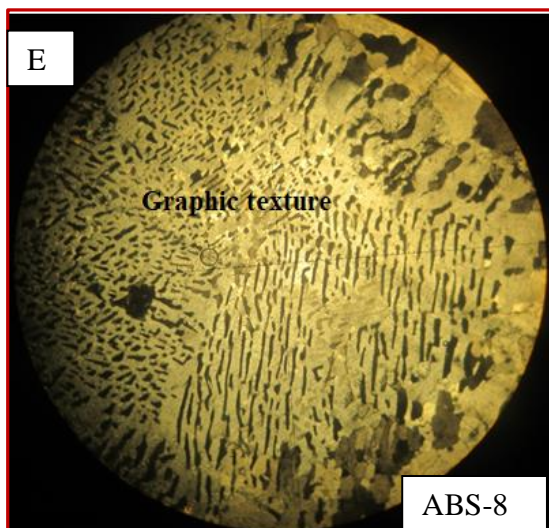
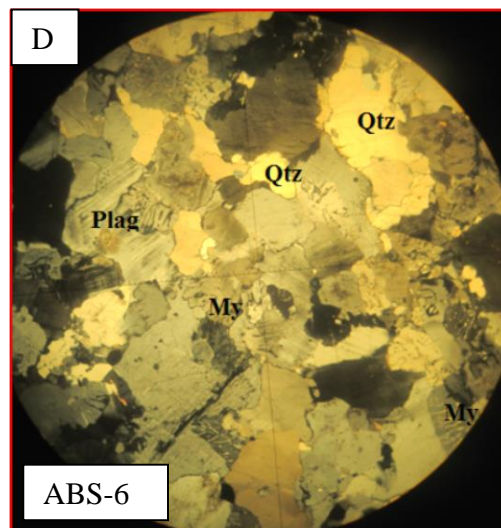
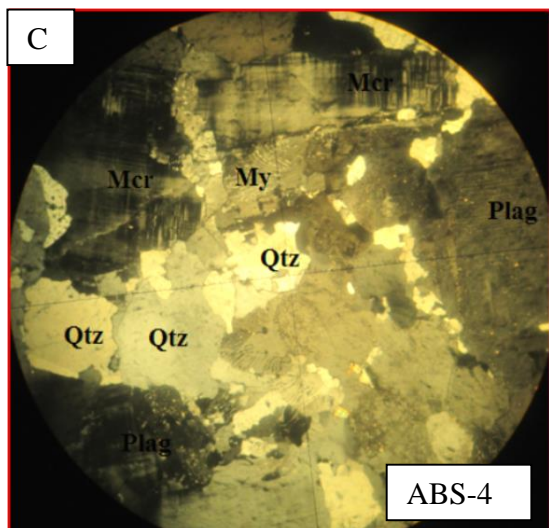


Figure 4.3. Quartz-Alkali feldspar-Plagioclase (Q-A-P) Classification Diagram of Granite, AG, alkali feldspar granite, SG, Syenogranite, MG, Monzogranite, AS,alkalifeldsapr granite, QS, quartzsyenite,QM, quartz monzonite, QD,quartz monzodiorite. Fields and nomenclature (after Streckeisen, 1976).





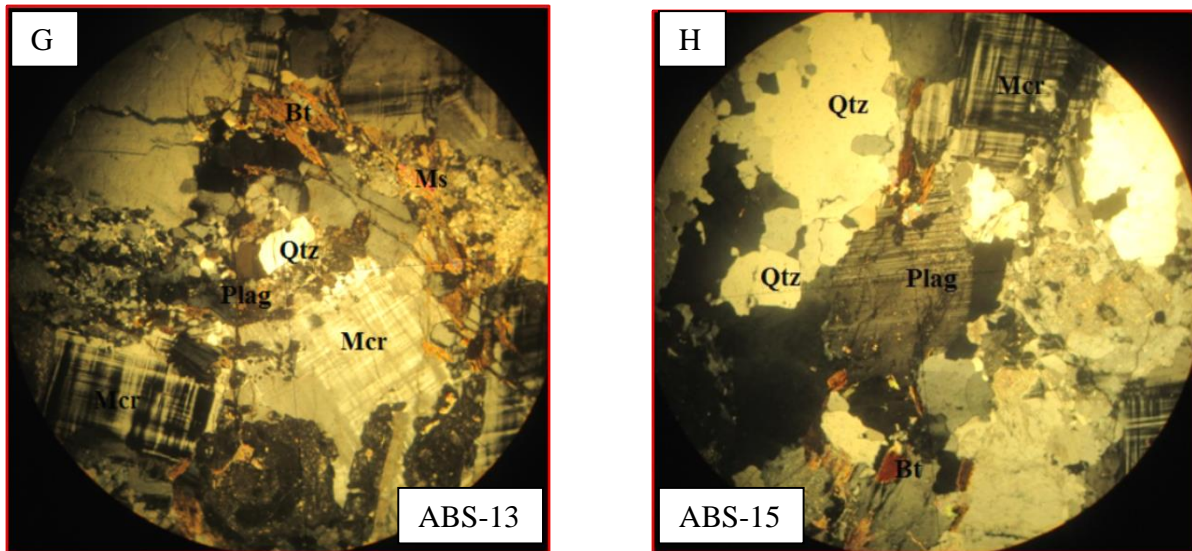


Figure 4.4. A-H: Microscopic photo-pictures of Granite unit. (A) part of granite unit with visible granular and myremekite texture. (B) large grain of biotite which is surrounded by quartz grains. (C) clear alteration of plagioclase to sercite. (D) Shows recrystallization of quartz grain. (E) clearly shows graphic texture. (F) large grain of plagioclase surrounded by biotite. (G) fine grained crystal of quartz and biotite are set in very large grain of K-feldspar and quartz crystals. (H) plagioclase crystals shows clear plysynthetic twinning.

4.2 Metamorphism

Both orthogneiss and granite of the study area were affected by regional metamorphism. The mineral assemblages and textural description of the rock units are given in the petrography portion of this research work. The analyzed gneiss sample ABS-10, ABS-11 and ABS-12 are compositionally dominated by K-feldspar (microcline), plagioclase and quartz. The dominance of felsic minerals and the chemistry of one sample from this unit typified as 77.4 wt. % SiO_2 indicates that the protolith of this rock is felsic igneous rock most probably granite. In contrary to this, sample ABS-7, ABS-16 and ABS-17 are compositionally dominated by hornblende, plagioclase and biotite; and the chemistry is characterized as 51.47-52.6 wt. % SiO_2 and relatively enriched by MgO , Fe_2O_3 and CaO . This indicates that the protolith of this rock is mafic igneous rock most probably basalt. The segregation of mafic and felsic rich compositional bands both at the mesoscale and in the thin section; the dominance of hornblende and plagioclase with

lesser amount of clinopyroxene and biotite and; the green brown pleochroic hornblende in the assemblage indicates that rock has been subjected to high grade metamorphism.

Mineral assemblage is generally very important to determine the grade of metamorphic rocks. The most dominant minerals of the rock units are shown below. The bold and underlined minerals are the critical minerals to evaluate the grade of metamorphism.

1. The Gneiss unit

❖ Mafic gneiss or hornblende-biotite gneiss

Hornblende + Plagioclase (andesine) + Clinopyroxene + Biotite + Quartz ± Chlorite ± Zircon ± Sphene ± Apatite + Opaque mineral.

❖ Granitic gneiss

K-feldspar (microcline) + Quartz + Plagioclase + Biotite + Muscovite/Sericite ± Chlorite ± Sphene + Opaque.

2. The granite unit

K-feldspar (microcline) + Quartz + Plagioclase + Biotite ± Muscovite/Sericite ± Zircon ± Opaque

In conclusion, these assemblages that are in bold and underlined minerals in the hornblende-biotite gneiss demonstrate that the rocks are experienced regional metamorphism in the upper amphibolite facies.

CHAPTER FIVE

5 GEOCHEMISTRY

5.1 INTRODUCTION

The main target of the geochemical data was to determine the palaeotectonic setting, petrogenetic evolution and the protolith of the basement rocks as well as to determine the behavior of elements during metamorphism. Ten samples are selected (6-granite and 4-gneiss) for whole rock geochemical analysis. The samples are carefully prepared in powdered form at the Institute of Geological Survey of Ethiopia. The powdered samples were sealed and packed into a plastic bag, and then submitted to the Australia Laboratory Science (ALS) for geochemical analysis in order to determine the concentration of major and trace elements.

Major elements including LOI (loss of ignition) were analyzed by Multi Element Inductively Coupled plasma 06 (ME-ICP06) whereas trace elements were determined by Multi Element Mass Spectrometry 81 (ME-MS 81) techniques in Ireland by Australian Laboratory Science. For detailed information on the procedure, precision, accuracy, and detection limits of ALS of ME-ICP06 and ME-MS81 analysis could be found at www.alsglob.com. All the major elements used in plots are recalculated, structured and presented on volatile-free base required for interpretation. To use the analyzed geochemical data for the purpose of this research the data have been integrated through different soft ware packages such as Microsoft Excel 2007, win rock and GCD kit version 3.00 soft ware packages are used to produce different geochemical diagrams. Having the analytical results for these samples, the results are interpreted in terms of both the major and trace elements. All the diagrams, descriptions and interpretations are according to the recalculated results presented on Table 5.1.

Table 5.1. Concentration of major and trace elements organized based on volatile free base recalculated values required for interpretation of the samples. Major oxides are in weight percent (wt %) and trace elements are in parts per million (ppm).

Granite							Orthogneiss			
Sample	ABS2	ABS4	ABS6	ABS8	ABS9	ABS15	ABS7	ABS12	ABS16	ABS17
			Major elements(ICP-AES)							
SiO ₂	68.8	73.55	74.98	76.13	73.85	77.54	52.6	72.26	51.97	51.47
TiO ₂	0.35	0.05	0.03	0.08	0.31	0.15	1.25	0.32	0.68	1.26
Al ₂ O ₃	17.5	14.9	13.8	13.24	13.3	12.04	17.62	14.82	18.3	14.89
Fe ₂ O ₃	3.19	1.15	1.13	1.43	3.56	1.69	10.79	2.88	8.38	11.36
MnO	0.07	0.02	0.01	0.01	0.03	0.02	0.16	0.04	0.13	0.18
MgO	0.62	0.09	0.02	0.03	0.41	0.15	5.01	0.52	7.28	6.71
CaO	1.69	0.09	0.98	0.84	0.87	0.83	8.59	1.89	8.16	9.63
Na ₂ O	3.8	3.8	3.38	3.51	3.08	2.8	3.23	4.32	2.99	3.54
K ₂ O	3.91	5.24	5.67	4.73	4.56	4.774	0.57	2.84	2.01	0.83
P ₂ O ₅	0.06	0.01	0.01	0	0.04	0.01	0.17	0.01	0.09	0.13
LOI	2.02	0.36	0.12	0.33	0.88	0.33	2.22	0.54	0.97	0.99
CaO/Na ₂ O	0.44	0.02	0.29	0.23	0.28	0.29	2.65	0.43	2.73	2.72
Na ₂ O/K ₂ O	0.97	0.72	0.59	0.74	0.68	0.59	5.66	1.52	1.49	4.27
K ₂ O/ Na ₂ O	1.02	1.37	1.67	1.34	1.48	1.70	0.18	0.66	0.7	0.23
Na ₂ O+K ₂ O	7.71	9.04	9.05	8.24	7.64	7.57	3.8	7.16	5	4.37
A/NK	1.88	2.02	1.94	1.20	1.44	1.22	3.03	1.40	2.57	2.17
A/CNK	1.31	1.17	1.02	1.04	1.23	1.05	0.82	1.30	0.77	0.71
Fe ₂ O ₃ /MgO	5.15	12.77	56.5	46.66	25.42	11.26	2.15	5.53	1.15	1.69
Total	99.99	98.9	100.01	100	100.0	100.00	99.99	99.9	99.99	100
Trace elements (ICP-MS)										

Sc	6	1	<1	1	2	2	28	3	12	34
V	37	<5	6	<5	29	12	265	12	123	252
Cr	10	20	10	10	10	20	30	20	60	190
Ni	5	7	3	9	16	5	34	8	106	62
Cs	1.97	2.31	1.4	1.29	1.78	1.65	0.36	1.25	5.82	0.37
Rb	145	141	133.5	145	152.5	109	9.5	62.1	88	12.1
Ba	1195	450	602	237	1115	1220	141	1405	226	93.3
Th	15.7									
	5	1.36	7.07	7.29	16.35	15.7	0.78	6.1	0.55	1.2
U	2.38	0.66	2.97	2.18	1.03	2.21	0.36	1.32	0.48	0.76
Nb	11.9	1.7	0.9	4.1	4.5	2.3	3	2.9	2.1	2.3
Ta	1.1	0.4	0.4	0.5	0.6	0.4	0.2	0.2	0.2	0.5
La	37.4	2	3.1	5	47.6	22.9	8.5	47.1	4.8	6
Ce	60.1	1.9	4.6	7.7	88.2	51.8	20.1	85.5	10.5	13.8
Pr	6.76	0.3	0.49	0.94	8.99	4.36	2.97	8.6	1.55	2.33
Pb	30	25	30	26	18	22	6	16	8	8
Sr	327	253	312	131	286	298	320	788	279	150
Nd	22.8	1.1	2	3.7	30.5	15.3	14.6	30.5	7.6	12.1
Sm	3.32	0.27	0.43	0.9	3.76	2.08	3.89	3.51	2.04	3.25
Zr	224	8	68	41	176	145	106	219	69	96
Hf	5.5	0.5	4.2	1.8	4.8	4	3	5.3	1.9	2.6
Eu	0.6	0.28	0.25	0.37	1.15	0.62	1.34	0.7	0.96	1.13
Gd	2.48	0.3	0.32	0.81	2.44	1.7	4.83	1.92	2.29	5.14
Tb	0.31	0.05	0.07	0.15	0.31	0.23	0.8	0.2	0.44	0.89
Dy	1.57	0.32	0.38	0.82	1.35	1.04	4.64	0.77	2.57	5.8
Ho	0.29	0.05	0.09	0.15	0.28	0.17	0.98	0.14	0.53	1.25
Er	0.79	0.18	0.34	0.52	0.79	0.49	2.81	0.47	1.43	3.64
Tm	0.12	0.03	0.06	0.09	0.09	0.05	0.42	0.07	0.21	0.52
Co	4	1	1	1	3	1	34	3	41	37
Y	8.1	1.6	2.6	25.4	5.2	7.3	4.7	4.1	13.9	30.4

Yb	0.69	0.2	0.37	0.52	0.69	0.34	2.44	0.48	1.35	3.32
Lu	0.11	0.02	0.09	0.08	0.1	0.06	0.34	0.08	0.19	0.51
total	137.34	7	12.59	21.75	186.25	101.14	68.66	180.04	36.46	59.68
Eu/Eu*	0.64	3.01	2.06	1.33	1.16	1.01	0.82	1.01	1.36	0.85
La _N /Yb _N	36.54	6.74	5.65	6.48	46.51	45.41	66.16	49.59	2.40	1.22
La _N /Sm _N	7.09	4.66	4.53	3.49	7.96	6.93	8.44	6.93	1.48	1.16
Gd _N /Yb _N	2.9	1.2	0.7	1.25	2.8	4.02	3.22	4.0	1.36	1.24
Y/Nb	0.68	0.94	2.88	6.19	1.15	3.17	1.56	1.41	6.61	13.21
La/Nb	3.14	1.17	3.44	1.21	10.57	9.95	2.83	16.24	2.28	2.60

5.2 Geochemistry of orthogneiss unit

5.2.1 Classification of orthogneiss

The FAM ternary diagram for classification of the orthogneiss of the study area put them in the calc-alkaline field. This indicates that the rock is formed at the subduction related environment.

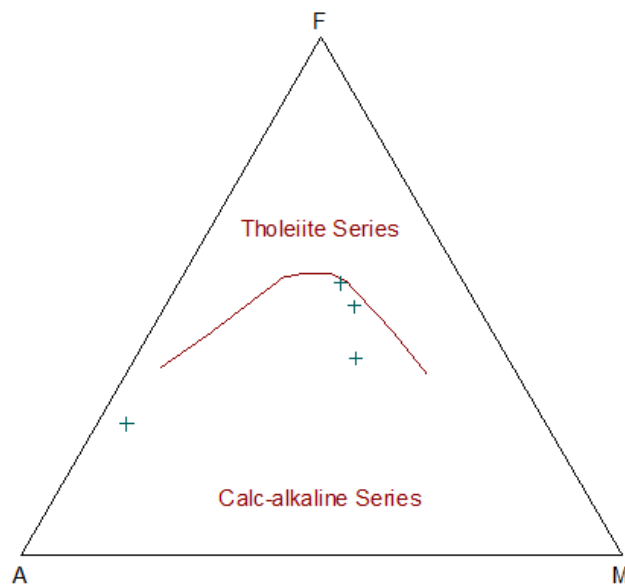


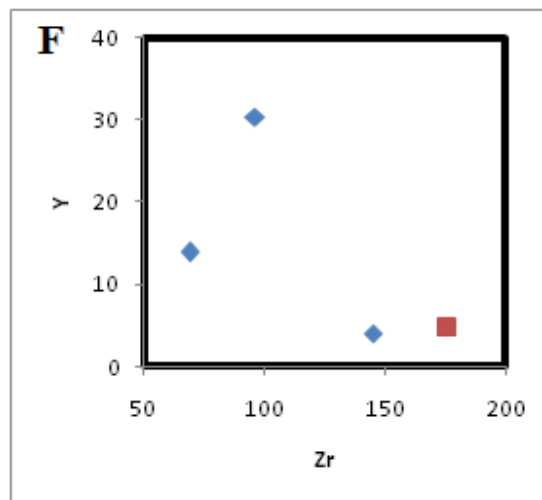
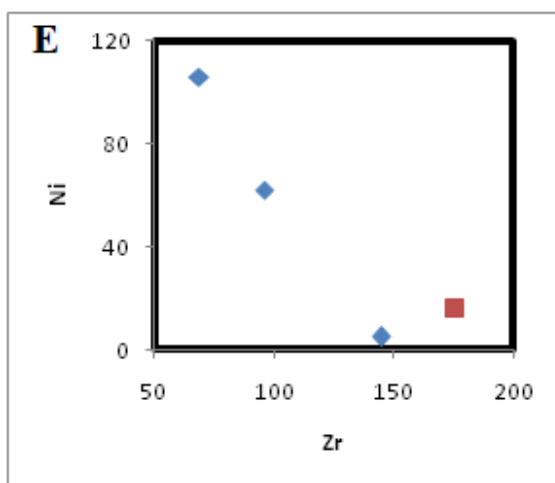
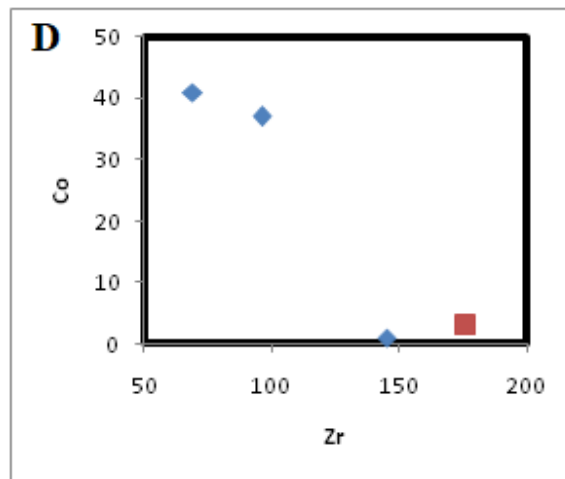
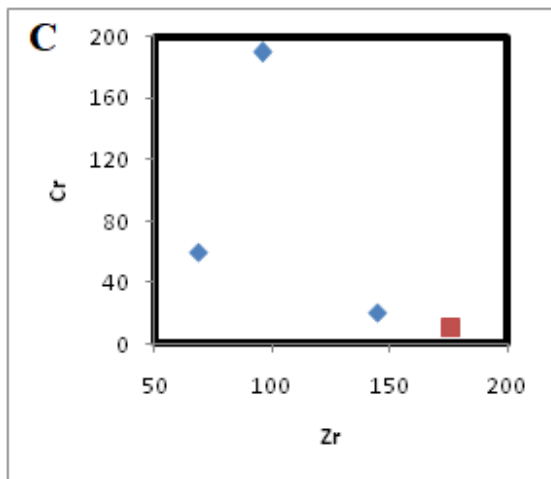
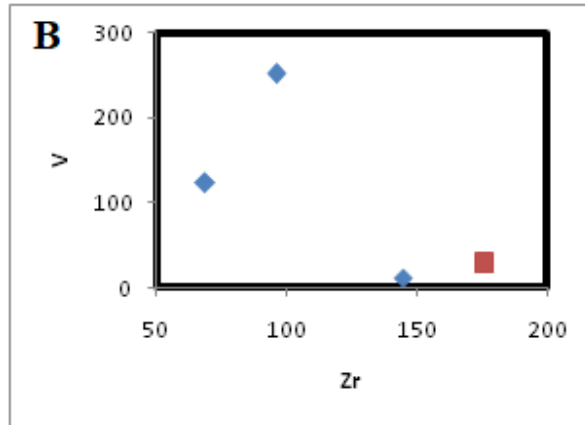
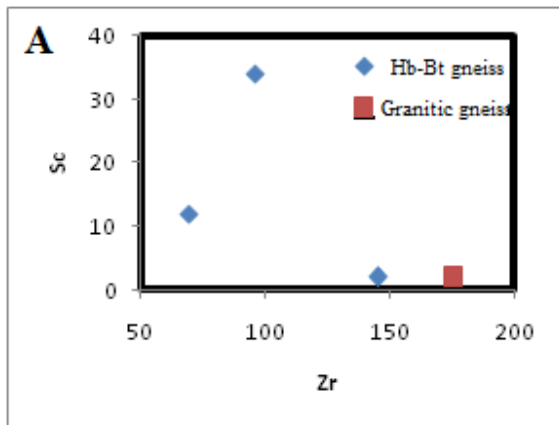
Figure 5.1. The AFM triangular diagram used to differentiate calc-alkaline series (CA) to tholeiitic series (TH) of orthogneiss rock of the study area: $A=Na_2O+K_2O$; $F=FeO_2+0.9Fe_2O_3$; $M=MgO$ using the criteria of Irvine and Baragar (1971).

5.2.2 Trace Element Geochemistry of Orthogneiss

5.2.2.1 Zr variation diagrams for trace elements

On the orthogneiss samples, the narrow range of SiO₂ and the upper amphibolite facies metamorphism to which this rock has been subjected has limited application of Harker variation diagrams to illustrate the path of crystallization. In addition to this, due to the ambiguity of the major element data, this study focuses only the information of the relatively immobile elements. Trace elements are plotted against Zr to evaluate their behavior and to establish their relative mobility of elements (Figure 5.2) because Zr is incompatible and immobile (Mulugeta Alene et al., 2000).

Nb, Th, U and Hf show apposite trend with Zr, this suggests that they have not been affected by metamorphism and hydrothermal alterations processes. Ni and Co show a negative trend with Zr. The negative trend of Co with Zr is indicative of that it is concentrated in early fractionating ferromagnesian minerals (Mulugeta Alene et al., 2000). The negative trend of Ni with Zr is due to fractionation of olivine, clinopyroxene and spinel in the early phase. V shows a scatter trend suggested that varying extent of ilmenite or titanomagnetite alteration (Mulugeta Alene et al., 2000). Rb and Sr show a broad scatter against zircon perhaps due to the mobility during the metamorphic processes.



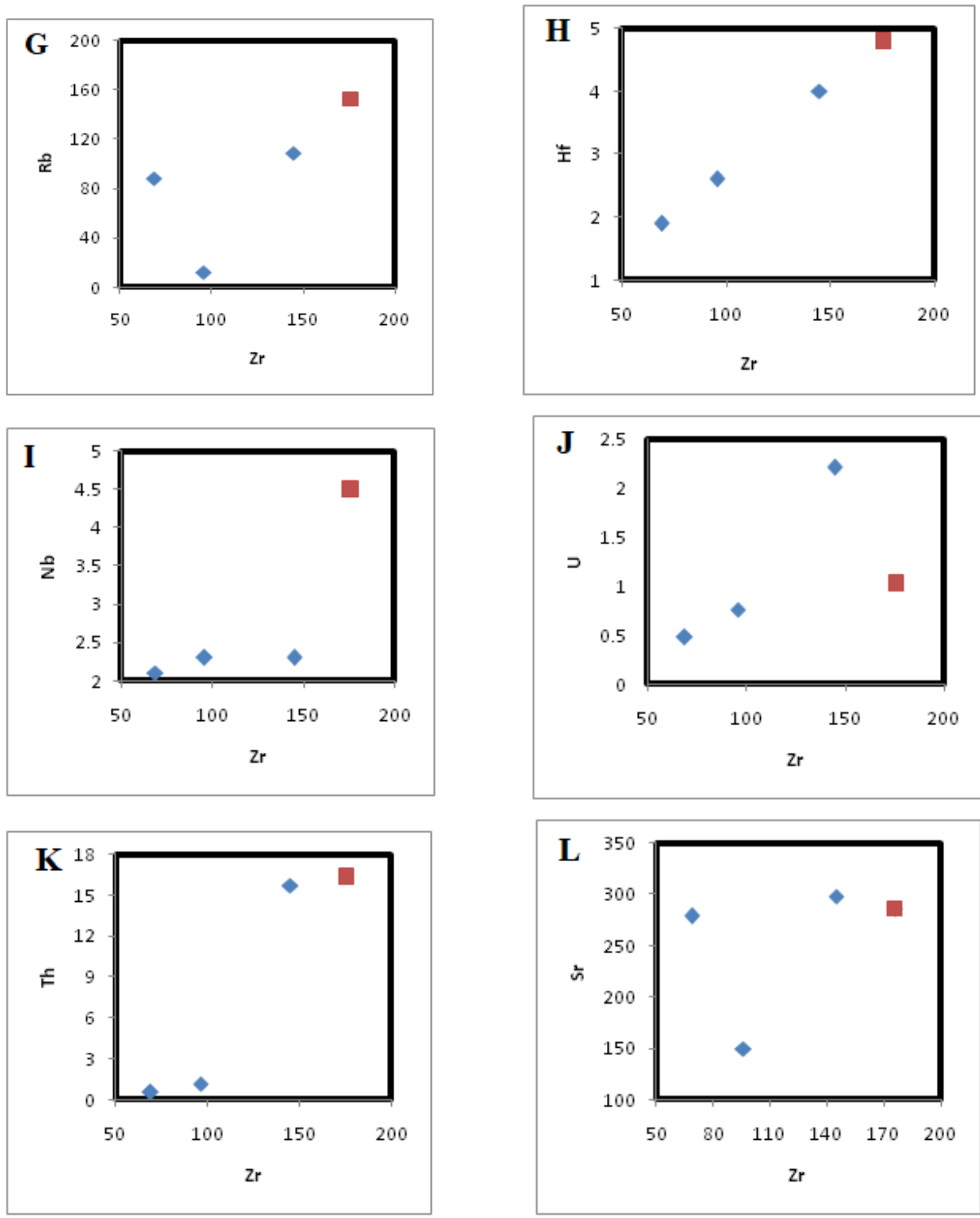


Figure 5.2. Zr variation diagrams for various trace elements (in ppm) of orthogneiss rock of the study area.

5.2.2.2 Petrogenesis of Orthogneiss

The orthogneiss of the study area has displayed two distinct REE patterns (Figure 5.3A). The REE abundance patterns of sample ABS-7 and ABS-12 show relatively strong light rare earth elements enrichment (LREE) and flat in heavy rare earth elements (HREE). The enrichment of LREE expressed by $[(La/Yb)_N]=66.16$ and $49.59]$ and the degree of HREE fractionation ranges between $[(Gd_N/Yb_N)= 3.22$ and $4]$. In contrary to this, samples ABS-16 and ABS-17 show flat REE patterns expressed by $[(La/Yb)_N]=2.40$ and $1.22]$ and the degree of HREE fractionation ranges between $[(Gd_N/Yb_N)= 1.36$ and $1.24]$. In addition to this, they show cross cutting pattern, implying that the contamination during fractional crystallization. Furthermore, the flat HREE patterns of samples ABS-7 and ABS-12 implying that garnet, which strongly partitions among the HREE, was not in equilibrium with the melt at the time of segregation (Winter, 2001). The flat REE pattern on samples ABS-16 and ABS-17 indicates that the REE abundances in these samples resulted from phase involving shallow fractionation (e.g olivine), which do not fractionate the REE (Winter, 2001). On sample ABS-7 and ABS-12 the relative stronger enrichment of LREE may imply strong fractionation process. Magma generation in the volcanic arc to back-arc transition environment may involve depleted MORB mantle source, more enriched OIB source mantle and subduction-zone component (partial melting of subducted oceanic lithosphere and the mantle wedge above the subducted lithospheric slab (Wilson, 1989). The calc-alkaline basalt is generated from subduction modified OIB source components (Thompson et al., 1984 as cited in Wilson, 1989). Furthermore, the low Th <3 ppm, La <16.8 ppm and low La/Sc (<1.1) and La/Y (<0.80) ratios could reflect provenance from an oceanic island arc setting (Bhatia and Crook, 1986 as cited in Mulugeta Alene et al., 2000). With the exception of granitic gneiss all samples have low Th <1.2 ppm, La <8.5 ppm and low La/Sc (<0.4) and La/Y (<0.3) ratios indicating that the rock is origin from oceanic island arc setting. From consistent negative slope in E-MORB and all OIBs are distinct from N-MORB (positive slope) and appear to originate in the lower enriched mantle reservoir, although very low degrees of partial melting may also produce LREE enriched melts from a primordial or slightly depleted source (Winter, 2001). In conclusion, the negative slope (Figure 5.3), the high $[(La/Yb)_N]$ ratio $=66.16$ to $2.40]$ (with an average of 34.28), the calc-alkaline affinity and their tectonic setting

(Figure 5.4) infer that the original rock of orthogneiss of the study area is originated from lower enriched mantle reservoir.

On the Primitive-mantle normalized multi-element variation diagram of orthogneiss (Sun and McDonough, 1989), (Figure 5.3B) display marked negative anomaly at Nb and P and marked positive anomaly at Rb, U, K, and Pb. The negative anomaly of Nb which is possibly due to the presence of a residual of Nb bearing minerals (Winter, 2001). In addition to this, the negative anomaly of Nb indicating that titaniferous minerals such as ilmenite or sphene were retained in the subducted oceanic crust (Wilson, 1989). Moreover, the large negative anomaly of Nb relative to the adjacent LIL elements is indicates high crustal contamination on this rock. Furthermore, the La/Nb ratio ranges between (2.28 to 16.24) indicates that, crustal contamination is high in this rock. The negative anomaly of P can be linked possibly due to the crystal fractionation of apatite during magmatic evolution. The positive anomaly of Rb, U, K, and Pb are an indicator of crustal contamination of magma. Furthermore, the positive anomaly of these elements could be linked to the mobility because these elements are highly mobile under secondary processes (hydrothermal activities, alterations and metamorphic processes). Island-arc and active continental margin basalts displaced to higher Th/Yb ratios, presumably reflecting the influence of subduction zone fluids enriched in Th in their petrogenesis (Wilson, 1989). The negative anomaly of Th in sample ABS-16 is due to low Th/Yb ratio (0.4) and implying that the subduction zone fluids are Th depleted. The slight LILE enrichment is the characteristics of either a subduction component or to a slight crustal contamination or both (Pearce, 1982 as cited Mulugeta Alene et al., 2000). Similarly The LIL elements of gneiss of the study area shows relatively strong enrichment of LIL elements this implying that the rock is derived by a subduction component or possibly with contamination of the continental crust or both. Over all, the analyzed samples are characterized by enrichment of large ion lithophile elements (Rb, Ba, Sr, Th, U and Pb) relative to high field strength elements (Nb, Y, Zr, Hf, Ti and Yb). Thus, this is probably due to their high mobility under the metamorphic conditions, alterations, weathering, erosion and hydrothermal activities.

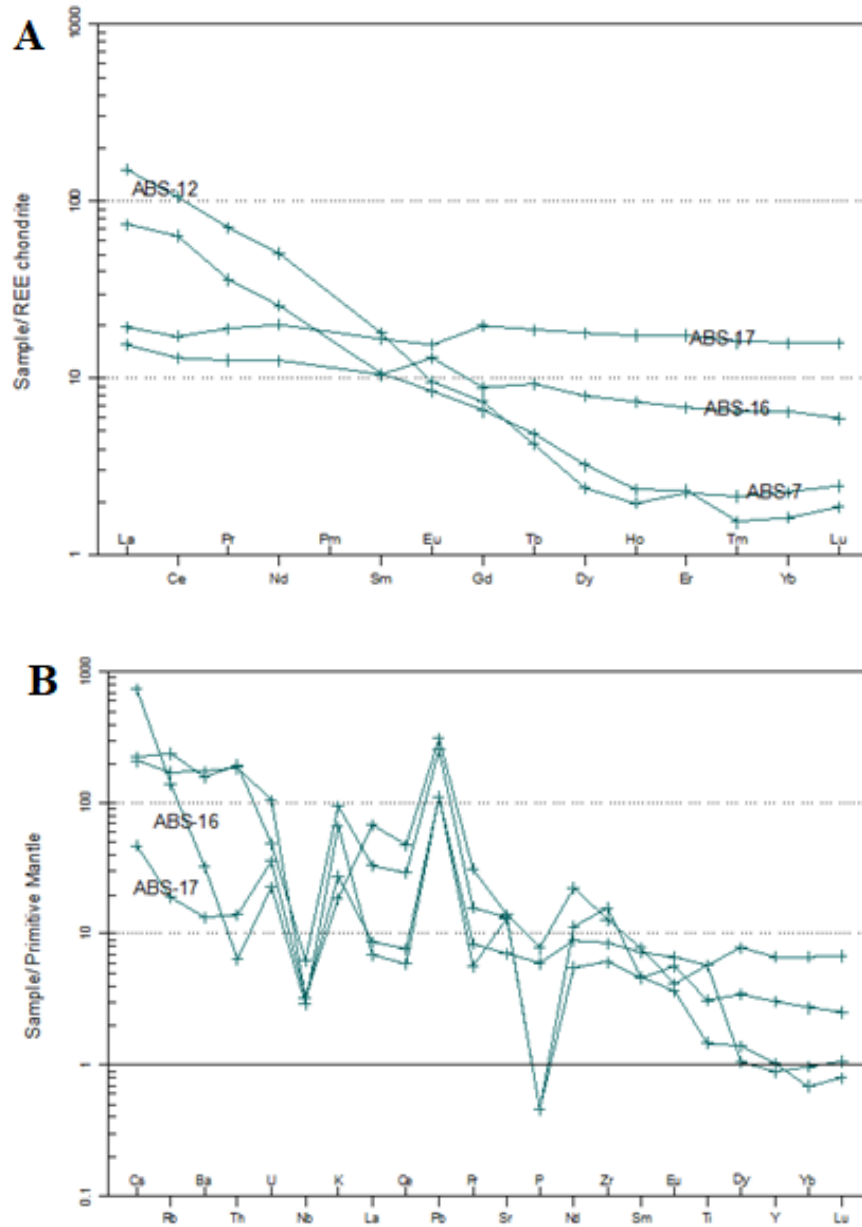


Figure 5.3.(A) Chondrite normalized REE pattern of orthogneiss rock of the study area. The concentration value of the rock samples are normalized to chondrite value determined by Boynton (1984) and (B) Primitive mantle normalized multi-element variation diagram for orthogneiss. The samples are normalized to primordial mantle of value determined by (Sun and McDonough, 1989).

5.2.2.3 Tectonic Setting of Orthogneiss

The study area has been affected by high-grade metamorphism. The interpretation of the tectonic setting of a metamorphosed and deformed terrain is difficult (B.Yibas et al., 2003). Gneiss of the study area is one of the deformed rocks affected by high grade metamorphism. This undoubtedly affected the chemistry of the LIL elements (such as K, Ba, Rb and Sr) which are highly mobile during metamorphism (B.Yibas et al., 2003). Therefore, the interpretation of the tectonic setting for this rock should largely depend on elements of high field strength elements (HFS). These elements are effectively immobile during metamorphism. The elements used in this discrimination diagram are (Zr, Th and Nb) are generally immobile under this condition. Moreover this, this diagram also separates tholeiitic and calc-alkaline magma series. The bulk of the gneiss samples plotted on Zr-Th-Nb (Figure 5.4) three samples plotted in the field of destructive plate margin i.e. falls inside calc-alkaline basalt field (CAB) and one sample plot on the margin of island arc tholeiitic (IAT), indicating that the original rock of the gneiss has been erupted in volcanic arc setting and has calc-alkaline and tholeiitic magma affinity.

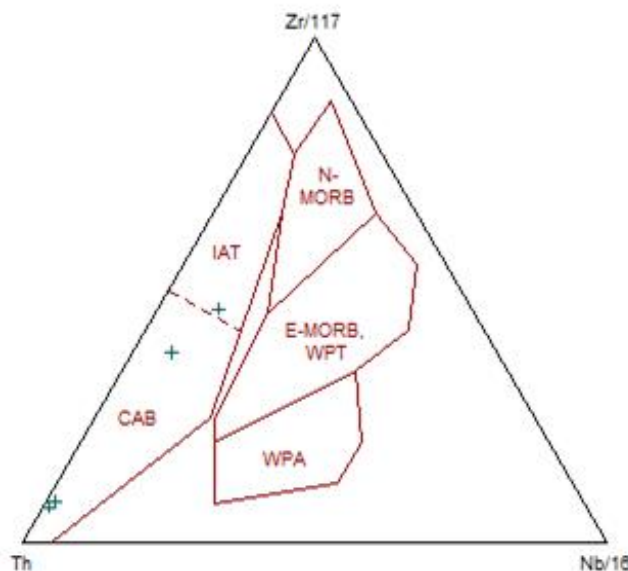


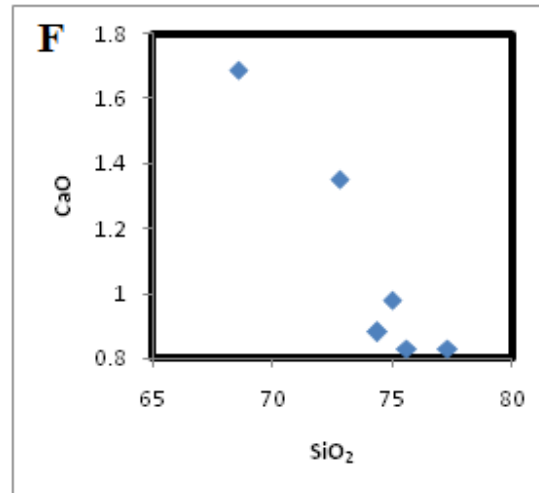
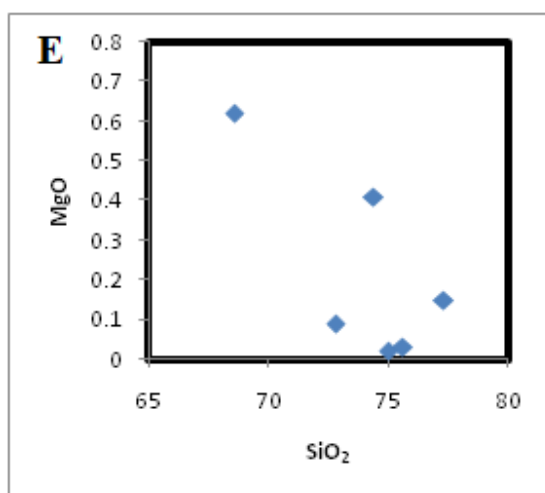
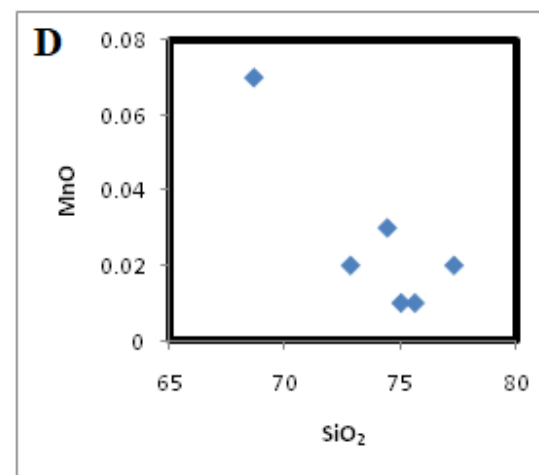
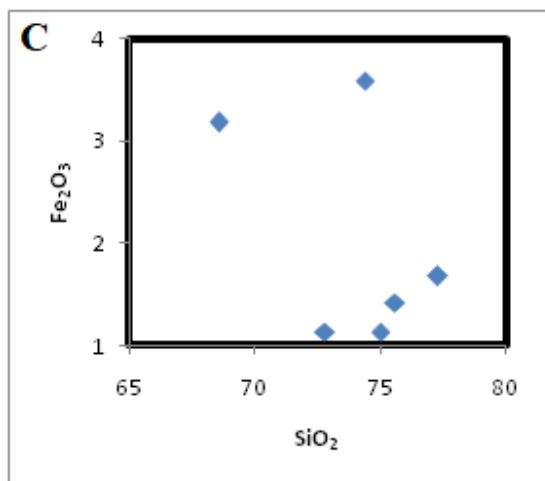
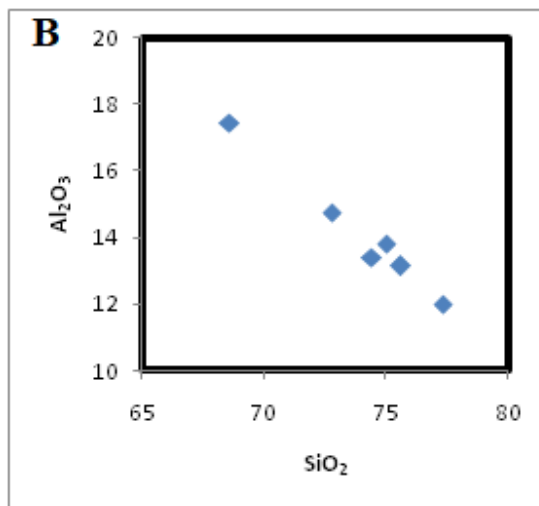
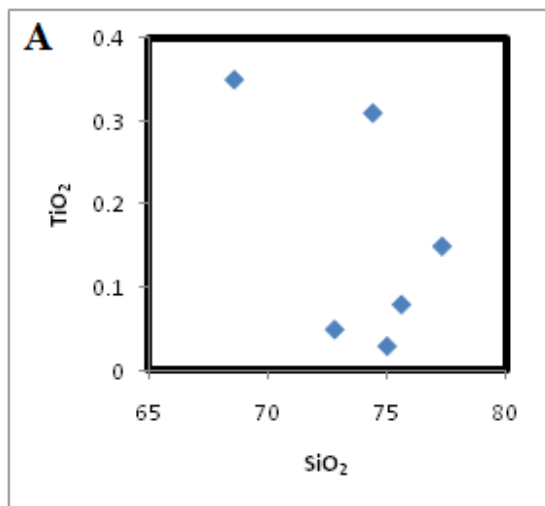
Figure 5.4. Zr-Th-Nb triangular diagram for gneiss of the study area (after Wood, 1980). Note N-MORB= Normal mid oceanic ridge, E-MORB= Enriched mid oceanic ridge, WPA= within plate tholeiites, IAT= Island arc tholeiites CAB= Calc alkaline basalts.

5.3 Geochemistry of Granite

5.3.1 Major Element Geochemistry of granite

Major elements are elements which are predominate in any rock analysis. They are Si, Ti, Al, Fe, Mn, Mg, Ca, Na, K and P, and their concentrations are expressed as wt. % in oxide form (Rollinson, 1993). This helps to visualize the property of those oxides as the function of the greater silica variability in felsic magmas. In addition to this, major element data are used for rock classification purpose and they have limited application in understanding the petrogenesis evolution since they are sensitive to weathering, hydrothermal fluid activities and metamorphic processes (Rollinson, 1993).

The Harker variation diagrams (Figure 5.5 A-I) defines a trend of granite rock. The plot is prepared for major elements on selected granite samples to refine the variation that is shown on the general major element variation diagrams of the rock. The analyzed granite samples listed in Table 5.1 are characterized by high SiO₂ and Al₂O₃ content 68.6-77.3 wt % ; 12.04-17.5 wt% and lower content of other major oxides. Such as, Fe₂O₃ 1.13-3.59 wt. %, MgO 0.02-0.62 wt. % and CaO 0.83-1.69 wt.%. The high SiO₂, Na₂O+K₂O and Al₂O₃, and low MgO, Fe₂O₃ and CaO concentrations imply that the primary magma was derived from partial melting of the lower crust (Zhu et al., 2009). In addition to this, the high SiO₂ 68.6-77.3 Wt % , total alkali concentrations Na₂O + K₂O 7.57-9.04 , and Fe₂O₃/MgO ratios 5.15-56.5 suggests that the studied granite rock experienced significant magmatic differentiation. The low CaO/Na₂O ratios (0.02-0.44), and higher K₂O/ Na₂O ratios (1.02-1.70) suggest that the samples are K₂O and enriched, with the predominance of K₂O over Na₂O. Overall, the studied samples (Figure 5.1) show negative trend on MgO, MnO, Al₂O₃, Na₂O and CaO with SiO₂, whereas the Fe₂O₃ and TiO₂ shows a scattered negative correlation with SiO₂. The K₂O show positive correlation with SiO₂. The negative trends of MgO, MnO, Al₂O₃, Na₂O, and CaO with SiO₂ indicates that, the normal differentiation of magma or crystal fractionation process in the evolution of the granite rock. The positive trend of K₂O with SiO₂ may reflect simultaneous removal of these two oxides from the magma most probably accomplished by fractionation of K-bearing minerals (mica). Primary magma is characterized by high MgO content > 6wt.%, Ni 250 -300 ppm and Cr 500- 600 ppm (Wilson, 1989). The low MgO content <0.62 wt %, Cr 10-20 ppm, Ni 3-16 ppm and Co 1-4 ppm in all the samples indicates that they were derived from highly differentiated magma source.



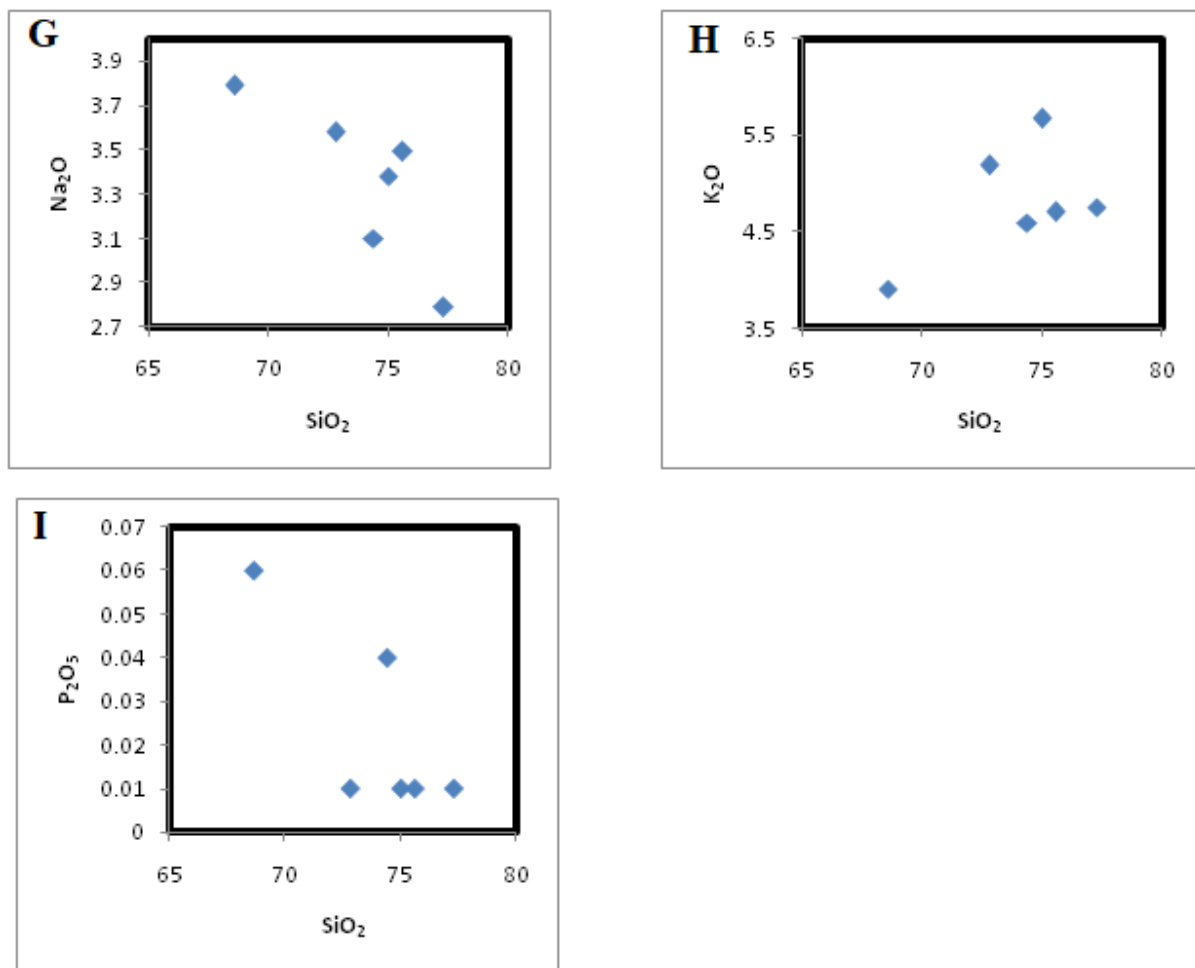


Figure 5.5. Harker variation diagrams for the granite rock of the study area. The major element concentrations are volatile free base and expressed by wt. %.

5.3.1.1 Classification of Granite

Based on the two chemical classification diagrams, SiO₂ versus Na₂O+K₂O (Figure 5.6A) adopted from Middlemost (1994) and Ab-An-Or (Figure 5.6B) adopted from O'Connor (1965), all the samples fall in the granite field. Alumina Saturation index diagram proposed by Shand (1943) (Figure 5.6C) shows that the granite of the study area are exclusively peraluminous as indicated by the values of A/CNK ranges between 1.02-1.31 and values of A/NK ranges between 1.20-2.02 where A: Al₂O₃, CNK: CaO+ Na₂O+K₂O respectively. It is worth noting that these values greater than one (see Appendix 3) meaning that they are peraluminous. The granite was also plotted on K₂O Vs SiO₂ proposed by Peccerillo and Taylor (1976) (Figure 5.6D) to determine the magmatic series of the rock. According to this diagram all the samples lie in High-K Calc-Alkaline magma affinity. The high-K nature of the granite of the study area could be a result of fractional crystallization and assimilation of crustal material during the upward movement of the magma to its emplacement place (Tesfaye Kebede et al., 1999).

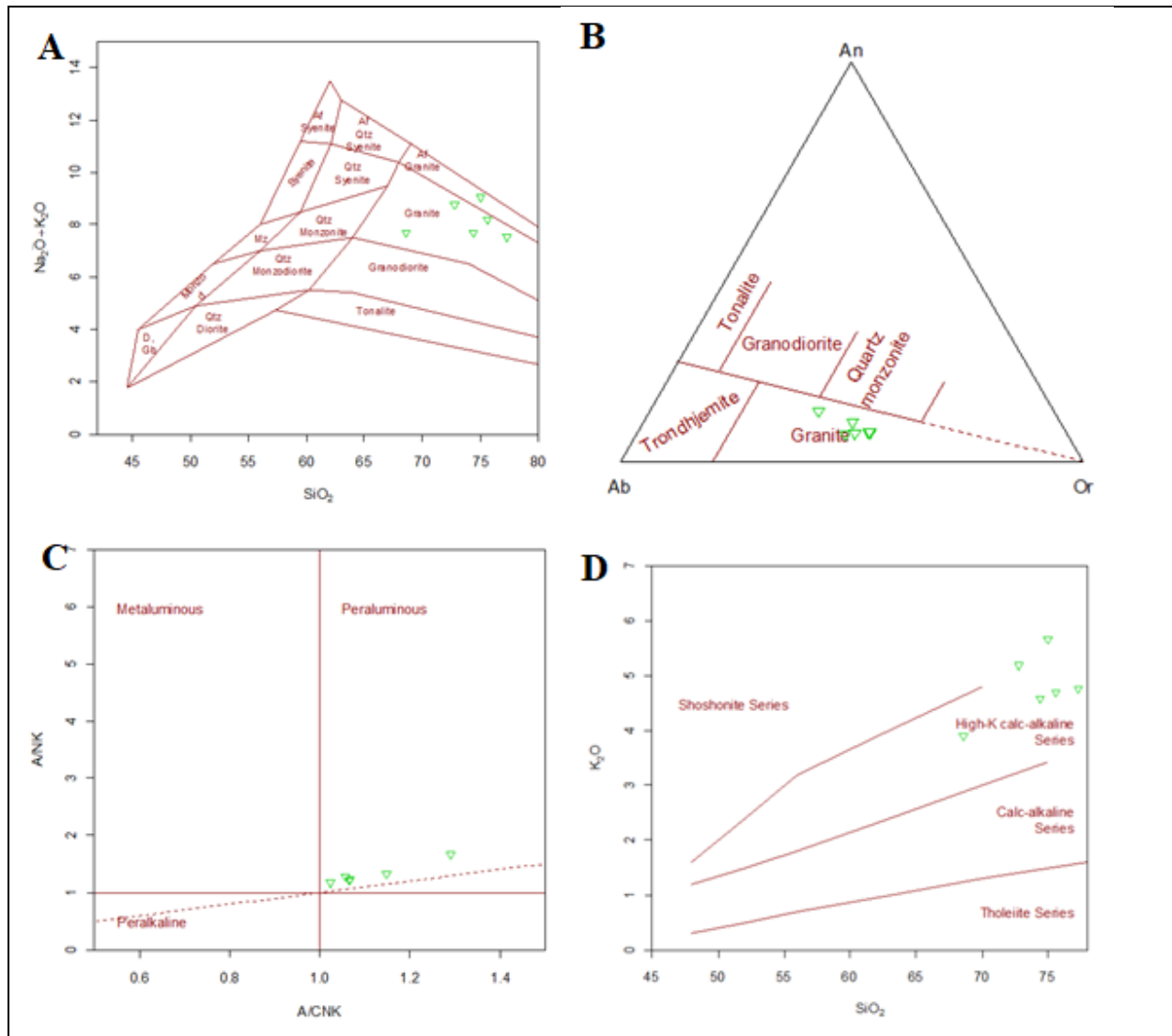


Figure 5.6. (A) Chemical classification diagram for granite rock of the study area based on TAS (SiO_2 Vs. $\text{Na}_2\text{O} + \text{K}_2\text{O}$) of (Middlemost, 1994), (B) Chemical classification diagram for granite rock of the study area based on Feldspar triangle (Ab-An-Or) of (O'Connor, 1965), (C) A/CNK ($\text{Al}_2\text{O}_3 / (\text{CaO} + \text{Na}_2\text{O} + \text{K}_2\text{O})$) Vs A/NK ($\text{Al}_2\text{O}_3 / (\text{Na}_2\text{O} + \text{K}_2\text{O})$) (in molar proportions) plot (Shand, 1943) discriminating metaluminous, peraluminous and peralkaline compositions of the granites rock samples of the study area and (D) The K_2O vs SiO_2 plot showing H-K nature of the rock (after Peccerillo and Taylor, 1976).

5.3.2 Trace Element Geochemistry of Granite

Trace elements are an element which is present in rock concentration is less than 0.1 wt. % and their concentration is expressed by in parts per million (ppm) or more rarely by parts per billion (ppb) (Rollison, 1993). Sometimes trace elements will form mineral species in their own right but most commonly they substitute for major elements in the rock forming minerals (Rollison, 1993). It can also be defined as elements that are not stoichiometric constituents of phases in the system of interest (White, 2013). In this study trace elements are used in order to understand the petrogenesis and palaeotectonic setting of both granite and gneiss rock by plotting chondrite normalized REE pattern, primordial mantle normalized spider diagram and trace element tectonic setting discrimination diagrams respectively.

5.3.2.1 Petrogenesis of Granite

The REE concentration of granite is normalized by chondrite according to Boynton (1994) is shown in (Figure 5.7A). On the chondrite normalized REE abundance plot, the analyzed samples relatively show slight to moderate enrichment of light rare earth elements (LREE) and a rather flat heavy rare earth elements (HREE) patterns (Figure 5.7A). Sample ABS-2, ABS-9 and ABS-15 are show relatively moderate LREE enrichment $[(La/Yb)_N$ 36.54, 46.51, 45.41] respectively. However, sample ABS-4, ABS-6, ABS-8 show slight LREE enrichment $[(La/Yb)_N$ (6.74, 5.65, 6.48]. the diagram show that the heavy REE are very weakly fractionated with almost flat pattern $[(Gd_N/Yb_N) = 0.7$ to 4.02]. In general the enrichment in the LREE ranges between $[(La/Yb)_N$ (5.65 to 46.51] relative to the HREE. According to winter (2001) increasing of LREE enrichment on sample ABS-9, ABS-2, and ABS-15 were indicating that the country rock is older and thicker. Eu/Eu^* is a measure of europium anomaly and the value less than one indicates negative anomaly (Rollinson, 1993). With the exception of one granite sample ABS-2 which show a negative Europium anomaly $[(Eu/Eu^*)$ 0.64], all the remaining samples show positive Europium anomaly $[(Eu/Eu^*)$ 1.01 to 3.01]. Europium anomalies are chiefly controlled by feldspars, particularly in felsic magmas for Eu^{+2} is compatible in plagioclase and potassium feldspar, in contrast to the Eu^{+3} REE, which are incompatible (Rollinson, 1993). Thus the negative Eu anomalies (Eu/Eu^*) is due to either removal of feldspar from the felsic melt by crystal fractionation or the partial melting of the rock in which feldspar is retained in the source (Rollinson, 1993). The positive Eu anomaly (Eu/Eu^*) could be attributed to a combination of the

larger degree of Eu fractionation and the amount of cumulus plagioclase in the magma (B.Yibas et al., 2003). Rollinson (1993) stated that REE patterns of the rocks show enrichment in LREE and depletion in HREE when the melting percentage decreases. However; the REE patterns of granite of the study area shows only slight to moderate variation between the abundances of LREE and HREE which indicates that there was slight to moderate percentage of melting. The flat HREE patterns of all samples may suggests a garnet free source, which reflects the shallower slab dip and lesser depth of magma genesis (Winter, 2001). The majorities of the orogenic granitoids originate at the crust-mantle interface and involve crust and mantle derived components (Barbarin, 1990). In addition to this, the crustal granitoids are produced by melting of crustal material due to tectonic thickening of the continental crust in an orogenic belt (Barbarin, 1990). Furthermore, crustal granitoids are calc-alkaline and peraluminous, mixed-origin granitoids are calc-alkaline and metaluminous whereas mantle derived granitoids are alkaline or peralkaline. The large negative anomaly of Nb, the large positive anomaly of Pb is a typical characteristic of granite melt derived from continental crust. Therefore the combination of negative Nb and positive Pb anomaly with calc-alkaline affinity and peraluminous nature may indicate that the granite of the study area originated from partial melting of continental crust.

On the primitive-mantle normalized trace element plots of granite (McDonough and Sun, 1989), (Figure 5.7B) all samples display marked troughs at Nb, P and Ti and peaks at Rb, K, Pb and Sr respectively. The large negative anomaly of Nb, P and Ti are possibly due to the fractionation of Ti-apatite bearing phase (Wilson, 1989). Nb trough is a characteristic of subduction zone magma (Winter, 2001). In addition, negative Nb anomalies are also characteristic of the continental crust and may be an indicator of crustal involvement in the magma processes (Rollinson, 1993). Furthermore, the positive anomaly of Pb is a typical characteristics continental crust. The enrichment of incompatible elements such as Rb, K, Pb and Sr is probably due to strong fractionation processes. A similarly high LIL/HFS pattern is now recognized as a distinctive feature of subduction zone magmas (Winter, 2001). The studied granite samples are characterized by enrichment of LILE in contrast to more compatible HFSE which intern an indicative of arc-related magmatism/ subduction-related and or calc-alkaline differentiation trend (Pearce et al., 1984). Moreover, more mobile LIL element concentrations may be controlled by aqueous fluids in subduction related setting but these elements are concentrated in

the continental crust and can also used as an indicator of crustal contamination of magma (Rollinson, 1993). The analyzed samples show cross cutting pattern on primitive-mantle-normalized trace element plots, implying the presence of crustal contamination during fractional crystallization.

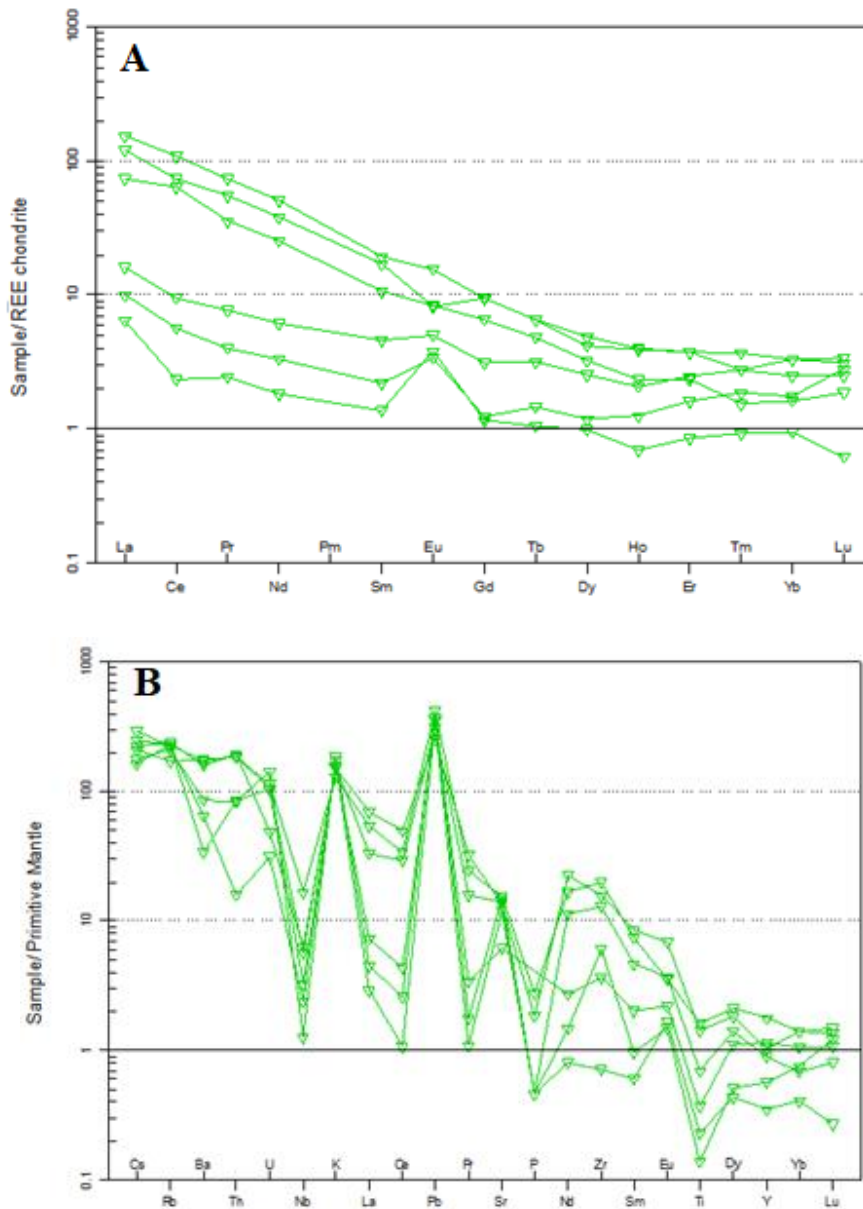


Figure 5.7. (A) Chondrite normalized REE pattern for granite rock of the study area. The concentration value of the rock samples are normalized to chondrite value determined by Boynton (1984) and (B)

Primitive mantle normalized mult-element variation diagram for granite rock of the study area. The samples are normalized to primordial mantle of value determined by (Sun and McDonough, 1989).

5.3.2.2 Tectonic Setting of Granite

The first systematic study of the geochemistry of granites from the known tectonic setting was made by Pearce et al. (1984 as cited in Rollinson (1993), who defined the term granite very loosely as any plutonic rock containing more than 5% of modal quartz. Classification of granitoids based on tectonic environments gives a conceptual framework to understand the occurrence of granitoids and their genesis (Winter, 2001). Tesfaye Kebede et al. (1999, 2001b) states that, beside the A-type granitoids volcanic granitoids and syn-collisional leucocratic granites are reported from the western Ethiopia. The granite of the study area has been subjected to very low degree of alteration, classification and tectonic setting discrimination is based on the immobile elements. In the classification of such rock types, we have to use elements such as Y, Yb, Rb, Nb, Ta and Hf to discriminate between granites from different tectonic settings (Pearce et al., 1984 as cited in Rollinson, 1993). Regardless of its mobility Rb has been used on the assumption that the effect of element mobility are much less in the granitic rock than in the basic rock, mostly because granitic rocks are generally less altered (Rollinson, 1993). Based on the tectonic setting (Pearce et al., 1984) granites are classified into oceanic ridge granite (ORG), within plate granite (WPG), volcanic arc granite (VAG) and Collisional granite (COLG). Taking all the tectonic setting discrimination diagrams of the granite Pearce et al. (1984) all the analyzed samples plotted on two major tectonic settings; the volcanic arc granite (VAG) and Syn-collisional granite (syn-COLG). On the Rb-(Y+Nb) (Figure 5.8A) two granite samples plotted on the syn-COLG field and four granite samples plotted on the volcanic arc granite field. Similarly, on the Ta-Yb binary plot (Figure 5.8D) one granite sample plotted on the syn-COLG field and five granite samples are plotted on the volcanic arc granite. On the other hand, on the Nb-Y and Rb-(Yb+Ta) on (Figure 5.8 B and C) all the granite samples are plotted on the volcanic arc granite field. In conclusion according to all the above tectonic setting diagrams adopted by Pearce et al. (1984) all the analyzed samples are plotted on the VAG field and Syn-COLG field, indicating that the granite of the study area erupted on VA and Syn-COLG environment. In addition, their enrichment in K, Rb, Th, Ce and Sm compared to Nb, Hf, Zr, Y and Yb is characteristic of volcanic arc (possibly I-type) granites (Pearce et al., 1984 as cited in

Mulugeta Alene et al., 2000). Such granite tectonic setting variation may be attributed to fractionation processes and /or varying contribution of different sources (cf.Landenbereger and Collins,1996; Forster et al.,1997 as cited in Tesfaye Kebede and Kobrel.C, 2003).

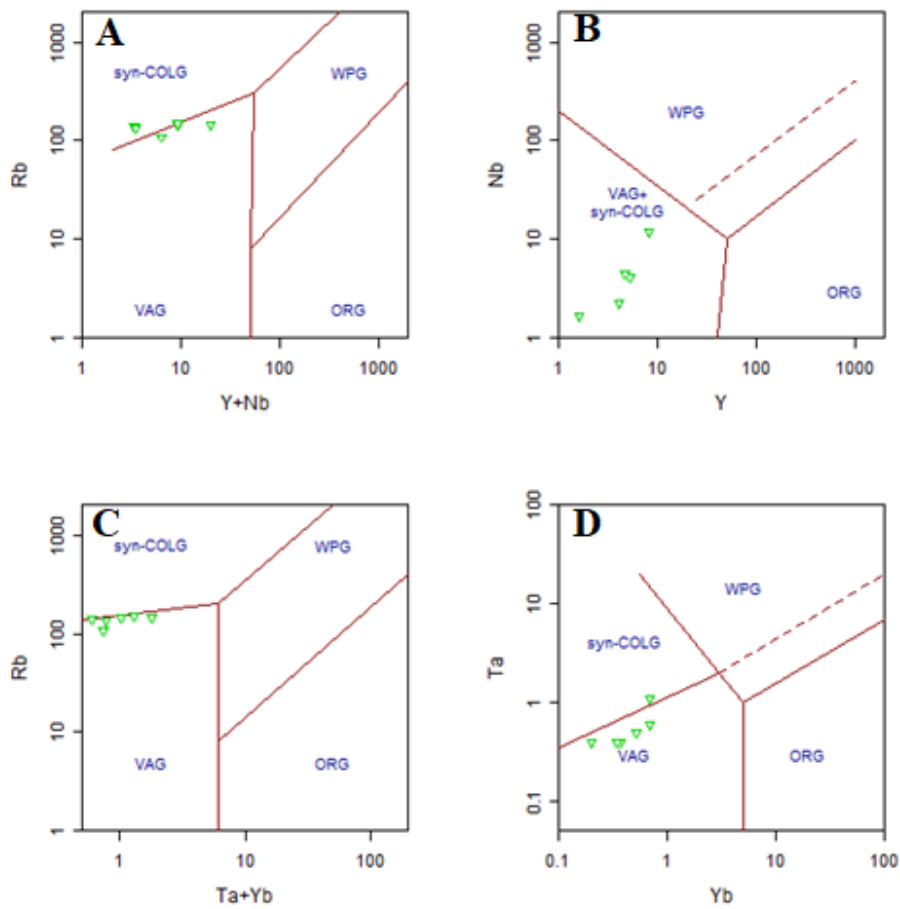


Figure 5.8. Nb-Y, Ta- Yb, Rb- Yb+ Ta and Rb-Y+Nb discrimination diagrams for granite rock of the study area (Pearce et al., 1984). Note syn-COLG= Syn-collision granites, VAG =Volcanic arc granite, WPG = Within-plate granites and ORG= Ocean ridge granites.

CHAPTER SIX

6 CONCLUSION AND RECOMMENDATION

6.1 CONCLUSION

Based on the integrations of petrographic and geochemical data of the granite and gneiss rocks of the study area, the following conclusions can be drawn:

1. The study area is a part of high grade metamorphic terrain of Western Ethiopian Precambrian shield (WES) that is dominated by both high grade metamorphic and Precambrian intrusive rock. The high grade metamorphic rock is represented by orthogneiss and the intrusive rock is represented by granite.
2. The segregation of mafic and felsic rich compositional bands both at the mesoscale and in the thin sections; the dominance of hornblende and plagioclase with lesser amount of clinopyroxene and biotite and; the green brown pleochroic hornblende in the assemblage indicates that the orthogneiss of the study area has been subjected to high grade metamorphism that belong to upper amphibolite facies conditions.
3. Petrographic study and geochemical analysis of the granitic gneissic samples (sample ABS-10, ABS-11 and ABS-12) are compositionally dominated by k-feldspar, plagioclase and quartz. The dominance of felsic minerals and the chemistry of one sample from this unit typified as (77.4 Wt. % SiO₂) and relatively low content of MgO, Fe₂O₃ and C indicates that the protolith of this rock is felsic igneous rock may be granite. In contrary to this, sample ABS-7, ABS-16 and ABS-17 are compositionally dominated by hornblende, plagioclase and biotite and the chemistry is typified 45-55 wt% SiO₂ and relatively enriched by MgO, Fe₂O₃ and CaO. This indicates that the protolith of this rock is mafic igneous rock most probably basalt.

4. The over all geochemical characterstics of the orthogneiss rock of the study area display calk-alkaline series. The descrimination diagram of after Wood (1980) suggests that the original rock of orthogneiss of the study area were developed in the volcanic arc tectonic setting. Furthermore,the rock shows two distinct REE patterns, (1) relatively slight to moderate light rare earth elements enrichment (LREE) and flat in heavy rare earth elements (HREE) and, (2) over all flat REE pattern.
5. Petrographicaly the studied granite samples are mainly composed of K-feldspar (microcline), quartz, plagioclase, biotite and muscovite/sericite, and accessory minerals such as zircon, chlorite, apatite and opaque also constitute the rock unit. They all fall on granite field of after Streckeisen (1979) classification diagram based on modal analysis
6. The overall geochemical characteristics of the granite of the study area displays high K-Calk-Alkaline series and peraluminous affinity. The descrimination diagrams of Rb-(Y+Nb), Ta-Yb, Rb-(Y+Nb) and Nb-Y granites suggested that the granite were developed in volcanic arc and syn-COLG tectonic setting environment. Moreover, chondorite normalized REE abundance plot, the granite rock relatively show slight to moderate enrichment of light rare earth elements (LREE) and a rather flat heavy rare earth elements (HREE) patterns, typical of intrusion in a destructive plate margin.

6.2 RECOMMENDATION

This work is targeted on studies the petrographic and geochemical study of basement rocks from the Abay (Blue Nile) river gorge area. The area is very narrow in terms of sampling and may not represent the wide variety of rocks, structures and processes of the area. For better understanding of the petrogenetic evolution, tectonic and metamorphic history of the area further studies with field data, sample on analytical data is required. Therefore, the following studies will be recommended:

- Large scale mapping, more detailed sampling (higher number of samples), structural mapping, field work and geochemical data with more samples are needed.
- Stratigraphic correlation and boundary relationship of the high grade basement rocks and Precambrian intrusive rocks are not differentiated yet. Large scale mapping is recommended to identify the undifferentiated unit.
- Using isotope data as proxies for correlation and radiometric data is very important for making Stratigraphic correlation.

REFERENCES

- Abbate, E., Bruni, P. and Sagri, M. (2015). *Geology of Ethiopia: A Review and Geomorphological Perspectives*, Springer Netherlands, 33-64pp.
- Abdelsalam, M.G. and Stern, R.J. (1996). Sutures and shear zones in Arabian-Nubian Shield. *Journal of African Earth Sciences*, **23**(3): 289–310.
- Aberra Mogessie, Kebede Belete, Hoinkes, G. and Ettinger, K. (1999). Platinum mineralization in the Yubdo ultramafic rocks, western Ethiopia. **In:** Mineral Deposits: Process to Processing, **1**:751–754.
- Allen, A. and Gebremedhin Tadesse (2003). Geological setting and tectonic subdivision of the Neoproterozoic orogenic belt of Tulu Dimtu, western Ethiopia. *Journal of African Earth Sciences*, **36**:329-343.
- Allen, A. and Gebremedhin Tadesse (2005). Reply to Discussion of geological setting and tectonic subdivision of the Neoproterozoic Orogenic Belt of Tulu Dimtu, Western Ethiopia. *Journal of African Earth Sciences*, **41**: 333-336.
- Asfawosson Asrat, Barbey, P. and Gleizes, G. (2001). Precambrian geology of Ethiopia: a review. *Africa Geoscience Review*, **8**(3):271-288.
- Asfawossen Asrat and Barbey, P. (2003). Petrology, geochronology and Sr–Nd isotopic geochemistry of the Konso pluton, south-western Ethiopia: implications for transition from convergence to extension in the Mozambique Belt. *Int. J. Earth. Sci. (Geol Rundsch)*, **92**:873-890.
- Avigad, D., Stern, R.J., Beyth, M., Miller, N. and Mc Williams, M.O. (2007). Detrital zircon U–Pb geochronology of Cryogenian diamictites and Lower Paleozoic sandstone in Ethiopia (Tigray): age constraints on Neoproterozoic glaciation and crustal evolution of the southern Arabian Nubian Shield. *Precambrian Research*, **154**: 88–106.

- Avigad, D. and Gvirtzman, Z. (2009). Late Neoproterozoic rise and fall of the northern Arabian–Nubian shield: The role of lithospheric mantle delamination and subsequent thermal subsidence, *Tectonophysics*, 477: (3–4): 217–22.
- Barbarin, B. (1990). Granitoids: main petrogenetic classifications in relation to origin and tectonic setting. *Geological Journal*, **25**: 227-238.
- Benzu Gold Mining Ethiopia PLC, (2013). Independent technical report on Dul-Menghe and Agusha License Benishangul Gumuz, Ethiopia, Gauteng, South Africa.
- Blades, M.L., Collins. A.S., Foden, J., Payne, J.L., Xu, X., Tadesse Alemu, Girma Woldetinsae, Clark, C. and Taylor, R.J.M. (2015). Age and Hafnium isotopic evolution of the Didessa and Kemashi Domain, western Ethiopia. *Precambrian Research*, **270**: 267-284.
- Braathen, A., Grenne T., Mulugeta Gebreselassie and Tadesse Worku (2001). Juxtaposition of Neoproterozoic units along the Baruda–Tulu Dimtu shear-belt in the East African Orogen of western Ethiopia. *Precambrian Research*, **107**: 215-234.
- Bhatia, M.R. and Crook, K.A.W. (1986) Trace element characteristics of graywackes and tectonic setting discrimination of sedimentary basins. *Contribution of Mineralogy and Petrology*, **92**: 181-193.
- Boynton, W.V. (1984). *Geochemistry of Rare Earth Elements: Meteoritic Studies*, Elsevier, Amsterdam, 63-114pp.
- De Wit, M.J. and Abera Aguma (1977). Geology of the ultramafic and associated rocks of Tullu Dimtu, Welega. Unpublished Report, 57, Ethiopian Institute of Geological Surveys, 23pp.
- De Wit, M.J., Berg, R., Balcha, B., Guyasa, A., Bekele, T. (1977). Geology of the Kata area, Welega. Unpublished Report, 65, Ethiopian Institute of Geological Surveys, 14p.
- Förster, H.J., Tischendorf, G. and Trumbull, R.B. (1997). An evaluation of the Rb vs. (Y+Nb) discrimination diagram to infer tectonic setting of silicic igneous rocks, *lithos*, **40**: 261-293.

- Gani, ND. and Abdelsalam, MG.(2006). Remote Sensing analysis of the Gorge of the Nile, Ethiopia with emphasis on Dejen-Gohatsion region. *Journal of Africa Earth Sciences*, **44**:135-150.
- Gebremedhin Tadesse and Mulugeta Tesfaye (1999). The geology of the Tosho Sheet (NC 36-11).Unpublished Technical Report, Regional Geology and Geochemistry Department, Ethiopian Institute of Geological Surveys,42pp.
- Gebremedhin Tadesse and Allen, A. (2005). Geology and Geochemistry of the Neoproterozoic Tuledimtu Ophiolite Suite, Western Ethiopia. *Journal of Africa Earth Sciences*, **41**:192-211.
- Getaneh Assefa, Giovanni, M. Paola, D.J. and Valer, R. (1981). Plate Tectonics and Metallogenic processes in Ethiopia (preliminary report). Unpublished report, Ethiopian Institute of Geological Surveys, Ethiopia.pp. 861-867.
- Grenne, T., Braathen, A., Mulugeta Gebreselassie and Tadesse Worku (1998). Results and models from fieldwork in the Meso-Neoproterozoic belt of western Ethiopia: the Wember Baruda-Bulen-Kilaj transect of the Metekel zone.Norges Geologiske Undersokelse Report 98.
- Grebennikov,A.V.(2014). A-type granites and related rocks: petrogenesis and classification, *Russian Geology and Geophysics*, **55**: 1074-1086.
- Irvine, T.N., and Baragar, W. (1971). A guide to the chemical classification of the common volcanic rocks. *Canadian journal of earth sciences*, **8**: 523-548.
- Johnson, P.R. and Woldehaimanot, B. (2003).Development of the Arabian–Nubian Shield perspectives on accretion and deformation in the northern East African Orogen and assembly of Gondwana. In: Yoshida, M., Windley, B.F., Dasgupta, S. (Eds.), Proterozoic East Gondwana: Supercontinent Assembly and Breakup. *Geological Society Special Publication*, **206**:289–326.

- Johnson, T.E., Teklewold Ayalew, Abera Mogessie, Johan, F.K. and Poujol, M. (2004). Constraints of the tectonometamorphic evolution of the western Ethiopian shield *Precambrian research*, **133**: 305-327.
- Kazmin, V. (1969). Geology of Tullu Kapi-Dalatti area. Unpublished Report, United-Nations Ethiopia Mineral Survey, pp.17.
- Kazmin, V. (1971). Precambrian of Ethiopia. *Nature*, **230**: 176-177.
- Kazmin, V. (1972). Geology of Ethiopia. Unpublished report, Ethiopian Institute of Geological Survey.
- Kazmin, V., Alemu Shiferaw and Tilahun Balcha (1978). The Ethiopian Basement: Stratigraphy and possible manner of evolution. *Geol. Rundsch*, **67**:531–546.
- Kroner, A. and Stern, R.J. (2004). Pan-African Orogeny, *Encyclopedia of Geology*, Elsevier, Amsterdam, **1**:1–12.
- Kusky, T.M., Abdelsalam, M., Stern, R.J. and Tucker, R.D. (2003). Preface: evolution of the East African and related orogens, and the assembly of Gondwana. *Precambrian Res.*, **123**:81-85.
- Landenberger, B. and Collins, W.J. (1996). Derivation of A-type granites from a dehydrated Charnockitic lower crust, evidence from the Chaelundi Complex, Eastern Australia. *J. Petrol.* **37**:145–170.
- Li, Z.X., Bogdanova, S.V., Collins, A.S., Davidson, A., DeWaele, B., Ernst, R.E., Fitzsimons, I.C.W., Fuchs, R.A., Gladkochub, D.P., Jacobs, J., Karlstrom, K.E., Lu, S., Natapov, L.M., Pease, V., Pisarevsky, S.A., Thrane, K. and Vernikovsky, V. (2008). Assembly, Configuration, and break-up history of Rodinia: a synthesis. *Precambrian Res.*, **160**:179-210.
- Lulu Tsige and Abdelsalam, M.G. (2005). Neoproterozoic-Early Paleozoic gravitational tectonic collapse in the southern part of the Arabian-Nubian Shield: The Bulbul Belt of southern Ethiopia. *Precambrian Research*, **138**: 297-318

- Lulu Tsige (2008). Geology of Bure map sheet NC-37/5. Ethiopian Institute of Geological Survey.No.18.
- McLennan, S.M. (1989). Rare earth elements in sedimentary rocks: Influence of provenance and sedimentary processes. In: Lipin B.R, McKay, G.A. (Eds.), *Geochemistry and Mineralogy of Rare Earth Elements*. Mineralogical Society of America, *Reviews in Mineralogy*, **21**: 169–200pp.
- Mengesha Tefera and Seife Michael Berhe (1987). Geology of Sheet NC, 36-16,(Gore Sheet). Ethiopian Institute of Geological Surveys.Unpublished manuscript.
- Mengesha Tefera, Tadiwos Chernet and Workineh Haro (1996). Explanation of the Geological map of Ethiopia. Ethiopian Institute of Geological Surveys, Addis Ababa,Ethiopia.
- Middlemost, E. A. K. (1994). Naming materials in the magma/igneous rock system. *Earth Sci.Rev.*, **37**:215-224.
- Moore, J.M.,Morgan, J.,Mengesha Tefera and Mengistu Teklay (1987). Geology of the Gore-Gambela Geotraverse, western Ethiopia. In: *Current Research in African Earth Science*, pp.109-112.A.A Balkema, Rotterdam.
- Mulugeta Alene, Ruffini, R. and Sacchi .R. (2000). Geochemistry and geotectonic setting of Neoproterozoic rocks from northern Ethiopia (Arabian-Nubian Shield). *Gondwana Res.*, **3**: 333-347.
- O'Connor, J. T. (1965). A classification for quartz-rich igneous rocks based on feldspar ratios. In: *US Geological Survey Professional Paper B525*. USGS, 79–84.
- Pearce,J.A.(1982). Trace element characerstics of lavas from destractive plate margins.In:Thorpe R.S.(Ed.),*Andesites:Orogenic Andesites and related rocks*,Wiley,New York, 525-548.
- Pearce, J.A., Harris, N.B.W. and Tindle, A.G. (1984). Trace element discrimination diagrams for the tectonic interpretation of granitic rocks. *Journal petrology*, **25**:956-983.

- Peccerillo, A. and Taylor S .R.(1976). Geochemistry of Eocene calc-alkaline volcanic rocks from the Kastamonu area, Northern Turkey, *Contrib Mineral Petrol*, **58**: 63-81pp.
- Rollinson, H.R. (1993).Using geochemical data: Evolution,presentation,interpretation:Longman Group UK Ltd.,352p.
- Seife Michael Berhe (1990). Ophiolites in Northeast and East Africa: implications for Proterozoic crustal growth. *Journal of Geological Society*, London, **147**: 41-57.
- Senbeto Chewaka (1980). Notes on the geology of part of Gimbi Sheet (NC36-12).Unpublished Report, Ethiopian Institute of Geological Surveys, 18pp.
- Shand, S.J. (1943). Eruptive Rocks. Their Genesis, Composition, Classification, and Their Relation to Ore-Deposits with a chapter on Meteorite. John Wiley and Sons., New York, pp. 444.
- Stern, R.J., Nielsen, K.C., Best, E., Sultan, M., Arvidson, R.E. and Kroner, A.(1990). Orientation of late Precambrian sutures in the Arabian-Nubian shield. *Geology*, **18**: 1103 - 1106.
- Stern, R.J., Nielsen, K.C., Best, E., Sultan, M., Arvidson, R.E. and Kroner, A.(1990). Orientation of late Precambrian sutures in the Arabian-Nubian shield. *Geology* **18**,1103± 1106.
- Stern, R.J. (1994). Arc assembly and continental collision in the Neoproterozoic East African orogen. *Ann. Rev. Earth Planet. Sci.*, **22**: 319±351.
- Stern,R.J., Kamal, A.,Mohamed,A Abdelsalam,G.,Simon, A. and Wilde,Qin Zhou.(2012). U-Pb Zircon geochronology of the eastern part of the Southern Ethiopian Shield. *Precambrian research*, 159-16.
- Streckeisen, A. (1974). Classification and nomenclature of plutonic rocks. *Geologische Rundschau*, **63**, 773–786.
- Tadesse Alemu and Tsegaye Abebe (2007). Geology and Tectonic Evolution of the pan-African Tulu Dimtu Belt, Western Ethiopia. *Online Journal of Earth Sciences*, **1**:24-42.

- Tadesse Yihunie and Fekadu Hailu (2007). Possible eastward tectonic transport and northward gravitational tectonic collapse in the Arabian-Nubian shield of western Ethiopia. *Journal of Africa Earth Sciences*, **49**:1-11.
- Teklewold Ayalew, Bell, K., Moore, J.M, J.M. and Parrish, R.R.(1990).U-Pb and Rb-Sr geochronology of the Western Ethiopian Shield. *Geology Soc .Am .Bull*, **102**:1309-1316.
- Teklewold Ayalew (1997). Metamorphic and structural evolution of the Gore-Gambella area western Ethiopia. *SINET*, **20**:235-259.
- Teklewold Ayalew and Peccerillo, A. (1998). Petrology and geochemistry of the Gore-Gambella plutonic rocks: implications for magma genesis and the tectonic setting of the pan-African Orogenic Belt of western Ethiopian. *Journal of African Earth Sciences*, **27**:397-416.
- Teklewold Ayalew and Johnson.,T.E. (2002). Geotectonic Evolution of the western Ethiopian shield. *SINET*, **25**:.227-252.
- Tenczer, V., Hauzenberger, C., Fritz, H., Wallbrecher, E., Muhongo, S., Aberra Mogessie, Hoinkees, G., Loizenb J. and Bauernhofer, A. (2005). The metamorphic evolution of the Mozambique Belt in Central Tanzania: new petrological and geochronological data. *Geophysical Research Abstracts*, **7**:xxx
- Tesfaye Kebede, Koeberl, C. and Koller, F. (1999). Geology, geochemistry and petrogenesis of intrusive rocks of the Wallagga area, western Ethiopia. *Journal of African Earth Sciences*, **29**:715–734.
- Tesfaye Kebede, Kloetzli, U.S. and Koeberl, C (2001). U/Pb and Pb/Pb zircon ages from granitoid rocks of Wallagga area: constraints on magmatic and tectonic evolution of Precambrian rocks of western Ethiopia. *Mineralogy and petrology*, **71**:251-271.
- Tesfaye Kebede, Koeberl, C. and Koller, F. (2001b). Magmatic evolution of the Suqii-Wagga garnet-bearing two-mica granite, Wallagga area, western Ethiopia. *Journal of African Earth Sciences*, **32**:193-221.

- Tesfaye Kebede and Koeberl, C.(2003). Petrogenesis of A-type granitoids from the Wallagga area, western Ethiopia: constraints from mineralogy, bulk-rock chemistry, a Nd and Sr Isotopic compositions. *Precambrian Research*, **121**:1–24.
- Thompson, R.N.,M.A. Morrison, G.L. Hendry. and Parry, S.J.(1984).An assessment of the relative roles of a crust and mantle in magma genesis: an elemental approach. *Phil Trans R.Soc. Lond.*, **310**:54990.
- UNDP (1972). Mineral Survey in two selected areas (Sidamo and Welega), Ethiopia.
- Vail, J.R. (1983). Pan-Africa crustal accretion in north-east Africa. *Journal of African Earth Sciences*. **1**:285-294.
- White, W.M. (2013). *Geochemistry*. John Wiley and Sons.
- Wilson,M.(1989).Igneous Petrogenesis a global tectonic approach,Unwin Hyman,London,480pp.
- Winter, J.D.(2001). An introduction to Igneous and Metamorphic petrology, Prince Hall Inc., Upper Saddle River, New Jersey.
- Wood, D.A. (1980). The application of a Th-Hf-Ta diagram to problems of tectonomagmatic classification and to establishing the nature of crustal contamination of basaltic lavas of the British Tertiary volcanic province. *Earth Planet. Sci. Lett.*, **50**: 11-30pp.
- Yibas, B. (2000). The Precambrian geology, tectonic evolution, and controls of gold mineralization in southern Ethiopia. Ph.D. Thesis (unpublished).University of the Witwatersrand, Johannesburg, South Africa, 448 pp.
- Yibas, B., Reimold, W.U., Anhaeusser, C.R., Koeberl, C. (2003). Geochemistry of the mafic of the ophiolitic fold and trust belts of southern Ethiopia: constraints on the tectonic regime during the Neoproterozoic (900-700Ma).

Zhu, DiCheng., MO XuanXue, WANG LiQuan, ZHAO ZhiDan, NIU Yaoling, ZHOU ChangYong & YANG YueHeng. (2009). Petrogenesis of highly fractionated I- type granites in the Zayu area of eastern Gangdese, Tibet: Constraints from zircon U-Pb geochronology, geochemistry and Sr-Nd-Hf isotopes. Science in China press, Springer.

APPENDICES

Appendix I. Field data

A) Field Characteristics and Hand specimen properties of the representative samples of the study area.

Sample code	Mineral content	Geographic location	Elevation(m)	Texture, color (fresh) structure
Granite unit				
ABS-1	Quartz, K-feldspar, Biotite	10°19'17.9"N 037°01'28.5"E	1441	Medium grained, light pink to pale pink, joint and fracture.
ABS-2	Quartz, K-feldspar, Biotite	10°19'06.4"N 037°01'34.4"E	1390	Medium grained, light gray, fracture
ABS-3	Quartz, K-feldspar, Biotite	10°18'51.4"N 037°01'43.1"E	1316	Coarse grained, whitish, quartz vein
ABS-4	Quartz, K-feldspar, Biotite	10°17'55.2"N 037°01'37.6"E	1134	Very coarse grained, whitish, fracture
ABS-5	k-feldspar, quartz and plagioclase	10°17'51.2"N 037°01'40.9"E	1130	Coarse grained, light gray to light gray, Quartz vein and fracture
ABS-6	k-feldspar, quartz and plagioclase	10°17'49.3"N 037°01'41.6"E	1123	Medium grained, whitish, joint
ABS-8	k-feldspar, plagioclase and quartz	10°283'00"N 036°97'00"E	1572	Very coarse grained, pinkish, joint
ABS-9	Quartz, biotite and feldspar	10°15'30.8"N 036°59'35.8"E	1519	Coarse grained light gray to greenish gray

				,fracture
ABS-13	k-feldspar, plagioclase and quartz	10°17'34.8"N 037°00'01.5"E	1108	Coarse grained, light pink
ABS-15	Quartz, biotite, plagioclase and k- feldspar	10°17'34.8"N 037°00'34.1"E	818	Medium grained, light gray, flow banding
Gneiss unit				
ABS-7	Biotite and feldspar	10°14'37.0"N 036°59'20.6"E	1580	Medium grained, gray
ABS-10	Biotite and feldspar	10°15'57.6"N 036°59'40.1"E	1460	Medium grained, darkish, fracture
ABS-11	Biotite and feldspar	10°17'11.4"N 037°00'16.8"E	1224	Medium grained, light gray, compositional banding
ABS-12	Biotite, feldspar and quartz	10°17'43.9"N 037°00'06.7"E	1136	Medium grained, light gray, quartz vein
ABS-14	Biotite, feldspar and quartz	10°312'00"N 036°99'00"E	886	Medium grained, light gray, fracture
ABS-16	Biotite, muscovite and feldspar	10°17'28.6"N 037°01'03.2"E	873	Medium grained, darkish ,compositional banding and quartz vein
ABS-17	Biotite, muscovite and feldspar	10°17'44.4"N 037°01'17.7"E	1008	Medium grained, darkish, compositional banding

Appendix II-Petrographic Data

A) Modal percentage of the representative rock samples.

Sample Name	Mineral name and their modal (%)											
	Granite samples											
	Qtz	Kfs	Plag	Ms/Ser	Bt	Opq	Zr	Pyr	Spn	Chl	Hbl	Apt
ABS-1	25	45	20	2	6	2	-	-	-	-	-	-
ABS-2	20	50	15	3	10	2	-	-	-	-	-	-
ABS-4	25	55	15	1	2	1	1	-	-	-	-	-
ABS-6	25	45	20	2	5	3	-	-	-	-	-	-
ABS-8	30	25	35	3	3	3	1	-	-	-	-	-
ABS-9	30	45	10	4	8	3	-	-	-	-	-	-
ABS-13	20	50	15	5	6	-	-	-	-	-	-	-
ABS-15	30	50	10	3	5	2	-	-	-	-	-	-
Gneiss samples												
ABS-7	20	-	25	-	8	1	-	3	-	3	40	-
ABS-10	30	40	15	-	10	2	-	-	2	-	-	-
ABS-11	35	45	10	2	5	2	-	-	-	2	-	1
ABS-12	30	45	14	3	5	2	1	-	-	-	-	-
ABS-16	15	-	30	-	5	2	-	5	4	-	35	1
ABS-17	20	-	25	-	10	2	-	5	4	-	38	1

B) Compiled thin section analysis results and descriptions, it represents the summary of all thin sections.

Component		Descriptions		
		Color	Shape	Texture
Kfs	Microcline	Dark gray to light gray	anhedral to subhedral	Micro-perthitic (intergrowth of quartz and feldspar), perthitic texture formed (inclusion of Pl, Qtz within Kfs) and cross hatched/ tartan twin is common to all.
Plagioclase		Light dark, light gray to alternative band color	anhedral to subhedral sometimes euhedral.	Perthitic of parallel streaks and (albite) occurred within Kfs (microcline) and alteration of Plagioclase to sericite with polysynthetic form.
Quartz		Whitish to Light gray , cloudy	anhedral to subhedral, sometimes euhedral elongated/ribbon	Fine to coarse, Intergranular (intergrowth with Kfs), graphic and granular texture.
Biotite		Dark brown to pale brown ,greenish	Subhedral to anhedral, elongated.	Flaky to tiny platy texture are common.
Muscovite		Pinkish, yellowish and purple	Elongated, subhedral to anhedral.	Fine grained to coarse grained, Flaky to tiny platy texture are common.
Hornblende		Brownish green to brown	anhedral, subhedral euhedral	Fine to medium grained and Intergranular.
Zircon and Sphene		Brown to red brown	Idioblastic	Very high relief, fine grained texture.
Chlorite		greenish	anhedral to subhedral	Very fine grained.

Opaque minerals	Black both in PPL and XPL	Subhedral to euhedral	Medium to coarse grained.
Epidote	Yellow of greenish-yellow	anhedral to Sub hedral	Fine grained.
Apatite	yellowish	anhedral	Fine grained.
Note: The representative rock samples of the area of prepared thin section samples mainly characterized by granular, Intergranular and myremekite, perthitic, graphitic texture, anhedral to subhedral crystal shapes are commonly observed.			

C) Recalculated modal percentage of major minerals in Granit samples.

Sample Name	Quartz (Q)	Alkali-feldspar (A)	Plagioclase (P)
ABS-1	27.77	50	22.22
ABS-2	23.52	55.55	17.64
ABS-4	26.31	57.89	15.78
ABS-6	27.77	50	22.22
ABS-8	33.33	27.77	38.88
ABS-9	35.29	52.94	11.76
ABS-13	23.52	58.82	17.64
ABS-15	33.33	55.55	11.11
Note: Granite of the area dominated by three major minerals alkali-feldspar, plagioclase and quartz.			

D) Petrographic Description

1. Hornblende-Biotite unit

Petrographic analysis of the representative samples (Figure 4.1 A-D) from Hornblende-Biotite Gneiss unit has been presented and interpreted as follow. Compositionally this unit is composed of hornblende, plagioclase, biotite, pyroxene and quartz. Trace amount of chlorite, sphene and opaque minerals also constitute the rock unit.

Description- Figure 4.1 A-D: Microscopic photo pictures of the Hornblende-Biotite Gneiss unit. **(A)** Sample # ABS-7 in XPL, 10 X magnifications, location (036°59'19.2"E:10°14'34"N). Mineral content: 40% hornblende, 35% plagioclase, 10% quartz, 8% biotite, 3% chlorite and 3% pyroxene (Cpx) and 1% opaque. This rock unit exhibits granular and foliated texture. Among the feldspar minerals plagioclase dominates the rock unit characterized by anhedral to subhedral shape and clearly shows twinning (polysynthetic twinning). Quartz grains have angular to sub angular shape and shows undulose extinction. The foliation is defined by mafic (hornblende and biotite) minerals but the felsic minerals plagioclase and quartz shows random orientation. Alteration of hornblende to chlorite is commonly developed. In addition, the abundance of certain minerals such as hornblende, plagioclase, biotite and small amount of clinopyroxene indicates that this rock is derived from mafic rock most probably basalt. **(B)** Sample # ABS-7 in PPL, 10 X the same location and mineral content with **(A)**. In this ppl view alteration of hornblende to chlorite is clearly observed. Furthermore, chlorite appears greenish gray in (PPL) at the right side of this thin section. **(C)** Sample # ABS-16 in XPL, 10 X magnifications, location (037°01'03.2"E:10°17'28.6"N). Mineral content: 38% hornblende, 30% plagioclase, 15% quartz, 5% biotite, 5% pyroxene, 4% sphene, 2% opaque and 1% apatite. This rock unit also exhibit granular texture. The biotite commonly shows flaky shape. In some part of the thin section the fine crystal of quartz is set in the larger crystal of plagioclase and biotite. The foliations are defined by biotite and hornblende; however, plagioclase and quartz shows random orientation. In this sample plagioclase also commonly twinned. Furthermore, the plagioclase is altered in some extent to sericite. The presence of Cpx may indicate that the rock reaches in the upper amphibolite facies. **(D)** Sample # ABS-17 in XPL, 10X magnifications, location (037°01'47"E:10°17'39.8"N). Mineral content: 48% hornblende, 25% plagioclase, 10% biotite,

5% quartz, 5% pyroxene, 4% sphene, 2% opaque and 1% apatite. This rock unit exhibit foliated texture. In some part of the thin section in plagioclase crystals micro fracturing are observed showing inclusions of opaque and sphene. Similarly in some part of the thin section in hornblende crystals inclusion of sphene is also observed. Quartz and plagioclase have angular to sub angular grain shape, whereas hornblende have elongated, subhedral to euhedral grain shape and show brownish green to brown color. It exhibits both the compositional variation and banding which is presumably due to metamorphic differentiation. The foliations are defined by mafic (hornblend) and felsic (plagioclase and quartz) minerals. In this rock sample also plagioclase altered in some extent in to sercite also observed.

2. Granitic gneiss unit

Petrographic study of the representative rock samples (Figure 4.2 A-D) from the granitic gneiss indicates that this rock is mainly composed of k-feldspar, quartz, plagioclase and biotite. Trace amount of muscovite/sericite, opaque, sphene and zircon also constitute the rock unit.

Description- Figure 4.2. A-D: Microscopic photo-pictures of granitic gneiss unit. **(A)** Sample # ABS-10 in XPL, 10 X magnifications, location (037°00'37.6"E:10°14'49.7"N). Mineral content: 40% k-feldspar (microcline), 30% quartz, 15% plagioclase, 10% biotite, 2% sphene and 2% opaque. This rock unit exhibit granular texture. Alteration of plagioclase and k-feldspar to sericite is commonly observed. Quartz grains have angular to sub-angular and exhibit undulose extinction. Most of the minerals do not show any preferred orientation; however, the faint foliations are defined by alignment of the mafic (biotite) mineral. The abundance of certain mineral assemblage such as k-feldspar, quartz and plagioclase and granular texture indicates that the protolith of the rock is felsic igneous rock most probably granite. **(B)** Sample # ABS-11 in XPL, 10 X magnifications, location (037°00'16.8"E:10°17'11.4"N). Mineral content: 40% k-feldspar (microcline), 35% quartz, 15% plagioclase 5% biotite, 2% muscovite/sericite, 2% chlorite, 2% opaque, and 1% apatite. This sample shows weak foliation defined by felsic (plagioclase, k-feldspar and quartz) and mafic (biotite) minerals. K-feldspar (microcline) and plagioclase shows euhedral to sub hedral grain shape, where as quartz grains have anhedral shape. Alteration of feldspar minerals to sercite is common as well. **(C)** The same view of picture (B) under PPL. **(D)** Sample# ABS-12 in XPL, 10X magnifications, location (037°00'06.7"E:10°17'43.9"N). Mineral content: 45% k-feldspar (microcline), 30% quartz, 15%

plagioclase, 5% biotite, 3% muscovite/sericite 1% opaque and 1% zircon. Most of minerals show preferred orientation defined by felsic (k-feldspar and plagioclase) and mafic (biotite) minerals. The angular to sub angular quartz grain shows undulose extinction whereas k-feldspar and plagioclase shows anhedral to sub-hedral grain shape. In addition, k-feldspar (microcline) and plagioclase exhibit irregular grain boundary formed probably due to deformation. Biotite has flaky texture, whereas quartz, k-feldspar and plagioclase have granular texture.

3. Granite unit

Description- Figure 4.2. A-D: Microscopic photo-pictures of granitic gneiss unit (A) Sample # ABS-1 in XPL, 10X magnifications, location (037°01'28.5"E: 10°19'17.9"N). Mineral content: 45% k-feldspar (microcline), 25% quartz, 20% plagioclase, 6% biotite, 2% opaque and 2% muscovite/sericite. Plagioclase and k-feldspar are altered in to sericite is observed in the thin section. The quartz grain appears in several forms: as coarse grained in the phenocryst; fine grained in the matrix; and as elongated quartz ribbons. This grain variation may be the result of deformation. Besides this, the quartz grains have anhedral to subhedral shape and exhibiting little undulose extinction. The presence of undulatory extinction in the quartz crystals and development of biotite and muscovite indicate that this unit is not post tectonic at least under this observation. Plagioclase shows polysynthetic twinning and K-feldspar (microcline) clearly shows cross hatched (tartan) twinning. In addition, the plagioclase feldspar shows elongated lath and lamellar texture. (B) Sample # ABS-2 in XPL, 10 X magnifications, location (037°01'34.4"E: 10°19'06.4"N). Mineral content: 50% k-feldspar (microcline), 20% quartz, 15% plagioclase, 10% biotite, 3% muscovite/sericite and 2% opaque. This rock unit exhibit granular texture. This sample has large grain of biotite which is surrounded by quartz grains. Furthermore, the plagioclase and k-feldspar altered in some extent to sericite is also present in the thin section. In some part of the thin section the usual polysynthetic twinning observed in plagioclase is not as such visible. Quartz grains are recrystallized and deformed. Beside this, the quartz grains show angular to sub angular shape whereas k-feldspar and plagioclase shows anhedral grain shape. Moreover, in the quartz grain micro fracturing is also well developed. (C) Sample # ABS-4 in XPL, 10 X magnifications, location (037°01'37.6" E: 10°17'55.2"N). Mineral content: 55% k-feldspar (microcline), 25% quartz, 15% plagioclase, 2% biotite, 1% muscovite/sericite, 1% zircon and 1% opaque. This rock unit exhibit granular, myremekite and in some part of the thin

section perthitic textures are well developed. Alteration of plagioclase and k-feldspar to sericite are commonly observed. K-feldspar and plagioclase shows euhedral to subhedral grain shape, whereas quartz grains have anhedral to subhedral shape. K-feldspar is generally perthitic microcline, which often contains inclusions of opaque minerals. **(D)** Sample # ABS-6 in XPL, 10X magnifications, location (037°01'41.6"E:10°17'49.3"N). Mineral content: 45% k-feldspar (microcline) 25% quartz, 20% plagioclase, 5% biotite, 3% opaque and 2% muscovite/sericite. This rock unit also show granular, intergranular and myremekite texture. Among the k-feldspar mineral microcline is the dominant mineral which constitutes the rock unit. Alterations of k-feldspar (microcline) and plagioclase to sericite are commonly observed. In some part of the thin section quartz grain occur as coarse grained aggregates and in other part of the thin section it displays fine grained in the matrix. Due to alteration effect the usual cross hatched (tartan) twinning of microcline and polysynthetic (albite) twinning of plagioclase is not as such visible it simply patches. **(E)** Sample # ABS-8 in XPL, 10 X magnifications, location (036°59'22.5"E:10°14'39.3"N). Mineral content: 35% plagioclase, 30% quartz, 25% k-feldspar, 3% muscovite/sericite, 3% biotite, 3% opaque and 1% zircon. This rock unit shows, granular, perthitic and graphic texture. In some part of the thin section alterations of plagioclase and k-feldspar are well developed. The quartz grain subhedral to euhedral grain shape, whereas K-feldspar and plagioclase shows anhedral to subhedral grain shape. Moreover, quartz appears in several forms: as small granular crystals in the matrix and in cluster forms graphic quartz in the k-feldspar. **(F)** Sample # ABS-9 in XPL, 10 X, magnifications, location (036°59'35.8"E:10°15'30.8"N). Mineral content: 45% k-feldspar(microcline), 30% quartz, 10% plagioclase, 8% biotite, 4% muscovite/sericite, 3% opaque. This rock unit shows intergranular and granular texture. In the larger crystal of plagioclase micro fracturing is well developed and within the micro fracture it consists of enormous amount of inclusion. Alteration of plagioclase to sericite is also commonly observed in the thin section. In some part of the thin section myrmekitic intergrowth of plagioclase and quartz are present. **(G)** Sample # ABS-13 in XPL, 10 X, magnifications, location (037°00'01.5"E:10°17'40.8"N). Mineral content: 50% k-feldspar (microcline), 20% quartz, 15% plagioclase, 6% biotite, 5% muscovite/sericite and 4% opaque. At places, a gradational change to rather fine grained of quartz, plagioclase, k-feldspar (microcline) are observed. Microcline is commonly shows cross hatched twinning (tartan). In some part of the thin section this rock unit shows a porphyritic texture formed by large crystals

(phenocrysts) of K-feldspars is set in a fine cloudy quartz and feldspar matrix associated with lesser amount of mafic mineral. In addition, clusters of plagioclase and quartz are visible in some part of the thin sections. **(H)** Sample # ABS-15 in XPL, 10 X, magnifications, location (037°00'34.1"E:10°17'34.8"N). Mineral content: 50% k-feldspar (microcline), 30% quartz, 10% plagioclase, 5% biotite, 3% muscovite/sericite and 2% opaque. This rock unit shows granular texture. Alteration of plagioclase and k-feldspar to sericite; and biotite to chlorite is well observed. The quartz grains have anhedral to sub hedral grain shape. Furthermore, the quartz grains are recrystallized and deformed. Moreover this, some of the quartz grain shows little undulatory extinction. Both plagioclase and k-feldspar (microcline) is commonly twined.

Appendix III. Geochemical data

A) Alumina Saturation Index granite of the study area A/CNK and A/NK.

Sample name	Al ₂ O ₃	CaO	Na ₂ O	K ₂ O	A/CNK	A/NK
ABS-2	0.17	0.03	0.06	0.04	1.31	1.88
ABS-4	0.14	0.009	0.06	0.05	1.17	2.02
ABS-6	0.13	0.017	0.05	0.06	1.02	1.94
ABS-8	0.12	0.015	0.05	0.05	1.04	1.20
ABS-9	0.13	0.015	0.04	0.05	1.23	1.44
ABS-15	0.11	0.014	0.04	0.05	1.05	1.22

Note: The granite of the area A/CNK and A/NK have range value from (1.02-1.31); (1.2.-2.02) respectively.